Combining cross-shore and longshore processes in long-term probabilistic coastline modelling

Development of a probabilistic framework

R.C.T. Smits

Delft University of Technology

TU Delft

CDR

Combining cross-shore and longshore processes in long-term probabilistic coastline modelling

Development of a probabilistic framework

by

R.C.T. Smits

in partial fulfilment of the requirements for the degree of

Master of Science
in Civil Engineering

at the Delft University of Technology,

to be defended publicly on Friday April 14, 2023 at 15:00.

Student Number:	4445481	
Date:	Tuesday 4th April, 2023	
Thesis Committee:	Prof. dr. ir. S.G.J. Aarninkhof	TU Delft, chair
	Prof. dr. ir. A.J.H.M. Reniers	TU Delft
	Ir. D.C. Heineke	CDR International B.V.
	Dr. ir. A. Dastgheib	IHE Delft Institute for Water Education

Cover: Kees Streefkerk

TU Delft Delft University of Technology

CDR International B.V.

Abstract

Many coasts around the world experience coastal erosion as a result of climate change, lack of sediment supply or human interventions. In the coming decades, coasts will be exposed to increased natural forcing because of climate change and sea level rise, leading to increased risks of coastal flooding and erosion. As sandy coasts are highly dynamic systems, it is difficult to assess the impact of these risks. Long-term coastal evolution is evaluated on large temporal and spatial scales, which introduce uncertainty. Hence, probabilistic estimates are required rather than single, deterministic values. Complex, process-based models have been developed to simulate morphological changes in coastal zones, but these come at large computational expense. As probabilistic approaches require a large number of simulations, it is necessary to reduce computational times as much as possible.

Variability in coastline position is induced by both cross-shore and longshore processes, which occur perpendicular and parallel to the coastline, respectively. Extreme storm events and sea level rise are responsible for the long-term cross-shore coastal dynamics, while gradients in longshore sediment transport act as the main driver for the longshore coastline changes. This study focuses on developing a framework to combine predictions of long-term cross-shore and longshore processes in a probabilistic way. The framework combines probabilistic predictions of cross-shore effects with deterministic estimates of longshore-induced coastline change. Two separate models are studied for the cross-shore and longshore component, namely the Probabilistic Coastline Recession (PCR) model and the ShorelineS model. Both models are computationally efficient due to the use of reduced complexity sediment transport formulations and a simplified representation of the beach profile.

The developed framework is validated by a case study of the IJmuiden coastline, the Netherlands, to assess the effects of the blockage of longshore sediment transport by the breakwaters between 1967 and 2007. Consequently, projections of coastline development are determined for the period of 2023 to 2100, for a range of IPCC sea level rise scenarios. To model storm erosion with the PCR model, a synthetic time series of storm events is simulated by establishing joint probabilities of wave forcing variates. Moreover, the PCR model provides stochastic estimates of coastline recession, enabled by the large number of simulations. Regarding ShorelineS, a representative wave climate based on data of local wave conditions was used to compute the longshore sediment transport.

The ShorelineS simulation over the hindcasted period clearly resulted in accretion on both sides of the breakwaters in the order of 100 to 900 meters, in accordance with field observations. This outcome indicates that limited threats of coastal erosion are currently present. However, when analysing the projections for 2023-2100, the PCR model predicted that a combination of storm impact and sea level rise can definitely lead to coastline recession, with a median retreat of 18 meters and 32 meters for the RCP2.6 and RCP8.5 sea level rise scenario, respectively. Moreover, the PCR model indicated that at some point the coastline erosion might be larger than 100 meters with a probability of 1.5% for RCP2.6 and 4% for RCP8.5. The combined projections confirm the importance of accounting for both cross-shore and longshore impacts on long-term coastline evolution and show that the developed framework is a useful method for this purpose.

For further research it is recommended to study long-term coastline evolution while including interaction between cross-shore and longshore processes, to analyse its contribution to long-term coastline changes. It is also advised to further investigate how to obtain stochastic projections of coastline development induced by longshore processes, as this study only presents the cross-shore component in a probabilistic way. Furthermore, stochastic projections of sea level rise and beach recovery can be studied as well.

Preface

This MSc thesis report marks the completion of my master's degree in Hydraulic Engineering at the Delft University of Technology. This research was carried out in collaboration with CDR International, an independent medium-sized engineering consultancy firm in the water sector.

I would like to express my gratitude to my thesis committee, who provided me with valuable expert knowledge throughout my graduation period. First of all, Stefan, thank you for being the chair of my committee and for your enthusiasm and positive attitude during the meetings. Thank you Ad, for your thorough, constructive feedback and for the useful insights in studies related to my research. Ali, thank you for assisting me with your in-depth knowledge on the PCR model and your admirable talent to come up with alternatives and solutions so quickly. Last but not least, David, thank you so much for the time and attention you have devoted to supervise me throughout my graduation project and for guiding me in the right direction. It was great to be close to you in the office and that you were always open for questions and fruitful discussions. I would also like to thank all the staff of CDR International for giving me the opportunity to work in a professional environment and for making me part of the close team.

I am proud of the research that is presented in this report. The report concludes my time at the Delft University of Technology and with that, my time as a student. I want to thank my friends and fellow students for making these years unforgettable. Finally, a very special thanks to my parents, my sisters and my girlfriend Floor, for always supporting me and for always listening to my endless stories about beaches, waves and Google Earth images. I could not have done this without you.

Ruben Smits
Delft, April 2023

Contents

List of Tables

List of Figures

Nomenclature

Abbreviations

Abbreviation	Definition
CDF	Cumulative Distribution Function
DoC	Depth of Closure
DoT	Depth of Transport
IPCC	Intergovernmental Panel on Climate Change (of the UN)
JPM	Joint Probability Method
LECZ	Low Elevation Coastal Zone
LST	Longshore Sediment Transport
MLW	Mean Low Water
MHW	Mean High Water
MSL	Mean Sea Level
NAP	Normaal Amsterdams Peil
PCR	Probabilistic Coastline Recession
RCP	Representative Concentration Pathway
RSLR	Relative Sea Level Rise
SLR	Sea Level Rise
SSL	Storm Surge Level
SSTS	Synthetic Storm Time Series
SWL	Still Water Level

1 Introduction

This introduction presents the motivation of this research and a description of the problem. In addition, the research objective and the main research question are presented, along with the sub-questions and the research approach. Finally, an overview of the structure of the report is given.

1.1. Research motivation

Many coasts around the world experience coastal recession as a result of climate change, lack of sediment supply or human interventions. Climate change induces accelerated sea level rise (SLR) and is the cause of more frequent and more severe storms, leading to an increase in coastal flood hazard all over the globe (Church et al., 2013; Vousdoukas et al., 2018). The combination of SLR, storm surge and storm waves results in high risks of socio-economic and environmental losses in the near-future (Ranasinghe, 2016, 2020). In addition, gradients in longshore sediment transport (LST), e.g. as a result of coastal structures or ports, can induce large coastline erosion (Bosboom & Stive, 2021). These risks could lead to a large increase in coastal protection costs (Hinkel et al., 2014), as well as in costs of forced population migration from vulnerable coastal areas (Hinkel et al., 2013).

The latter is a serious concern, since coastal zones belong to the most heavily populated and developed land zones in the world (Luijendijk et al., 2018; Small & Nicholls, 2003). To illustrate, almost 10% of the world population lives in the vulnerable Low Elevation Coastal Zone (LECZ) - i.e. the contiguous area along the coast that is less than 10 metres above sea level (McGranahan et al., 2007; Vafeidis et al., 2011). Also, approximately 40% of the world's population is estimated to live within 100 kilometres of the coast (Shi & Singh, 2003).

Coastal population and economic activities are seen to be growing due to the attraction of coastal areas, which increases the number of people affected by coastal hazards (Neumann et al., 2015). Hence, it can be stated that the need for sound, integrated coastal zone management is urgent in order to ensure human and property safety (Ranasinghe, 2016, 2020; Waterman, 2010). Coastal zone management is based on risk assessment, which requires extensive knowledge about future coastal erosion hazard in the form of accurate, long-term predictions of coastline changes. Therefore, probabilistic projections rather than single, deterministic values are necessary (Callaghan et al., 2008; Wainwright et al., 2014).

Long-term coastline evolution is induced by both cross-shore and longshore processes, which occur perpendicular and parallel to the coastline, respectively. Ranasinghe et al. (2012) proposed the physics-based Probabilistic Coastline Recession (PCR) model for risk-based coastal zone management purposes. The model provides stochastic estimates of coastal recession based on governing physical cross-shore processes: storm events, SLR and beach recovery. The PCR model, however, does not consider longshore processes. Long-term coastline evolution induced by gradients in LST can be modelled with the ShorelineS model (Roelvink et al., 2020). This is a free-form coastline model which is capable of modelling the long-term response of a coastline after a human intervention (i.e. a structure or port), however it does not account for coastline changes induced by cross-shore processes.

Previous studies have indicated that a coupling between a cross-shore and a longshore model might add significant value when modelling the behaviour of coastlines dominated by LST gradients or by human interventions (Bitaki, 2019; Da Cruz, 2018; Hallin et al., 2019; Krijnen, 2021). For some coastal areas around the world, gradients in LST can be the main driver for structural changes in coastlines, while SLR and severe storms can induce structural coastline retreat as well. In addition, cross-shore coastline displacement induces changes in coastal orientation and thus changes to the LST as well. In order to obtain accurate and reliable coastline recession predictions, it is therefore necessary to investigate the possibilities of combining cross-shore and longshore processes in modelling long-term coastline evolution.

1.2. Problem definition

The large - and growing - coastal population and the valuable coastal assets are endangered by the effects of climate change and human interventions. To understand, manage and mitigate those effects, the use of probabilistic, risk-based management approaches increases rapidly. Many coastline models used for this purpose account for cross-shore and longshore physical processes individually and separately. However, in reality, cross-shore and longshore processes may have a combined influence on coastal evolution and can even interact. In addition, estimating future developments induces uncertainties. Hence, a probabilistic approach is required to enable uncertainty ranges in the long-term projections of coastline development. In literature, a knowledge gap is found for a common method to account for both cross-shore and longshore impacts on long-term coastline changes in a probabilistic way. In order to aim for improved estimates of future coastline evolution, this study investigates the possibilities to combine long-term cross-shore and longshore predictions of coastline change using a stochastic approach.

1.3. Objective and research question

The main motivation behind this study is to improve the accuracy of long-term projections of coastline evolution including an uncertainty range. These projections can be used by decision-makers to optimize coastal zone management strategies and to minimize the vulnerability of coastal areas to the impacts of climate change and human interventions. The objective of this research is to study the possibilities of combining cross-shore and longshore processes in modelling long-term coastline changes, in a probabilistic way. The following research question is defined:

How can cross-shore and longshore nearshore processes be combined in long-term, probabilistic coastline modelling, in order to obtain stochastic projections of long-term coastline evolution?

In order to answer the main research question and to analyse all involved processes, two sub-questions are introduced:

Sub-question 1	What are the relevant physical processes reponsible for long-term coastline evolution?
Sub-question 2	How can the relevant physical processes be modelled to obtain long-term projections of coastline evolution?
Sub-question 3	What is the added value of a framework that combines the relevant processes compared to existing methods?

1.4. Research approach

In this MSc research, the research objective is approached by developing and studying different frameworks to model long-term coastline evolution induced by both cross-shore and longshore processes, and to present it in a probabilistic way. Based on applicability in engineering purposes, computational time and model performances, it is chosen to conduct this research with the use of the PCR model and the ShorelineS model. This decision is elaborated in Chapter 3.

First, a study is performed to all relevant physical processes, to cross-shore and longshore coastal modelling and to the modelling procedures of ShorelineS and PCR. Consequently, multiple frameworks are developed to describe the modelling possibilities of both cross-shore and longshore processes, including their interaction. In order to study the developed frameworks and to analyse the performance, a case study of the coastline near IJmuiden is implemented. In this area, gradients in LST are present due to the breakwaters protecting the port entrance channel. Figure 1.1 shows a schematic overview of the research approach.

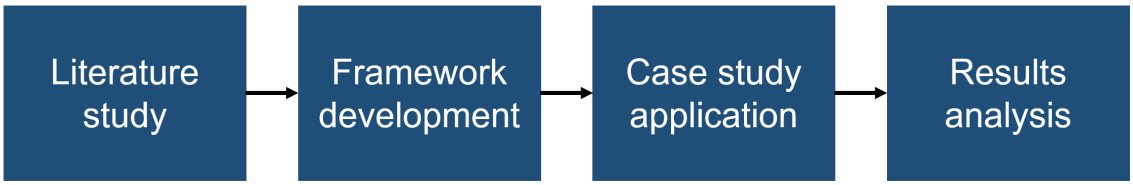

Figure 1.1: Schematic overview of research approach.

Frameworks
According to the described research approach, the following frameworks have been defined:

1. Cross-shore and longshore processes are modelled separately;
2. Longshore processes respond to cross-shore storm erosion;
3. Cross-shore processes respond to changed coastline orientation induced by LST gradients;
4. Both processes are coupled and fully interact with each other.

The developed frameworks are further explained in Chapter 4.

Scope of present study
The scope of the present study is confined to Framework 1. This is mainly due to the assumptions of the implemented models, but also because it is hypothesised that the framework is an acceptable method to obtain estimates of coastline development. The results are analysed and presented in a probabilistic way, in order to obtain long-term projections of coastline change including an uncertainty range. Additionally, the small exceedance probabilities of coastline erosion are studied, which are relevant for coastal engineering purposes. The established scope means that in this research no interaction effects between cross-shore and longshore processes are taken into account.

Physical processes
Within this research, the scope is confined to certain physical nearshore processes. For the longshore transport processes, the relevant process is coastline change induced by gradients in LST.

Regarding the cross-shore transport processes, it is focused on:

- Erosion due to extreme storm events;
- Recovery of the coastline during (calm) periods in between storms;
- Coastline retreat as a result of (relative) sea level rise.

All mentioned processes are thoroughly discussed in Section 2.3.

Temporal and spatial scales
The focus of this research will be on processes with timescales of years to decades. Cross-shore variations of smaller timescales (e.g. storm events) are part of the study, but the focus lies on their long-term effects. The corresponding spatial scales of interest range from metres to kilometres for cross-shore purposes and an extension to tens of kilometres for alongshore observations. Large-scale geographical characteristics (e.g. long-term oceanographic changes) and very small scales (e.g. wave ripples) are both out of scope.

1.5. Report structure

In addition to this introduction, Chapter 2 provides extra background information on the research topic, the relevant nearshore processes and the coastline models in the form of a literature review. Chapter 3 presents the decision for the models implemented in this research and elaborates on the modelling procedures. In Chapter 4 the developed frameworks to combine cross-shore and longshore processes are described and discussed. The selected framework is applied to a case study in Chapter 5. Next, the obtained results of this study are presented and analysed in Chapter 6, after which the research approach and the findings are discussed in Chapter 7. Finally, Chapter 8 presents the conclusions of this research and the answers to the research questions, as well as recommendations of elements requiring further investigation.

2

Literature review

This chapter presents a literature review in order to provide the necessary background information on the studied subject. First, more context is presented on the field of study of coastal morphology, including the relevant physical nearshore processes involved. Also, the relevance of probabilistic modelling in coastal zone management is highlighted. After, an introduction is given to the world of coastal modelling, along with a discussion of several interesting models which have been used in relevant previous studies.

2.1. Long-term, probabilistic coastal zone management

As described in Section 1.1, population and developments in coastal zones are actively growing, while climate change and human-induced threats for these attractive but vulnerable areas are increasingly present. This leads to an urgent need for sound, integrated coastal zone management (Ranasinghe, 2016; Waterman, 2010). The consequences of coastal flooding and erosion are enormous, so accurate estimations of coastal recession probabilities are crucial.

As coastal protection approaches and structures need to be designed for long (engineering) timescales of decades to centuries, large uncertainties have to be dealt with regarding future wave climates, storm events and SLR. These uncertainties must be integrated in coastal zone management frameworks by implementing uncertainties in wave climate and stochastic forcing in coastal modelling (Callaghan et al., 2008; Ranasinghe, 2020). This induced a movement of coastal zone management from deterministic towards risk-based, probabilistic approaches, which has led to the development of frameworks that yield probabilistic estimates of coastal recession - such as the PCR model (Ranasinghe et al., 2012).

In this study, it is focused on a probabilistic approach for modelling long-term coastline development. A probabilistic framework can account for (uncertainties in) temporal and spatial variability in the relevant parameters, such as the wave climate, and it can include uncertainty ranges in the derived projections of, e.g., coastline change. Statistical methods can be used to include joint probabilities and/or dependencies between variates. In coastal modelling, for instance, this enables the simulation and extrapolation of extreme wave events instead of only using a benchmark event, i.e. the largest measured historical storm event. Also, a probabilistic approach can be used to design for specific safety standards with corresponding failure probabilities.

2.2. Coastal morphology

2.2.1. Coastal zone

The study to all the processes involved in investigating and modelling coastline changes can be described by the term coastal morphology (TU Delft, n.d.), covering all sources of coastal energy, coastal hydrodynamics, coastal sediment transport and coastal morphodynamics. In short: all natural and human-induced processes ongoing in the coastal zone. In order to properly study those processes, it is thus important to agree on a clear definition of the coastal zone. According to Hinrichsen (1998, as cited in Winter, 2011), it is the part of the land most affected by its proximity to the sea and the part of the ocean most affected by its proximity to the land. More specifically, the landward limit extends as far as the influence of the tides and storm waves reaches (Bosboom & Stive, 2021). The seaward limit can be seen as the external limit of oscillatory waves, where the interaction between waves and sediments begins (Stanica & Ungureanu, 2010). Of course, the depth of such a limit depends on changing wave characteristics and catastrophic events such as tsunamis or extreme storms.

Depth of closure
This resulted in the definition of the so-called depth of closure (Hallermeier, 1978): the depth, empirically determined, beyond which repeated field observations of the bed height over a certain period of time (months to years) show no significant changes. See Figure 2.1. Landward of the depth limit d_i, the coastal profile is dynamic, but the bed dynamics occur mostly at depths smaller than depth limit d_l. Figure 2.1 also shows the inactive, offshore coastal zone and the active nearshore zone called shoreface. The shoreface can be divided in the shoal zone (where wave heights are increasing) and the highly dynamic surf zone/littoral zone (where waves are breaking).

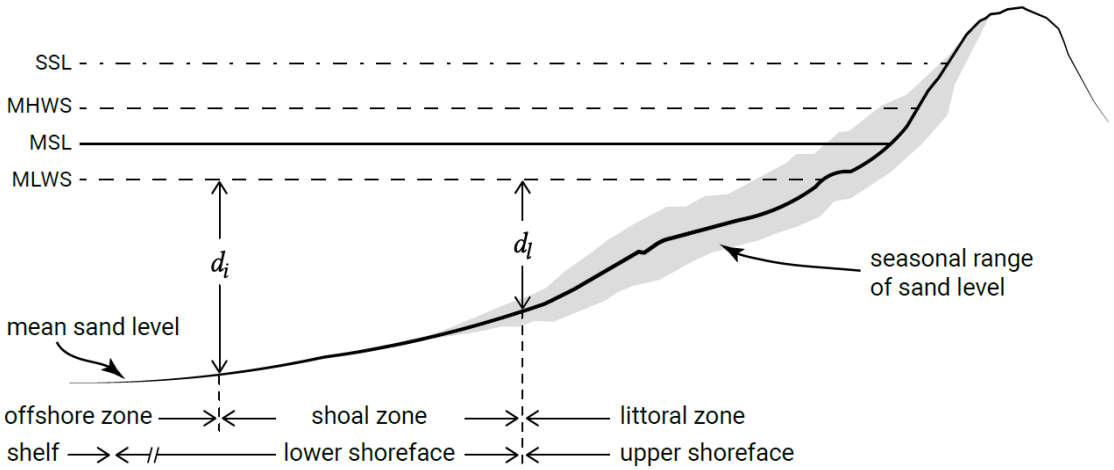

Figure 2.1: Cross-sectional view of the coastal zone (Bosboom & Stive, 2021).

Temporal scale
It must be noted that the described coastal zone limits also depend on the timescale of interest. The definitions mentioned above are based on a timescale of years to a hundred years, which is relevant for (coastal) engineering purposes (Bosboom & Stive, 2021). A further description on studying different coastal features corresponding to different timescales will be described in Sections 2.2.4 and 2.4, including the relation to coastal modelling.

2.2.2. Hydrodynamics

The described coastal zone is a highly dynamic and energetic environment. The relevant forcing processes can be defined by the term coastal hydrodynamics. In general, hydrodynamics is the study of fluids in motion. Coastal hydrodynamics cover waves, tides, storm surges, currents and other meteorological phenomena that reach the coastal zone. Those processes influence the physical shape and structure, i.e. the morphology, of a coastal system (Bosboom & Stive, 2021). In addition, also terrestrial

forces (e.g. river outflow) and atmospheric forces (coastal winds, local climate and weather conditions) have significant impact on coastal morphology. Further elaboration on all nearshore processes inducing coastline changes is given in Section 2.3.

2.2.3. Morphodynamics

Generally, morphodynamics can be defined as the mutual adjustment of fluid dynamics and topography involving sediment transport (Wright & Thom, 1977, as cited in Winter, 2011). It is the interplay between hydrodynamics (fluid motions, as described in Section 2.2.2) and sediment dynamics (erosion, deposition, transport and resulting morphological changes). The main processes are often schematised as a looped series of fluid motion, sediment transport and morphological change (Figure 2.2). It is noted that in reality this is not a closed loop, as natural systems are continuously exposed to unsteady forcing.

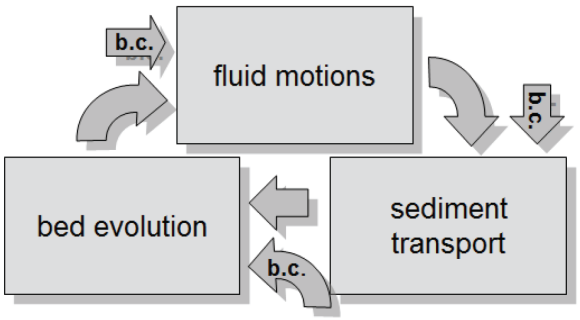

Figure 2.2: Schematic loop of coastal morphodynamics under the influence of boundary conditions (Winter, 2011).

Coupled with coastal engineering specifically, coastal morphodynamics is defined as the mutual adjustment of morphology and hydrodynamic processes involving sediment transport (Bosboom & Stive, 2021). Changes in the morphology of coastal systems depend on spatial and temporal fluctuations in sediment transport rates. A sediment surplus or deficit in a certain area results in morphological changes, leading to changes in the depth-dependent waves and tides, consequently leading to changes in sediment transport rates, which again induces morphological changes, and so on. Summarized, a feedback named morphodynamics exists between hydrodynamic processes and morphology, which is provided by sediment transport. Bosboom and Stive (2021) describe this dependency with a continuity equation or mass balance:

$$\frac{\partial z_b}{\partial t} + \frac{\partial S_x}{\partial x} + \frac{\partial S_y}{\partial y} = V \tag{2.1}$$

in which:

$z_b(x, y, t)$	bed level above a certain horizontal datum [m]
$S_x(x, y, t)$, $S_y(x, y, t)$	sediment transport rates per m width of flow [$m^3/m/s$]
$V(x, y, t)$	sink or source term per unit area [$m^3/m^2/s$]

2.2.4. Temporal and spatial scales

Coastal morphodynamics involve a wide range of different temporal and spatial scales. Spatial scales refer to the dimensions (e.g. in metres) of particular morphological coastal features. The temporal scale is the period of time (e.g. in years) required for characteristic morphological developments. In other words, the total duration needed for a morphological system to reach a new equilibrium situation after disturbance by nature or by humans (Bosboom & Stive, 2021). Based on observations, it is stated that morphological timescales are directly coupled to the spatial scales of the morphological units, as seen in Figure 2.3.

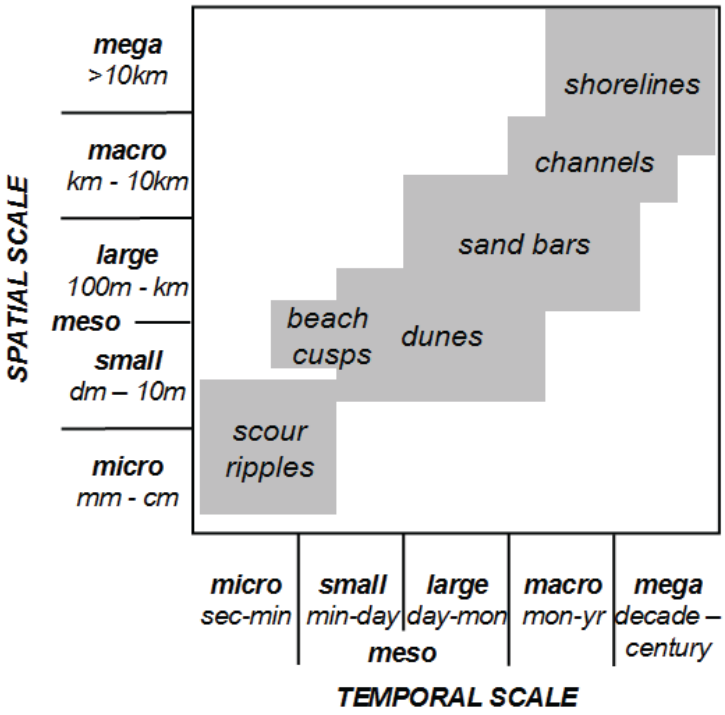

Figure 2.3: Connection of temporal and spatial scales with typical coastal morphological features (Winter, 2011).

As also illustrated in Figure 2.3, coastal systems range from the microscopic interaction of turbulent fluid motions with single particles, to meso-scale dynamics of bed forms, to macro-scale seasonal adaptations of coastal profiles or tidal channels, to the mega-scale evolution of shorelines and shelf systems over decades to centuries (Winter, 2011). As mentioned in Section 2.2.1, engineering timescales range from years to decades, the timescale on which the net effects of not only natural coastal behaviour, but also of human interventions are visible. Long-term oceanic changes and coastal evolution on larger timescales than indicated in Figure 2.3 can be considered as a given for engineering purposes, i.e. the boundary conditions for the studied processes.

2.3. Physical processes leading to coastline changes

Changes in coastline position are a result of (changes in) physical nearshore processes, both natural and human-induced. Natural causes are for instance increased intensity and/or frequency of storm surges and long-term sea level rise, both induced by climate change as described in Section 1.1. Examples due to human interventions are changes in wave impact on coastlines or in sediment supply, which can occur after construction of a coastal breakwater, a dam in a river or after a beach nourishment.

Structural erosion
The unwanted effect of those (changes in) nearshore processes is coastal erosion. Coastal erosion can be defined as the encroachment of land by the sea (Salman et al., 2004). Episodic erosion can happen due to severe winds or waves, after which the coastline recovers to its equilibrium situation. The main concern is the case in which the coastline does not return to its original position: structural erosion. Structural erosion describes the case of a long-term erosional trend. To obtain insight in structural erosion of a coastline of interest, the episodic impacts of storm events and local sediment dynamics are eliminated by averaging the coastline changes over a sufficiently long period of time. Moreover, seasonal variability, where a cross-shore profile responds differently to summer and winter conditions, is not classified as structural erosion.

Relevant processes
Nearshore processes can be divided in cross-shore and longshore processes, occurring perpendicular and parallel to the coastline, respectively. See Figure 2.4. Cross-shore and longshore transport processes occur on both short-term (e.g. seasonal to multi-annual) and long-term (e.g. decadal to centennial) timescales. The following sections will elaborate on the relevant natural and human-induced processes in the coastal zone and the different effects of those processes.

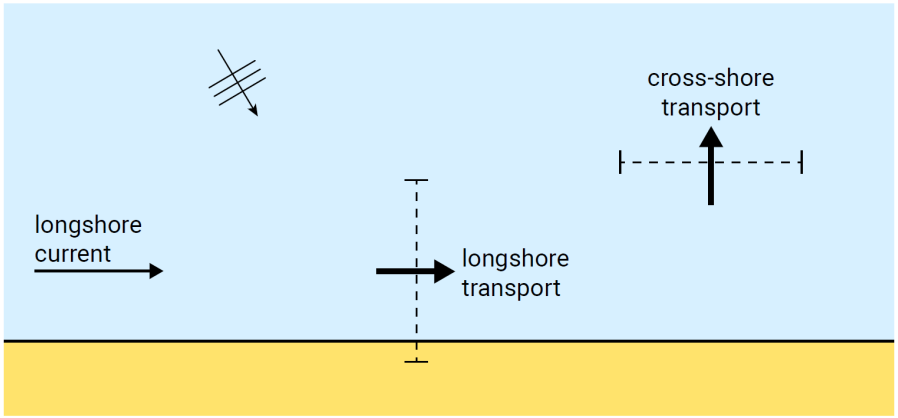

Figure 2.4: Distinction between the directions of cross-shore and longshore transport (Bosboom & Stive, 2021).

2.3.1. Cross-shore processes

Sea level rise
The first described process responsible for structural cross-shore erosion is relative sea level rise (RSLR), i.e. the total vertical land movement as a result of SLR and land subsidence. SLR is caused by three major factors: sea water thermal expansion due to global warming, melting of glaciers and ice caps, and loss of ice mass from Greenland and Antarctica (Church et al., 2013; Wong et al., 2014). Even though no sediment is lost from the cross-shore profile, the profile adjusts to an increased mean sea level (MSL), hence the shoreline moves backwards (Bruun, 1962). This shoreline retreat is depicted in Figure 2.12 in Section 2.4.4, in which the process and the description by Bruun are further explained. The timescale of this process is rather long, but when studying long-term coastal development, RSLR is certainly a cause for structural erosion.

Wave breaking
One of the general processes leading to cross-shore coastline changes is the breaking of (severe) waves. Breaking waves in the surf zone form a ball of turbulent water on the front of the wave, the 'roller', of which the size is dependent on the intensity of wave breaking (Svendsen, 1984). See Figure 2.5. On steep slopes, wave breaking is very intensive (plunging breakers), resulting in large rollers. These rollers result in an energy loss, perceived as a reduction in the wave height. This cross-shore gradient in the wave orbital motion, i.e. in the radiation stress, exerts a stress in the cross-shore direction (which generates a water level set-up at the coastline). Also, part of the generated turbulence in the wave roller is ”injected” in the water column underneath the wave, which can result in sediment stir-up - since the sediment concentration is higher in the lower half of the water column. Hence, the roller is important for sediment transport as it contains an amount of sediment mass that moves forward to the coastline with the velocity of the wave (de Schipper, 2019).

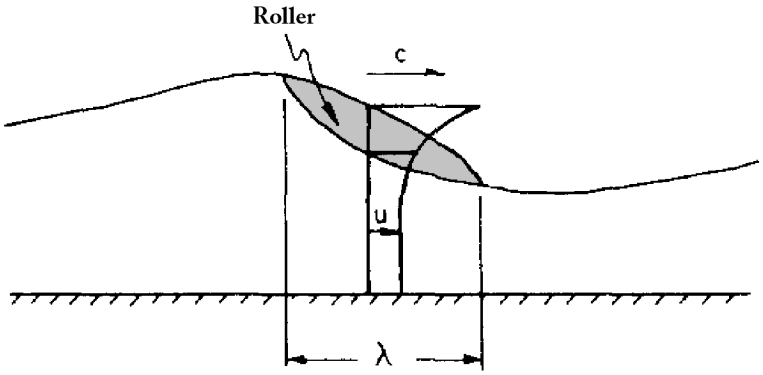

Figure 2.5: Breaking waves create a 'roller' (modified from Svendsen (1984)).

Storm erosion
The piling up of water during a storm event is called surge. Changes in water levels and wave characteristics induce changes in cross-shore sediment transport rates and thus changes in cross-shore profiles (Bosboom & Stive, 2021). During a severe storm, the waves generated in the open sea will be much larger than in a normal situation, hence the wave breaking is much more severe, leading to large changes in the cross-shore profile due to erosion of the dune and the upper part of the beach (Larson et al., 2016). The larger the berm width of the beach, the better the dune is protected against erosion by wave attack (Hanson et al., 2010).

Eroded sand is transported offshore by the strong (dominant) return current under the breaking waves (i.e. undertow, to compensate for the onshore mass flux by those breaking waves). The large-scale turbulence due to the impact of incoming breaking waves increases the sediment carrying capacity of this offshore-directed return current (Van Rijn, 2013a). The sand is settled further seaward, forming a new cross-shore profile. In addition, part of the dune face might collapse and ”slide” downwards when it has become too steep. Since the new cross-shore profile is considerably more resistant against the storm waves, erosion rates will decrease as the storm proceeds. A typical post-storm cross-shore profile is depicted in Figure 2.6. The storm impact is clearly illustrated.

As a result of RSLR, waves may break even closer to the coastline due to depth-induced breaking, which can result in even larger erosion during a storm event. Also, event grouping, in which two consecutive storm events happen in a short amount of time, causes a significant increase in storm impact.

Coastline recovery
It is noted that during calm, low energy conditions between storm events, in the absence of RSLR and LST gradients, the coastal profile recovers to the pre-storm situation due to waves, tide and wind (Figure 2.7). This is due to the fact that there is a constant amount of sediment in the active coastal zone (Bosboom & Stive, 2021). The sediment is only redistributed over the cross-sectional area, as described in the previous paragraph and Figure 2.6. After a storm, moderate ('normal') waves transport the settled sediment in onshore direction (under water), due to asymmetry in onshore and offshore

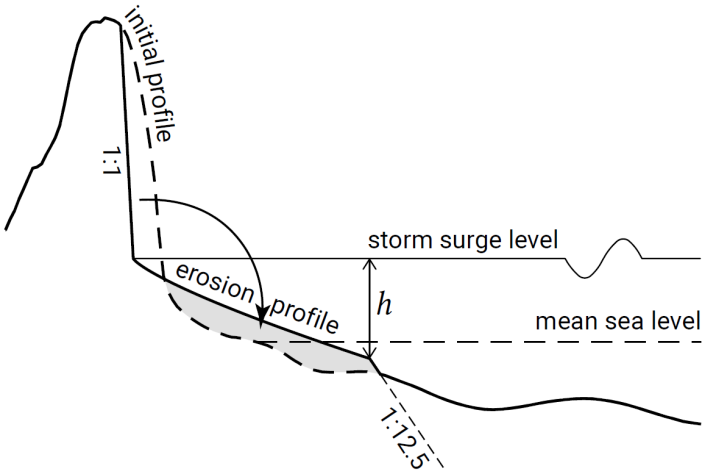

Figure 2.6: Illustration of storm impact on the cross-shore profile (Bosboom & Stive, 2021).

directed orbital velocity distributions. Moreover, tidal asymmetries and/or flood-dominant systems can cause a net import of sediment, contributing to the recovery of the coastline. In addition, the wind transports the sediment on the beach (above water) and rebuilds the dunes: aeolian sediment transport (de Vries et al., 2012). Lastly, if a gradient in LST occurs after an extreme storm event, the longshore current will also be part of the coastal recovery, transporting sediment to the eroded area (see next Section 2.3.2 on the longshore processes).

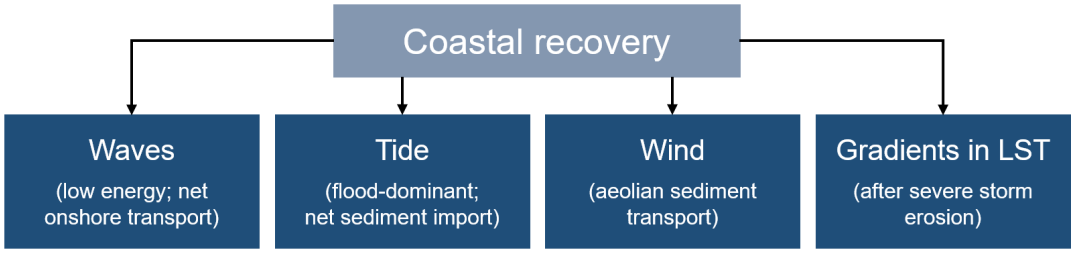

Figure 2.7: Relevant processes contributing to coastal recovery.

This is the reason that storm erosion is not necessarily seen as structural erosion (but as temporary). However, the described recovery generally happens on a much larger timescale than the storm erosion. So, rapid storm-driven erosion and slow post-storm recovery can induce chronic coastline retreat and permanent changes to the coastal system (Larson et al., 2016). That's why the previously mentioned event grouping is an important factor to take into account. Moreover, sometimes there actually is a structural loss of sediment in the active zone after a storm, as a result of the longshore current. This combined effect of cross-shore and longshore processes is further described in Section 2.3.3. It is also noted that in the case of storm-driven overwash, when sediment is transported landward over the dunes and cannot return (or if there are no dunes at all), the described coastal recovery is obviously weakened.

Other processes

Finally, other relevant processes in cross-shore coastline changes are tide-induced sediment transport (Gatto et al., 2017), aeolian transport (wind-driven sediment transport, de Vries et al. (2012)) and density-driven sediment transport (e.g. the mixing of salt and fresh water in estuaries - estuarine circulation, or the mixing of sediment-poor and -rich water in harbours (van Prooijen & van Maren, 2022)). Sometimes even temperature differences between water bodies induce sediment transport. Those processes are also only seen as drivers for temporary coastline changes and do not play a role in (long-term) structural coastal erosion.

2.3.2. Longshore processes

Gradients in longshore transport
In alongshore direction, coastline changes occur in the case of gradients in longshore sediment transport (LST). A gradient in LST means an increase or decrease in the sediment transport in the transport direction, i.e. a structural gain or loss of sediment in a coastal section. This gradient leads to structural changes in coastline position (Bosboom & Stive, 2021). See Figure 2.8. If the gradient is zero, so constant LST over the coastal section, there are no changes in morphology. This phenomenon corresponds to the described relation in Equation 2.1.

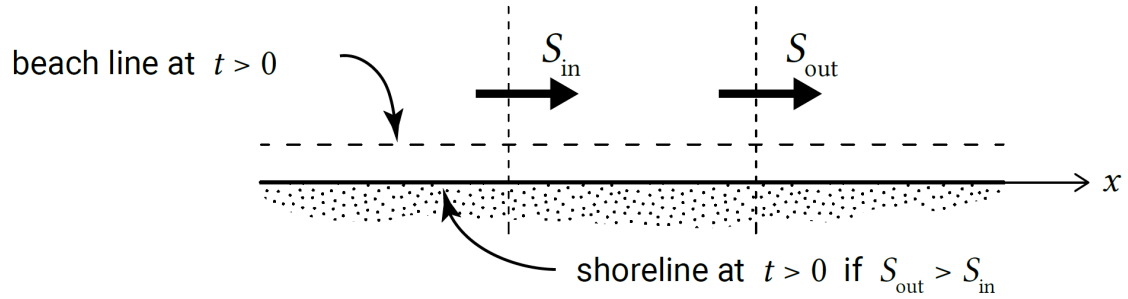

Figure 2.8: Longshore transport continuity (Bosboom & Stive, 2021).

Longshore current
The LST is driven by a longshore current, which is generated by the breaking of obliquely incident waves in the surf zone (under an angle φ_b). At the point of breaking, the momentum of the wave (i.e. the radiation stress) is transferred to the water column and hence to the mean flow. See Figure 2.9 below. The flow velocity of this wave-induced longshore current does not have a uniform cross-shore distribution, as can be seen in the figure. The depicted shape of the longshore current is common for sandy coastal zones. Regarding sediment transport, the breaking waves stir up sediment from the bed and the wave-driven longshore current consequently transports this sediment along the coast. As a result, the sediment transport also has a non-uniform cross-shore distribution, being larger for larger current velocities. Multiple formulations have been developed to describe this longshore sediment transport (e.g. Van Rijn (2013b), USACE (1984)), dependent on the bed profile, wave and current conditions, and sediment characteristics.

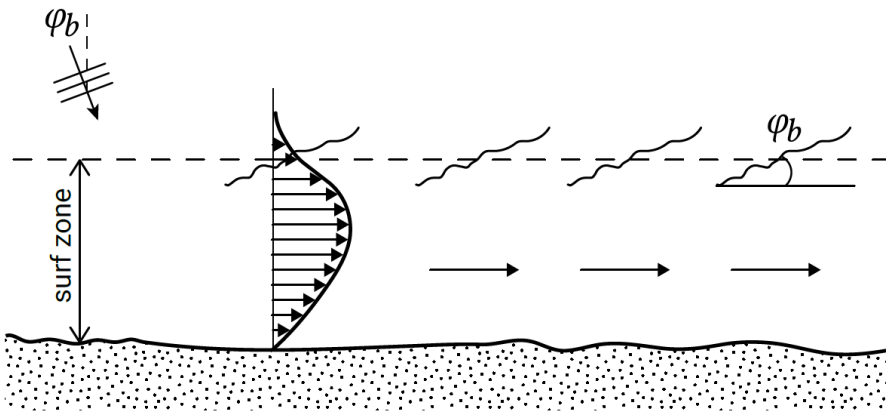

Figure 2.9: Wave-driven longshore current in the case of obliquely incident waves (Bosboom & Stive, 2021).

Single line theory
In addition, a tidal or wind-induced current can be present along a coastline, which interferes with the wave-driven longshore current. This makes the morphodynamics rather complicated, and as such, most coastline models are based on wave-driven longshore transport only. In that case, the so-called single line theory is applicable (Pelnard-Considère, 1956, as cited in (Hallin, 2019)), in which is assumed that the shape of the cross-shore profile does not change (Bosboom & Stive, 2021). Multiple coastline models work with this assumption, such as the PCR and ShorelineS model which will be described in Section 2.4. Coastline changes are modelled as such that the entire cross-shore profile moves seaward or landward, see Figure 2.10. The depth of the active profile (Section 2.2.1) is an important point of attention here.

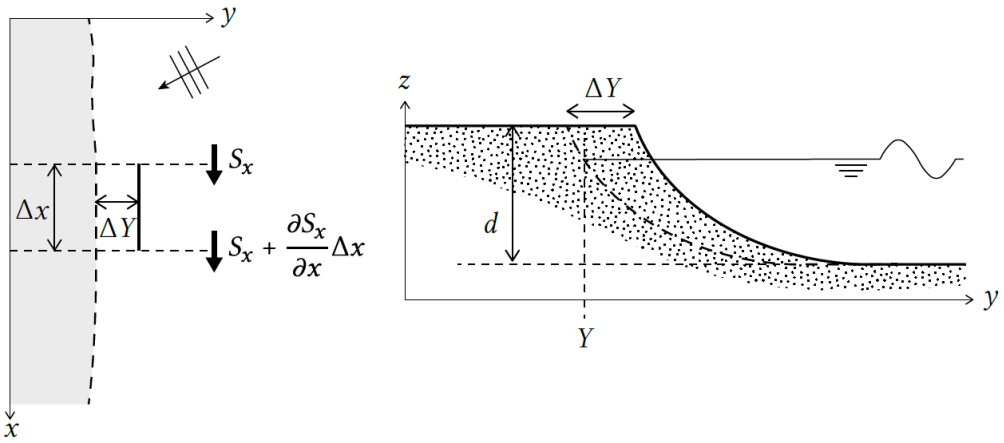

Figure 2.10: Longshore transport and coastal change in a coastline model (Bosboom & Stive, 2021).

Human interventions
Engineering activities are often set up from a local point of view without actively considering their potential regional impact. If on a uniform coastline, as assumed so far, a breakwater, groyne or harbour is constructed, the longshore current and thus the LST are abruptly interrupted. This leads to a large gradient in sediment transport and consequently to large problematic coastal erosion behind the structure. It is noted that engineering problems are often related to longshore transport gradients, because changes in LST induce large disruption in the coastal zone and because they are most often induced by humans themselves. Major human activities leading to coastline changes are summarized below. Those interventions can have impact on extremely large reaches of coastlines and may even cross country borders, making it very difficult to achieve uniform coastal zone management strategies.

- Construction of coastal defence structures;
- Harbour construction;
- Navigation improvement, dredging;
- Mining of sand and gas;
- Land reclamation;
- River regulation works (e.g. dams);
- Vegetation clearing;
- Water extraction;
- Works in neighbouring river catchment areas reducing sediment supply to the coast.

Tidal inlets
Highly dynamic coastal areas such as tidal inlets have complicated sediment transport patterns due to (wave-driven or tidal) longshore currents, in which the inlet can act as a sink or source for LST, influencing the development of adjacent coastlines. Also, tidal bars and spits can be formed which may shield other parts of the coastline from waves and currents. In coastline models such as ShorelineS (Section 3.3), tidal inlets can be implemented as a source or sink of sediment.

2.3.3. Combination cross-shore and longshore processes

In Sections 2.3.1 and 2.3.2 it is described that RSLR and gradients in LST are the processes that cause structural erosion, and that storm events do not. As described in Paragraph 2.3.1, storms only result in temporary erosion since no sediment is lost in the active zone, and 'normal' natural conditions in between storm events induce a recovery of the coastal profile.

However, when a gradient in LST is present in a coastal section, the eroded sediment from the upper part of the cross-section (i.e. the dune) is transported out of the coastal section in alongshore direction (Bosboom & Stive, 2021). Hence, after a storm event, the eroded material will not return to its original position, despite the normal, calm wave conditions and the accreting wind effects. This process results in structural erosion of the dunes and maybe even the hinterland. To summarize, it is the cross-shore storm erosion which is responsible for the fact that the upper part of the profile is eroded and deposited on the beach and foreshore, but the final structural erosion is mainly caused by the longshore current transporting the eroded material away. So, in this case, the cross-shore storm erosion actually plays a significant role in structural (dune) erosion.

2.3.4. Interaction cross-shore and longshore processes

Next to the described phenomenon in the previous section, it is an important observation that in reality, cross-shore and longshore processes interact. This means they often have a combined influence on coastal development. It is especially the case for coastlines dominated by longshore currents and wave-driven LST, so-called drift-aligned coastal areas (Hughes, 2016). Here, also cross-shore impacts of storm events and SLR are still present and influence the shoreline evolution (Sections 2.3.1 and 2.3.3). Hence, processes of both directions have to be taken into account in order to obtain accurate predictions. This can be done within a single model, or separate model outputs can be combined afterwards.

Below, the relevant effects of the interaction of cross-shore and longshore processes in the coastal zone are described, which need to be considered when modelling the (long-term) evolution of coastlines. In Chapter 4 it is defined how the discussed interaction effects are implemented in this MSc research.

Cross-shore effects on longshore processes
Episodic erosion of a coastline, e.g. storm-induced, can cause a change in coastline orientation and in the cross-shore coastal profile. Such a change influences the sediment transport rates in the alongshore direction since this transport is dependent on the angle of the incoming waves (via the S-φ curve (Bosboom & Stive, 2021)). In other words, cross-shore storm erosion might change or induce gradients in LST, which are responsible for the long-term evolution of the coastline. For regular coastlines without complex plan-view shapes such as spits, this change in orientation can be neglected in modelling cross-shore and longshore interactions (Vitousek et al., 2017). Regarding this MSc research, this might be an important assumption to incorporate in the combination of the PCR and ShorelineS models.

Schepper et al. (2021) studied a cross-shore shoreline model (ShoreFor) including multiple temporal scales, in order to investigate the separate effects of extreme forcing events and long-term shoreline trends. Often, only particular spatial-temporal scales are taken into account, in which the shoreline is forced by waves and it responds on corresponding timescales (e.g. a beach erodes and recovers after an individual storm). However, extreme forcing events can have a considerable and, more importantly, persistent shoreline impact. Schepper et al. (2021) found at a certain study site (Narrabeen-Collaroy Beach, Australia) that short-term high-intensity forcing events have a large and persistent impact on the quasi-seasonal shoreline evolution. This indicates that long-term coastline change due to LST gradients can be influenced by short-term storm events.

Longshore effects on cross-shore processes
Also gradients in LST can cause alterations in shoreline orientation, for instance by accretion or erosion near a coastal structure. This change in coastline orientation can affect the amount of storm-induced (cross-shore) erosion since this is dependent on the angle of the incoming waves, e.g. reduced wave heights due to refraction effects. This interaction effect is difficult to incorporate in coastline modelling, but it can be highly important at certain sites, for example at the lee side of a breakwater. At such a location, additional processes such as sheltering/shadowing of waves are relevant, having a large impact on the amount of wave-induced coastline erosion and its recovery.

Schepper et al. (2021) also modelled the effect of long-term shoreline variations on extreme event impacts. The response of a coastline to a high-intensity forcing event of a small temporal scale (e.g. a storm) depends on whether that coastline is eroded or accreted on a larger temporal scale (e.g. due to a seasonal variation), i.e. on the initial state of the beach. This can be explained by the sediment transport efficiency, which is higher for accreted beaches (narrow surf zone, reflective beach), resulting in a faster beach response. The reason for this is that for accreted beaches and narrow surf zones, more offshore sand supply (e.g. from sand bar(s)) is migrated closer to the shoreline. This process works the other way around for eroded beaches and wide surf zones (i.e. a dissipative beach). The surf zone width is determined by antecedent forcing conditions.

In Schepper et al. (2021), it was seen at all studied sites that short-term forcing events are affected by longer-term shoreline variations: overall accreted beaches showed faster responses to storms/monsoons due to sand supply being close to the shoreline, resulting in high sediment transport efficiencies.

2.4. Coastal modelling

According to Winter (2011), modelling can be described as the process of conception and formulation, coding and compiling, verification, calibration, validation and application. Relevant physical processes have to be known, formulated as (mathematical) equations, discretized (translated to a form that can be calculated numerically), and implemented (coded and compiled) into computational modules.

Regarding coastal zone management, the most advanced way to obtain coastal retreat predictions is by the use of numerical models. Numerical models are capable of estimating a system's response to certain forcing, based on (simplified) descriptions of fundamental system physics (Ranasinghe, 2020). Examples of such forcing in coastal systems are wind, waves and currents, occurring in cross-shore direction (e.g. storm events) and along the coastline (e.g. longshore currents).

2.4.1. Types of models

Models are representations of system behaviour and can be simplifications or interpretations of data (conceptual models), physical models or models based on mathematical formulations. Mathematical models can be analytical (based on representative equations and parameters), (semi-)empirical (relations based on measured data, with or without assumptions) or process-oriented (based on the theoretical understanding of the underlying physical processes).

Process-based models can vary a lot in complexity, which is mainly dependent on the spatial dimension of the model, e.g. one-dimensional (1D), two-dimensional depth-averaged (2DH) or three-dimensional (3D). The more detailed and complex the model, the higher the required grid resolution and the smaller the required simulation time-steps. This results in high computational demands. Therefore, simplified process-based models are upcoming, in which specific parts of the input (e.g. the wave climate data) are reduced in complexity. This is further described below in Section 2.4.2.

Regarding coastal morphodynamics modelling, the hydrodynamics, the sediment transport and bed evolution models are coupled to simulate the physical system. A distinction can be made between a *coastal profile* model, describing the evolution of cross-shore profiles over time, and a *coastline* model, describing the long-term evolution of a coastline with a constant cross-shore profile. The latter is applicable in this MSc research and will be further discussed in Chapter 3.

2.4.2. Reduced complexity modelling

Computational time vs. model resolution
This research focuses on the balance between reliable, accurate output of coastal models and their computational expense. A choice has to be made on the balance between grid cells sufficiently small to capture coastline development at the required spatial and temporal scale, and sufficiently large to reduce computation time as much as possible. The optimal balance is clearly dependent on the application of the model: the larger the coastal features and the coastal area of interest, the less detailed morphodynamic models are necessary - and possible (Winter, 2011). It must be noted that within numerical models, the grid spacing and time step are dependent on each other via principles such as the Courant number. That is, for small spatial steps, the time step can not be too large, otherwise it would not detect every grid cell (i.e. it would skip certain cells). In coastal morphology, complex, two-dimensional horizontal (2DH) process-based models have been studied (McCall et al., 2010; Roelvink et al., 2009; van Dongeren et al., 2018), but they come with large computational expense due to the very dense grids and hence the small time steps. Moreover, studies of long-term coastal development on large spatial scales require less detailed predictions (as local short-term morphological variations are negligible), so less complex models will suffice.

Simplifications
Ranasinghe (2020) describes the principle of reduced complexity modelling in which simplified descriptions of fundamental system physics are used, e.g. a simplified wave climate or a constant beach profile. These simplifications enable multiple simulations (thousands of simulations in minutes) and thus rapid probabilistic estimates of the system's (long-term) response, which are highly desirable for risk-informed

coastal zone management approaches as described in Section 2.1. A lot of these computationally efficient process-based models have been proven reliable, although mainly for larger timescales of years to decades. Coastline models that fit in this reduced complexity description are the models used in this research, PCR and ShorelineS, which will be thoroughly introduced in sections 3.2 and 3.3.

2.4.3. Uncertainties in coastal modelling

Types of uncertainty
Predictions of morphological coastline development obtained by numerical modelling contain many uncertainties, which can be divided in two types: intrinsic and epistemic. Intrinsic uncertainty arises from natural processes and forcing (i.e. wave climate variability), both in space and time, whereas epistemic uncertainty is related to knowledge, models and methods (Kroon et al., 2020, see Figure 2.11). Model uncertainty can be described by model inadequacy (if processes such as coastal recovery are simplified or missing), parameter uncertainty (in case of limited knowledge on parameters like grain size or settling velocity) and numerical limitations (e.g. due to model resolution). Another form of epistemic uncertainty is observation uncertainty, for instance induced by inaccuracies in used instruments.

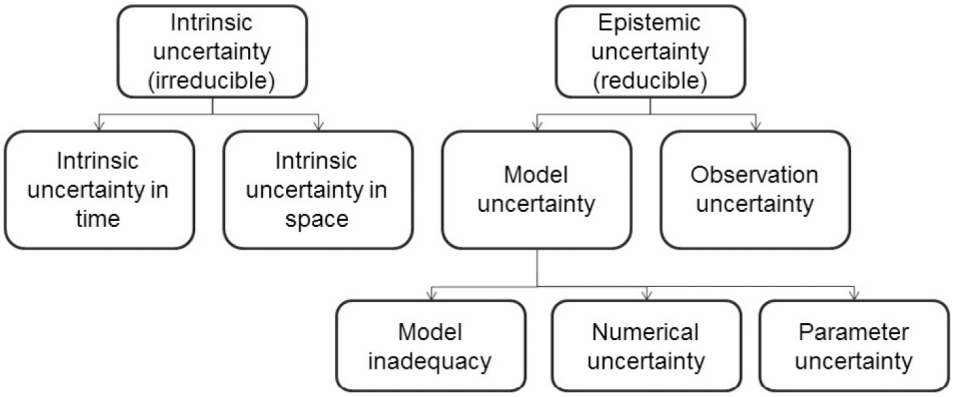

Figure 2.11: Types of uncertainty in morphological modelling (Kroon et al., 2020).

Model uncertainty over intrinsic uncertainty
In probabilistic frameworks, it is dealt with intrinsic uncertainty (in the form of variability in wave climate), but model uncertainty is often not covered, mainly in order to reduce computational costs. Kroon et al. (2020) studied the relative importance of epistemic versus intrinsic uncertainty and showed that model uncertainty becomes dominant over wave climate variability for medium-term timescales (years). Namely, for a long simulation period, years with extreme wave conditions are compensated by calmer years, while on the other hand, model uncertainty is a cumulative effect which increases with each time step. It is stated that although Kroon et al. (2020) studied a large scale nourishment in particular, the results are expected to be applicable to any sandy solution in the coastal zone, dependent on model sophistication and variation of local wave conditions. It was concluded that the uncertainty in model settings may be the principal source of uncertainty, especially when predicting large scale coastal development with simplified models on a multi-year timescale.

Link with ShorelineS
In the study of this report it is focused on a probabilistic framework, often using less complex models (to obtain quick insights in coastal development), thus increasing the relevance of model uncertainty assessment within the framework. The described results can be an important link for the ShorelineS model. Due to the large timescale of the model, a reduced wave climate can be used as realistic input, reducing the computational expense of the simulations significantly.

2.4.4. Modelling cross-shore processes

Over the last decades, multiple numerical models have been developed, ranging from simple functions to highly advanced models. To indicate the wide variety in complexity and performance of such models, a few will be discussed in the next sections. A distinction is made between cross-shore models, longshore models and models which aim to simulate the interaction between cross-shore and longshore processes. First, several cross-shore models are presented:

Bruun rule
The Bruun rule (Bruun, 1962) is a simple two-dimensional mass conservation principle which estimates the landward and upward displacement of the cross-shore profile in response to a certain SLR, as follows (see also Figure 2.12):

$$R = \frac{L \cdot SLR}{B + h} \tag{2.2}$$

in which:

- h maximum depth until which there is nearshore-offshore material exchange
- L horizontal distance from the shoreline to depth h
- B berm or dune elevation estimate for the eroded area

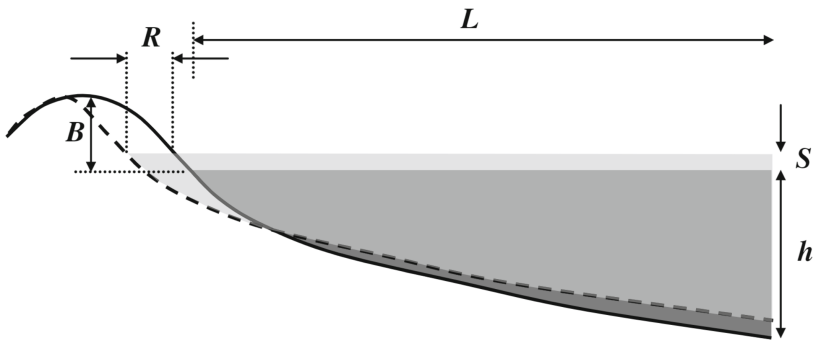

Figure 2.12: Schematic view of the Bruun rule application (Ranasinghe et al., 2012).

The Bruun rule has limited applicability as a result of many assumptions: it has major uncertainty in the definition of the slope of the active profile, it assumes cross-shore sediment transport only, is only applicable for an equilibrium profile, assumes uniform sediment size along profile, has an extremely wide variability if SLR uncertainties are taken into account, and even more (Ranasinghe & Stive, 2009).

Nevertheless, the Bruun rule has been used ever since its development and is still used today, as a result of its simplicity and the absence of quick and efficient alternatives. However, nowadays, the concerns regarding accelerated SLR and the increase in coastal zone development require highly accurate and site specific predictions of coastal recession, which the broadly indicative and uncertain estimates of the Bruun rule can not deliver. The need for small-scale, process-based numerical models in coastal planning and management resulted in the development of the PCR model (Ranasinghe et al., 2012).

XBeach
A process-based nearshore numerical model, XBeach, is used to simulate the natural coastal response during time-varying storm and hurricane conditions, including dune erosion, overwash and breaching (Roelvink et al., 2009). It is a highly advanced model which is able to solve cross-shore and longshore hydrodynamics and morphodynamics. The model is validated with a series of analytical, laboratory and field test cases. Due to the fact that the model is time-dependent and two-dimensional depth-averaged (2DH), the modelling time scale is limited to typical storm event durations (i.e. hours to days). Therefore, it is not (yet) suitable for studying long-term coastline evolution.

SBEACH
SBEACH (Larson & Kraus, 1989) is a two-dimensional numerical model for simulating storm-induced beach change and post-storm recovery, developed by the U.S. Army Corps of Engineers. It calculates dune and beach erosion produced by storm waves and water levels. Wave height and set-up across the profile are calculated to obtain the net cross-shore sand transport rate. Gradients in longshore transport are not considered. The model was initially developed using data from large wave tanks and afterwards verified based on field measurements.

DUROS+
DUROS+ is a deterministic, cross-shore dune erosion model which estimates the post-storm equilibrium profile (Ruessink et al., 2012). The actual erosion profile and the dune retreat are computed based on the shape of an equilibrium profile and a cross-shore balance between erosion and sedimentation. The model is thoroughly investigated with physical laboratory experiments.

CS-model
The CS-model (Larson et al., 2004) is an analytical wave impact dune erosion model, based on the assumption that there is a linear relationship between the wave impact and the weight of sand eroded from the dune. The model is based on a set of semi-empirical, physics-based sand transport equations, which require site-specific data for calibration and validation in order to achieve a good model performance. It simulates cross-shore sediment transport and long-term beach and dune evolution in individual transects. Included processes are dune erosion and overwash, dune build-up by aeolian transport, beach-bar exchange, and sea level rise.

Dunerule
The Dunerule model is an empirical function which was proposed by Van Rijn (2013a) and originates from the cross-shore model CROSMOR, which is based on a 'wave by wave' modelling approach solving the wave energy equation for each individual wave. Dunerule was developed by studying the effects of various key parameters on the computed dune erosion for a reference case that is defined by Vellinga (1982, as cited in Li (2014)). Li calibrated and validated the model for a specific coastal profile along the Holland coast with the use of XBeach. To achieve this, Li used 298 storm events with different combinations of wave conditions to estimate the DUNERULE model coefficients.

PCR model
The PCR model (Ranasinghe et al., 2012) is a physics-based model which can provide probabilistic estimates of coastal recession based on governing physical processes in cross-shore direction, i.e. storm erosion, recovery and long-term sea level rise (SLR). The PCR model is thoroughly elaborated in Chapter 3.

2.4.5. Modelling longshore processes

Long-term coastal evolution due to gradients in longshore transport is mostly modelled with coastline models based on the single line theory (see Section 2.3.2):

UnibestCL+
The Unibest-CL+ model (Tonnon et al., 2018) is a coastline model which consists of the Unibest-LT module and the Unibest-CL module. The LT module computes the longshore sediment transport (LST) based on tide- and wave-induced longshore currents, from which the CL module simulates the development of the coastline under the influence of the computed gradients in LST. The calculated transport rates are coupled to the angle of the coastline orientation, which enables the model to efficiently derive the transport rates at every grid cell. The model includes the principal processes of wave energy changes due to bottom refraction, shoaling, dissipation by wave breaking and bottom friction.

GENESIS
GENESIS (Hanson & Kraus, 1989) is designed to simulate long-term shoreline change based on spatial and temporal changes in longshore sand transport. It can cover spatial and temporal scales in the ranges of 1 to 100 km and 1 to 100 months, respectively. Moreover, it can account for (combinations

of) coastal structures, influencing the LST. The GENESIS model is originally intended for coastal engineering projects specifically. It is said that it performs sufficiently efficient and accurate for projects with limited data availability.

LITPACK
DHI Group developed the LITPACK model to simulate the evolution of coastlines affected by structures, sediment sources and climate changes (DHI Group, n.d.). It was developed to support the design and evaluation of coastal management strategies. The model covers sediment transport across a profile as well as the integrated littoral drift rates. It also accounts for variations in the hydrodynamics by accurately calculating wave propagation towards the coast and related wave-driven currents as well as longshore transport. Moreover, it is also possible to analyse the effects of construction using several different profiles in the longshore direction and various coastal structures.

ShorelineS
The ShorelineS model (Roelvink et al., 2020) is a free-form coastline model which can describe long-term, longshore coastal transformations based on longshore transport gradients, driven by a CERC-like sediment transport formula. As for the PCR model, also the ShorelineS model is further explained in Chapter 3.

2.4.6. Modelling interaction processes

Currently, in engineering practice, cross-shore and longshore processes are mostly modelled in isolation (Robinet et al., 2018). Often, (variability of) the longshore component is neglected as cross-shore storm erosion is assumed to be governing for coastline changes. To validate newly developed models, sometimes even specific coastal regions and/or sections with limited to no (effect of) LST are chosen on purpose - in order to justify the assumption (Ranasinghe et al., 2012). Such coastal areas are defined as swash-aligned beaches, where the wave crests arrive parallel to the shoreline due to a specific offshore wave direction, or caused by refraction and/or diffraction in embayed (pocket) beaches (Hughes, 2016). Moreover, even for (drift-aligned) coastlines where LST is clearly present, it is often assumed negligible in engineering research. However, this assumption is usually only applicable during the (short) periods with stormy conditions, i.e. when the cross-shore processes are actually governing. Therefore, for long-term modelling of coastline evolution, it is of high importance to take into account both cross-shore and longshore processes, including their interaction.

The following section will highlight several different models developed to predict shoreline response to both cross-shore and longshore sediment transport processes on different timescales. Each model shows the importance of combining and/or coupling cross-shore and longshore sediment transport in predicting coastal development in areas where gradients in LST are present. That is, for each model, using only cross-shore or longshore transport resulted in incorrect or incomplete predictions of shoreline development compared to observed and/or measured data.

Advanced models
Scientists and researchers have developed multiple highly advanced models in which longshore and cross-shore processes are coupled. For instance, complex process-based 2DH models such as XBeach (Roelvink et al., 2009) can solve coupled equations for cross-shore and longshore hydro- and morphodynamics on the timescale of wave groups, involving variation in hydrodynamic forcing and morphological development in the longshore dimension. An important implication, however, is the large computational expense as a result of the high level of complexity (as introduced in Section 2.4.2). This is not in line with a probabilistic, long-term focus in which rapid estimates are desired. As for XBeach, the additional problem is that it can not be used to predict shoreline evolution on larger timescales (i.e. years, decades) at all.

XBeach-G and LST parameterization
The first described method is a coupling of XBeach-G (for gravel beaches) and a parametric formulation of the LST by Bergillos et al. (2017). The main objective of the research was to study the profile response to storm waves from varying directions, considering different cross-shore distributions of LST by means of a parameterization based on the LST equation of Van Rijn (2014, as cited in Bergillos

et al., 2017). After each storm event, the shape of the final beach profile modelled with XBeach-G was modified considering the LST volume gradients and the different cross-shore distributions of LST, prior to modelling the next profile response to the next storm event. The study focused on the short-term response of the morphology of the cross-shore beach profile of gravel beaches. This completely does not match the objective of this MSc Thesis research, but it proved the necessity of combining cross-shore and longshore processes to model coastline development in coastal areas where LST gradients play a role.

CoSMoS-COAST model
Another model integrating longshore and cross-shore processes, is able to predict long-term shoreline response: the Coastal One-line Assimilated Simulation Tool (CoSMoS-COAST) by Vitousek et al. (2017). The model applies a synthesis of individual process-based shoreline change models representing unique and addable components, assuming a constant cross-shore profile. The governing equation describing shoreline change is a sum of LST gradients (one-line model), cross-shore transport (shoreline model), SLR (shoreline recession model, Bruun rule) and long-term shoreline trend (unresolved processes). The mathematical formulation of the different components (in the same order as above) is given by:

$$\frac{\partial Y}{\partial t} = -\frac{1}{d}\frac{\partial Q}{\partial X} + CE^{1/2}\Delta E - \frac{c}{\tan\beta}\frac{\partial S}{\partial t} + \mathsf{v}_{\mathsf{lt}} \tag{2.3}$$

The model uses data assimilation to account for unresolved sediment transport processes such as fluvial discharge, regional sediment supply and long-term erosion. This is done by using historical shoreline positions of a 15-year hindcast period, in order to improve estimates of model parameters and thus improve confidence in the model's predictive capability.

An important limitation is that CoSMoS-COAST does not include feedback between the shoreline and wave changes, which can only be assumed if the shoreline orientation does not change significantly. Hence, no complex shoreline plan-view shapes such as sand spits, islands and headlands can be modelled. Also, due to the use of a specific cross-shore model to resolve the cross-shore transport component, the shoreline is not able to move well away from its equilibrium position. However, CoSMoS-COAST is able to perform very well along regular coasts with long-term monitoring programs.

LX-Shore model
A model which has the potential to address complex shoreline plan-view shapes, including non-erodable areas, is the LX-Shore model by Robinet et al. (2018). In this model, the coastal area is divided in a cellular grid, in which each cell is filled with a sediment fraction F ranging from 0 to 1, based on the Coastal Evolution Model (CEM) as implemented by Ashton and Murray (2006, as cited in Robinet et al., 2018). At each time step, the breaking wave parameters determine the longshore and cross-shore sediment transport modules and thus the shoreline change (via the sediment balance). For each shoreline cell, the calculated net sediment flux into or out of the cell determines a new F for this cell, following the equation:

$$F(t+\Delta t) = F(t) + \Delta F_l(t) + \Delta F_c(t) \tag{2.4}$$

in which:

t	time
Δt	simulation time step
$\Delta F_l(t)$	sediment fraction variations induced by longshore processes
$\Delta F_c(t)$	sediment fraction variations induced by cross-shore processes

Within each cell, the shoreline position and orientation are determined based on the sediment fraction of the cell and its neighbouring cells. This is followed by interpolation of all shoreline position estimates to obtain the complete shoreline. The derived shoreline position and orientation control the breaking wave parameters and sediment fluxes at each time step.

Also here, a constant cross-shore profile shape is assumed, so the LX-Shore model is not capable of modelling sites where large temporal variations of this profile shape are expected. In addition, no SLR and no sediment sources/sinks (i.e. influence of estuaries and tidal inlets) are taken into account. This also holds for the effects of overwash (which can occur in case of gentle-slope beaches or low elevation dunes). Another note is that no use is made of in-situ bathymetric data, so application of LX-Shore to real sites is not possible (yet).

Regarding a probabilistic approach, the most important advantage of the LX-Shore model (as well as for CoSMoS-COAST) is the low computation time, mainly as a result of the constant cross-shore profile simplification. This enables performing a large amount of simulations to obtain probabilistic coastline development projections, including uncertainties in the wave forcing, storm events and SLR. This is a very important element for the research of this MSc Thesis. The PCR and ShorelineS models (Sections 3.2 and 3.3) also have the potential to be used for this purpose.

GenCade model
Another model which is discussed here, is the one-line model GenCade (Hanson et al., 2010, 2011). It origins from a synthesis of GENESIS (Hanson & Kraus, 1989), a project-scale, engineering design-level model, and Cascade (Larson et al., 2003, as also cited in (Frey et al., 2012)), a regional-scale, planning-level model. The GenCade model is able to simulate long-term beach and dune change in response to cross-shore processes (i.e. dune build-up by wind and dune erosion by storms) and by gradients in longshore transport. The berm plays a key role since dune erosion by wave attack depends on the berm width, as well as the amount of sand transported to the dune by wind.

To simulate the total shoreline change, the berm translations due to cross-shore interaction between the dune and berm are linearly added to the contribution by the gradient in longshore transport rate. The governing equation for the rate of change of shoreline position is as follows:

$$\frac{\partial y}{\partial t} = -\frac{1}{D_B + D_C}\left(\frac{\partial Q}{\partial x} - q_o + q_w\right) \tag{2.5}$$

in which:

D_B	vertical distance between berm crest and MSL
D_C	depth of closure
$\frac{\partial Q}{\partial x}$	gradient in longshore transport rate
q_o	erosion rate due to wave impact
q_w	rate of onshore sand transport by wind

Hanson et al. (2010) also focused on the sensitivity of shoreline evolution to climate change induced changes in wave height. Since in this study the cross-shore interaction between the dune and berm is included, it was found that for increased wave heights (i.e. larger cross-shore transport), the system contains less sand available for transport due to larger sand losses from the dune. As a result, the location of the dune toe is more landward, reducing the wave impact on the dune for larger waves and higher water levels. This contradictory effect highlights the complexity of the dune-berm system and indicates the importance of sequencing regarding the forcing.

GenCade follows the single-line theory, i.e. the beach profile shape is constant (see Section 2.3.2 and Figure 2.10). According to this theory, it is also assumed that LST rates only arise from wave breaking and longshore currents, being proportional to the breaking wave height and direction with respect to the local shoreline orientation (Frey et al., 2012). Implementing tide- or wind-induced LST is only possible in the presence of breaking waves. Moreover, it is assumed that sand is transported alongshore between two well-defined limiting elevations on the profile, i.e. a restriction of profile movement between defined shoreward and seaward depth limits. Lastly, also the detailed structure of the nearshore circulation is ignored and a long-term trend in shoreline evolution is assumed to be present.

CS-model + longshore model

Hallin et al. (2018) and Palalane and Larson (2019) studied the long-term evolution of dunes under interacting cross-shore and longshore processes, investigating the interaction between longshore transport gradients and the beach and dune evolution on decadal timescales. It includes exchange of sediment between the beach and the dune and obtained LST gradients are added as a source or a sink in the model. Different approaches were used for computing the rate of - and thus gradients in - longshore transport, such as transport formulations from Bayram et al. (2007) or CERC (USACE, 1984), or the LST gradients were derived from JARKUS data. The semi-empirical CS-model (Larson et al., 2016), see Section 3.2.4, was used for modelling the cross-shore coastline changes.

Krijnen (2021) also used the CS-model as a cross-shore *coastal profile* model to study the coupling with LST gradients derived from an longshore *coastline* model: Unibest-CL+, by Deltares. The longshore coastline changes are multiplied with the active profile height to obtain volume changes per meter, which are then translated to the CS-model prior to modelling cross-shore volume changes. As a result of this coupling, the effects of cross-shore processes on the local and temporal LST gradients are taken into account by enabling the CS-model to give feedback to Unibest-CL+. These effects involve changes in coastline orientation as discussed in Section 2.3.4. In addition, the coupling even enables the implementation of time-varying LST gradients into the already existing CS-model. A schematic overview of the model coupling is depicted in Figure 2.13, where CL indicates the longshore Unibest-CL+ model and CS the cross-shore CS-model.

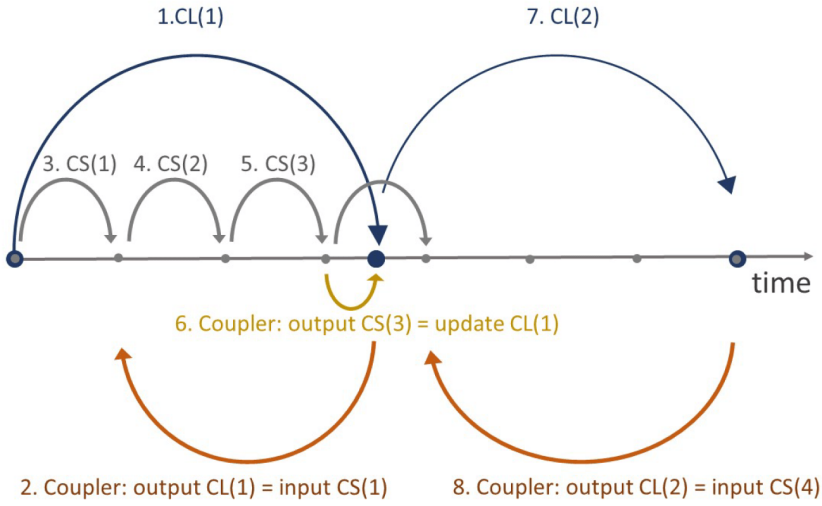

Figure 2.13: Schematic overview of the model coupling by (Krijnen, 2021).

Both studies performed satisfactory in simulating an impressive variety of relevant sediment transport processes, i.e. dune erosion and overwash, aeolian dune build-up, beach erosion and accretion due to gradients in longshore sediment transport, adaptation to sea level rise and response to nourishments. The coupled models demonstrated their potential for long-term risk assessments for flood prone areas protected by dunes, as well as for nourishment strategies.

The CS-model is ideal for long-term purposes as it uses reduced-complexity transport equations and a simplified schematization of the beach profile, but it requires a lot of site-specific data for calibration and validation in order to deliver reliable results. Also, it must be noted that the discussed researches are not fully in line with the MSc research of this report since a coastal profile model, dune-beach exchange and dune volume evolution are involved, whereas PCR and ShorelineS are one-line models assuming a constant cross-shore profile shape.

PonTos-model
In order to model long-term and large scale morphological evolution, Steetzel et al. (1998) developed the conceptual PonTos-model, originally intended for the Dutch coast. The behaviour-oriented model is based on the multi-layer concept, in which the cross-shore profile is schematized as a number of mutually coupled layers, defined between fixed profile depths (see Figure 2.14). Subsequent layers refer to layers positioned further seaward. The actual position of a layer is determined via the sediment balance of the cross-shore profile.

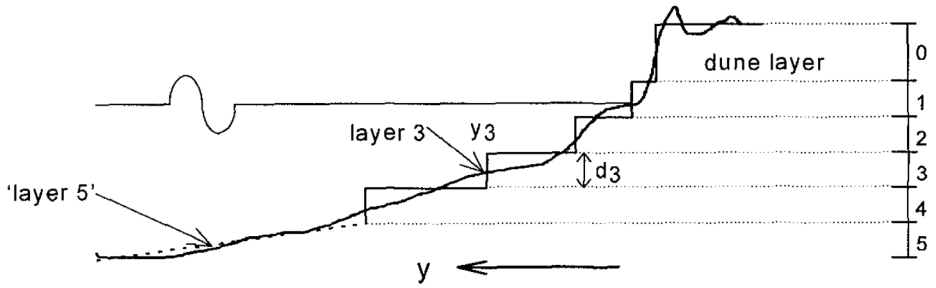

Figure 2.14: Layer schematization of the cross-shore profile in the PonTos model (Steetzel et al., 1998).

Cross-shore transport determines the interaction between the layers, based on the principle of a wave-based equilibrium profile. If the slope deviates from this equilibrium slope, cross-shore exchange of sand between the layers occurs. In longshore direction the layers respond to gradients in the longshore transport in the considered region, which depend on the orientation of a specific layer and the direction of the incoming waves. The total wave-induced longshore sediment transport is distributed over the different layers, depending on the level of the layer boundaries relative to the water level. The model can also account for tide-induced longshore transport in a specific layer, by computing the transport rate in vertical direction - i.e. between the layers.

Eventually, the yearly-averaged sediment transport patterns determine the coastal evolution. In the layer-approach, the volume in a specific computational cell or layer is represented by the specific position of the layer in cross-shore direction. A change in a cell's volume, based on cross-shore and longshore transport (and a source or sink term in the cell), yields a cross-shore shift in the position of a layer.

The longshore and cross-shore transport processes are modelled separately and are summed up in the determination of the described cell's volume change. Also, since the cross-shore transport is based on an equilibrium slope, relatively small variations in the wave climate can already lead to relatively large variations in the profile slope (for initially gentle profiles). Lastly, also the shoaling and refraction effects are not accounted for. Based on validation results, including those effects is expected to improve the model reliability (Steetzel et al., 1998).

COCOONED model
COCOONED (Antolínez et al., 2019) is a coastal response model which combines interactions between longshore transport, cross-shore transport, water level variations and foredune erosion, at several temporal and spatial scales. It can also include sequencing and clustering of storm events. A schematic of the coastal evolution model is depicted in Figure 2.15, in which Y_S represents the shoreline position, Y_D the foredune toe position and Q_L the gradient in LST rate. One of the main characteristics in this model is the adaptation of the cross-shore baseline through adjustments to long-term water level variations (e.g. SLR), updates in shoreline position from a cumulative LST imbalance, short- to medium-term adjustments due to sediment supply and sediment inputs from the foredune erosion.

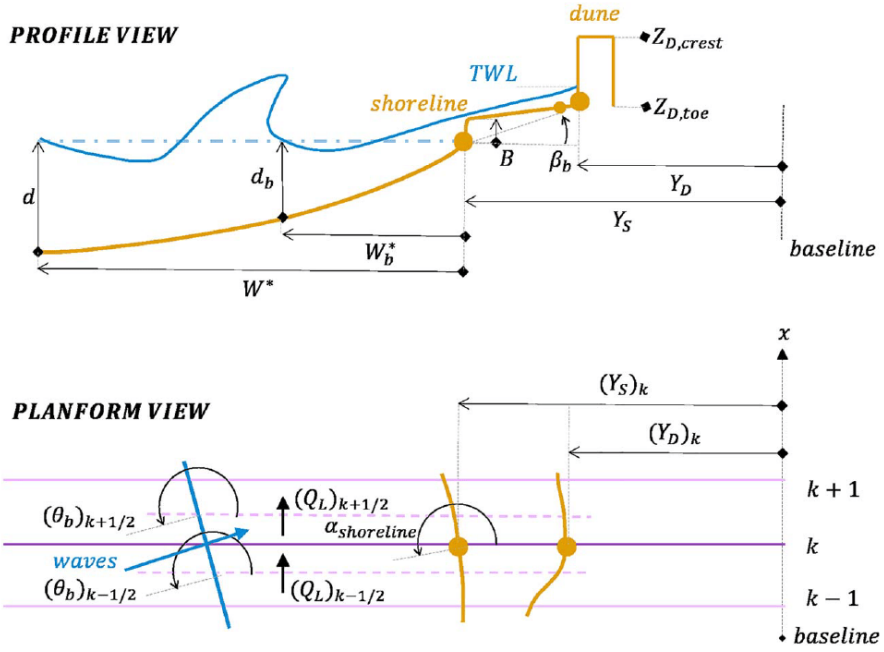

Figure 2.15: Schematic showing the setup of the coastal evolution model (Antolínez et al., 2019).

The governing equations of the model, presented below, describe an longshore transport one-line model (first term on the right side of Equation 2.6), a cross-shore equilibrium shoreline model (accounting for wave action and varying water levels, second term Equation 2.6), a foredune erosion model (based on waves and water level oscillations, Equations 2.7 and 2.8), and a term describing the influence of sediment supply. The equations below are coupled via Y_D which defines $Y_{S,eq}$.

$$\frac{\partial Y_S}{\partial t} = \frac{-1}{d}\frac{\partial Q_L}{\partial x} + K_C(Y_{S,eq} - Y_S) + \frac{-1}{d}(q_x + q_y) \tag{2.6}$$

$$\frac{\partial V_D}{\partial t} = (Z_{D,toe} - TWL)\frac{\partial Y_D}{\partial t} \tag{2.7}$$

$$\frac{\partial Y_D}{\partial t} = \frac{1}{T_s}(Y_{D,eq} - Y_D) \tag{2.8}$$

in which:

t	time
x	alongshore coordinate
d	depth of closure
K_C	erosional/accretional rate
$\frac{q_x}{d}$	longshore related sediment source
$\frac{q_y}{d}$	cross-shore related sediment source
V_D	eroded foredune volume
$Z_{D,toe}$	foredune toe elevation
TWL	total water level
T_s	response time

The COCOONED model implements certain assumptions and simplifications in order to simulate the interaction of several processes. Although these assumptions might cause less reliable model results, they can be important to reduce the complexity and thus computational time of this and other coastal models.

- Within the COCOONED model, the foredune model only accounts for erosion. Thus, full recovery over the summer is assumed. The reason for the foredune recovery not being modeled is the fact that aeolian processes and vegetation interactions complicates the analysis.
- Also, the model uses a simplified approach in which erosion/accretion only occurs in the upper shoreface profile and is distributed over the full shoreface all at once, i.e. delays in the erosion/accretion distribution to the lower parts of the shoreface profile are neglected.
- In addition, although severe storms can transport sediment from the beach and upper shoreface landward (inducing shoreline erosion and foredune growth), the berm profile is set to be constant during the simulations.
- During the simulation, the erosion/accretion rates K_C are kept constant, thus neglecting effects such as differences in grain size characteristics.
- Overtopping is not taken into account in the model: when the TWL exceeds the foredune crest elevation, the model assumes the maximum TWL would equal the foredune crest elevation.
- Regarding longshore transport, the CERC formula is used, neglecting the sediment grain size and the beach slope. Other formulas can be used to include these important parameters.
- Lastly, local variations in wave conditions (e.g. due to complicated nearshore bathymetry) are not considered, so areas close to jetties or headlands are not reproduced well.

2.5. Key points of Chapter 2

- Coastal zone management strategies and designs for coastal (protection) structures are developed for large temporal and spatial scales. This comes with large uncertainty regarding future wave conditions, storm events and sea level rise.
- A probabilistic approach can account for uncertainty in the wave forcing variates as well as in the estimates of future, long-term coastal evolution. This can assist in designing according to specific safety standards with corresponding failure probabilities.
- Physical processes leading to coastline changes can be divided in cross-shore and longshore processes, occurring perpendicular and parallel to the coastline, respectively.
- Relevant cross-shore processes that might lead to structural coastline erosion are storm events and sea level rise. Regarding longshore processes, this is mainly caused by gradients in longshore sediment transport.
- Cross-shore and longshore processes can interact, as the processes can induce changes in the coastal profile and in the coastline orientation, which influences the other processes.
- Morphological changes to the coastal system can be modelled with coastal profile models, describing the evolution of cross-shore profiles, and coastline models, assuming a constant cross-shore profile. The latter is relevant for long-term modelling purposes as implementing a constant cross-shore profile reduces the computational time.
- For every coastal modelling study, it is important to aim for an optimal balance between reliable, accurate results and the computational expense.
- Studies have found that for long-term coastal modelling purposes, the model uncertainty becomes dominant over the uncertainty in wave conditions.

3

Coastline models

This chapter describes the coastline models which are used in this research. The reasoning behind the decision for the particular models is presented, as well as detailed descriptions of the models. In addition, the relevant implemented assumptions are discussed.

3.1. Introduction

As introduced in Section 1.4, this study focuses on long-term projections of coastline development and how to present these in a probabilistic way. In order to generate multiple predictions that cover a range of possible future scenarios, a large number of simulations is needed to perform a Monte Carlo analysis. A requirement for this is an acceptable (i.e. small) simulation time of the used models; the models need to be robust and computationally efficient. As a result of this, based on applicability in engineering purposes, model performances and computational time, it is chosen to conduct this research with the use of the Probabilistic Coastline Recession (PCR) model (Ranasinghe et al., 2012) and the ShorelineS model (Roelvink et al., 2020). Figure 3.1 shows the relevant processes considered in this study and by which model they are covered.

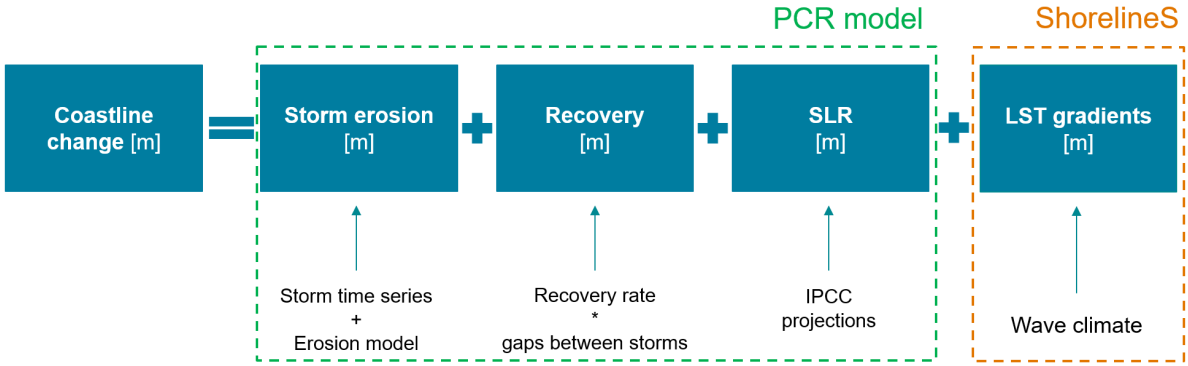

Figure 3.1: Relevant processes and models considered in this study.

PCR model
The PCR model provides probabilistic estimates of coastal recession based on governing physical processes in cross-shore direction, i.e. storm erosion, recovery in between storm events and long-term sea level rise (SLR). Due to the fact that most components are modelled separately, the model has a very low computational time. Hence, the modelling cycle can be repeated thousands of times, which enables a statistical analysis of the obtained results. This makes the PCR model perfectly suitable for being used in a probabilistic framework. Moreover, the low computational time makes it possible to model multiple coastline transects, from which a full coastline can be simulated.

ShorelineS model
The ShorelineS model describes long-term, alongshore coastline development based on gradients in longshore sediment transport (LST). The coastline changes can be computed with multiple transport formulations. The advantage of the ShorelineS model is that it is a free-form coastline model: it describes the coastline as a chain of grid points that can move, expand and shrink freely. The ShorelineS model is developed due to the fact that at timescales beyond events and seasons, coastline evolution of sandy beaches is often dominated by gradients in wave-driven LST. Event-scale and seasonal variations, which are mostly due to cross-shore transport, are not (yet) considered in this model.

Elaborate information on both models is presented in this chapter. It discusses all the required input information and the implementation procedures of the models.

3.2. Probabilistic Coastline Recession (PCR) model

3.2.1. Introduction

The PCR model uses a physics-based approach to provide stochastic estimates of coastal recession. The output of the PCR model is a time series of computed coastline positions for a certain period of time (e.g. 100 years). This process can be simulated for multiple coastline transects and for many times (e.g. 100,000 times - due to PCR's low computational time), resulting in many time series representing a full coastline. These time series are then statistically analysed to obtain the cumulative distribution function (CDF) of coastline change for the simulated period (Dastgheib et al., 2022).

This probabilistic approach makes the PCR method highly suitable for risk-based approaches in coastal zone management. Moreover, instead of conservative, restricting deterministic methods, probabilistic approaches enable economically optimal designs to fully utilise the potential of coastal areas (Dastgheib et al., 2018).

Implementation
The PCR model requires specific input data, such as the initial position of the studied coastline, information on the wave climate, water level data, a time series of storm events and gaps between them, the coastline recovery rate in between storms and a definition of the (uncertainty in) future SLR. Moreover, a specific erosion model needs to be determined in order to calculate the coastline retreat during storms. See Figure 3.1 for the relevant processes in the PCR model. In the next sections, these input components will be thoroughly described, as well as their implementation into the PCR model.

3.2.2. Framework

The PCR method consists of the following key elements, which are repeated over a bootstrap cycle (Ranasinghe et al., 2012). This cycle and the conceptual framework of the PCR model, as introduced by Dastgheib et al. (2022), are presented in Figure 3.2.

1. **Storm time series**

   A time series of storm events (and the time gap between those events) is generated as input, using a data set of historical wave conditions. The storm characteristics are derived from joint probability distributions of the variates in the available wave data set. Hence, it departs completely from the deterministic approach in which a benchmark event is used, i.e. the largest measured historical storm event (Callaghan et al., 2008).

   If an appropriate method is selected to simulate the time between events, the model can account for event grouping. This is important, since Kriebel and Dean (1993, as cited in Callaghan et al., 2008) showed a dependency of erosion volumes on storm duration: shorter duration events having the same peak wave height result in less beach erosion.

2. **Erosion model**

   From the generated storm time series, the coastal recession for each storm event is estimated using an appropriate erosion model, by focusing on a defined coastline indicator (such as dune toe position or mean sea level). The erosion model should be wisely chosen, taking computational time and effort into consideration.

3. **Sea level rise**

   Then, estimate the SLR and the corresponding coastline retreat at the time that each storm in the time series occurs. IPCC projections can be used in this step (Church et al., 2013).

4. **Coastline recovery**

   In addition, it is important that the recovery of the coastline in between storm events is allowed for; a sound assumption for an appropriate recovery rate has to be determined. The location of the coastline before the next storm is calculated considering the coastline recovery and SLR within the time gap between storms.

5. **Coastline change**

   The position of the chosen coastline indicator is tracked and stored throughout the full simulation period. Subtract the initial position of the coastline indicator from its final calculated position to estimate coastline change during the simulated period.

6. **Repetition**

   Consequently, the estimation steps are repeated until exceedance probabilities larger than 0.01% converge. This is called bootstrapping, explaining the bootstrap cycle as mentioned above. The number of required repetitions depends on the study or project, but sufficient data is needed in order to have accurate results for (very) low probabilities.

All described components of the PCR framework are more thoroughly discussed in the next sections of this chapter.

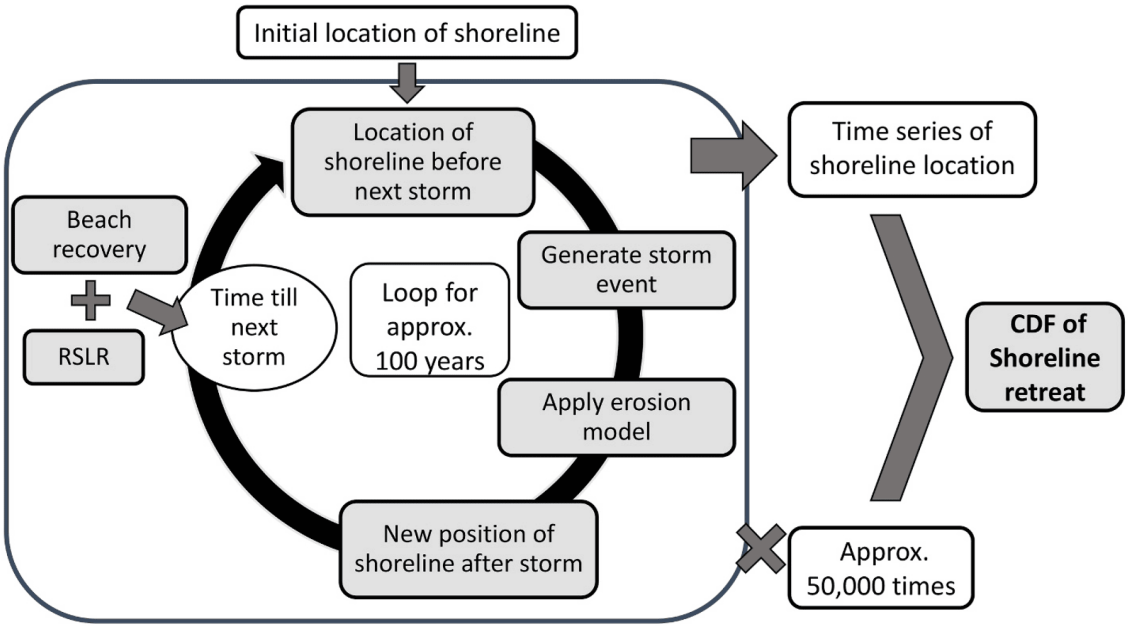

Figure 3.2: Conceptual framework of PCR model implementation (Dastgheib et al., 2022).

Limitations
Apart from the described advantages, the PCR model also has its limitations (R. Ranasinghe & A. Dastgheib, personal communication, June 15, 2022), being:

- The omission of longshore sediment transport (LST) gradients in the computations, discussed in Section 1.1. Again, for coastlines where LST gradients play a significant role or for coastlines where hard structures influence the LST, this is an important element to add to the PCR model. This will be the main topic of this research.
- The assumption that the cross-shore profile remains constant after each storm event and only moves backwards and forwards. Multiple studies are being done into the effect of storm events on profile changes and also the effect of SLR, when waves break closer to the coastline. Namely, a time-varying cross-shore profile would influence the recovery rate in between storms, as well as the actual storm erosion of the specific profile (Da Cruz, 2018). This assumption is out of the scope of the research in this report.
- The assumption of a constant coastline recovery rate in between storms, in absence of SLR. In other words, a coastline in equilibrium is assumed, which in reality is often not the case, especially when a coastline is dominated by LST or when a coastal structure has been constructed (Bitaki, 2019), see also Sections 2.3.1 and 2.3.3. It is evident that it is not realistic to assume that after a storm with twice as much erosion, the coastline recovers twice as fast. The recovery rate can be obtained by historical measurements of the study area, or by implementing additional coastline models into the research.
- The choice of the dune erosion model, which influences the PCR model output significantly. A sound balance has to be considered of the computational time of the erosion model and the added value to the PCR output. Studies have shown that increasing the level of sophistication of the erosion function does not necessarily ensures better results, especially given the fact that the PCR model is developed for relatively quick and efficient insights in coastline recession.
- The storm event definition; from what wave height exceedance is it called a storm? This highly depends on the location of the study area and can not be assumed universally equal.
- Lastly, climate change driven variations in the wave climate, other than SLR, are not taken into account for the (long) simulation period in the PCR framework. Additional models can (and must) be used to account for changes in wave climate and also in storm frequency for the simulated future period.

3.2.3. Synthetic storm time series

The main input of the PCR model is a time series of storm characteristics for the duration of the simulated period. This storm time series is derived following the methods as used in previous PCR model applications. From a wave data set, information is gathered using the Joint Probability Method (JPM) (Callaghan et al., 2008). Wave climate variates always have an internal physical connection, and thus often a mutual (partial) dependency (Li, van Gelder, Ranasinghe, et al., 2014). With the JPM, the joint probability between basic forcing variates such as wave height, period and direction, event duration and event spacing can be determined. The focus lies on extreme storm events, which are crucial for coastal engineering purposes. The obtained joint probabilities can be used in Monte Carlo simulations to derive a time series of (extreme) storms and their associated characteristics. Also event grouping can be accounted for, in which two closely spaced storms can cause significantly more erosion.

The obtained synthetic storm time series (SSTS) can be implemented in the PCR model. As input into the erosion model, storm conditions can be randomly generated from the defined extreme value probability as well as joint probability distributions (Dastgheib et al., 2022). Hence, a sound decision is to be made for an appropriate storm erosion function which simulates the eroded volumes after each storm event.

In this research, the SSTS is generated by performing the following steps (modified from Ranasinghe et al. (2012)):

1. Identify meteorologically independent storm events;
2. Fit extreme value distributions to the maximum wave height per storm event, the still water level and the storm duration;
3. Fit the dependency distribution between wave height and storm duration (using copula functions);
4. Fit a conditional distribution between wave height and wave period;
5. Determine the empirical distribution for wave direction;
6. Analyse the gaps between storms to calculate the mean number of events per month in order to fit a non-homogeneous Poisson distribution to the gaps between storms;
7. Generate the total number of storm events using the fitted distributions, including storm spacing (i.e. generate the SSTS).

Storm definition and identification
In this research, storm events are defined based on wave conditions. A storm event is the period in which the measured wave height is above a certain threshold (e.g. the 97th-percentile value of the wave height data), for at least 6 consecutive hours. See Figure 3.3. Also, in order to call it a storm event, the still water level (SWL) must be above a certain threshold as well (e.g. 0.50 m +MSL). Moreover, if the time between two storm events is less than 12 hours, the two identified storm events will be considered as one single event: storm grouping. It must be noted that the total number of identified storms from a data set is highly sensitive to this definition of a storm event.

In addition, dependent on the used erosion model, it is possible to account for a varying water level during a storm event, in order to represent reality. Hence, multiple SWL values might be generated for a single storm event. If only a (maximum) water level is taken to calculate the storm erosion of a single event, the estimated amount of erosion will be unrealistic and often too large (Caroline Hallin, personal communication, November 15, 2022). This especially holds for storm events with a large duration.

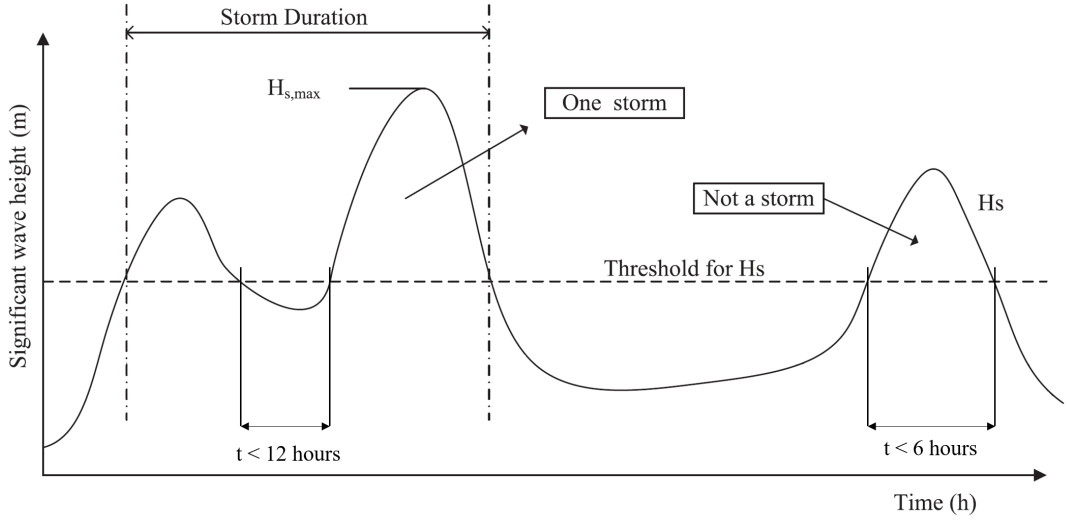

Figure 3.3: Definition of independent storm events, modified from Li (2014).

Statistical analysis
For each detected storm event, specific storm characteristics are derived: the maximum significant wave height during the detected storm event, the peak wave period, still water level, mean wave direction, event duration and the gap between two consecutive events. After the storm events are identified, a statistical analysis of these characteristics is performed. That is, the storm characteristics are fitted to theoretical or empirical distributions and moreover, dependency distributions can be fitted between different storm characteristics using for instance a copula method. A copula is a multivariate probability distribution which is able to correlate two (or more) variables without changing their marginal distributions (Li, van Gelder, Ranasinghe, et al., 2014).

The main goal is to describe the detected extreme wave height values by a specific probability distribution, such that for return periods longer than the duration of the measured data, a realistic extreme wave height can be determined. The extrapolation from observed to unobserved values (i.e. the small exceedance probabilities) is crucial for coastal protection and engineering design.

Generation of the storm time series
Finally, the storm event time series is generated as follows:

1. First, two random numbers are generated from a joint CDF of max. Hs during storm event and the storm duration using a copula method: one for the probability of exceedance of the max. Hs, one for the probability of exceedance of the storm duration;
2. Consequently, the values for the generated Hs and duration are obtained from their individual cumulative distributions using the generated probabilities;
3. The still water level (SWL) is derived from a fitted distribution by generating a random probability of exceedance. (Again, it is noted that multiple SWL values could be generated for a single storm event);
4. Next, the Tp is retrieved from a fitted Hs-Tp function, corresponding to the generated Hs;
5. The wave direction is sampled from a fitted distribution;
6. Lastly, the gap between events is randomly generated using a non-homogeneous Poisson distribution, with a λ parameter that depends on the month in which the storm event takes place.

This way, a database of storm characteristics is obtained for the total desired simulation period. Each storm event consists of a wave height, a duration, a still water level, a peak wave period and a mean wave direction (see Figure 3.4). By generating these storm events beforehand, the computational time of the PCR model simulation is reduced significantly.

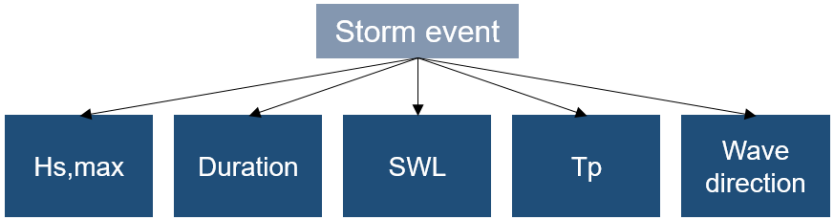

Figure 3.4: Generated storm characteristics per event.

3.2.4. Erosion model

The amount of dune erosion (and the corresponding coastline displacement) related to each storm event is calculated with an erosion function. The requirement of a low computational time to allow for a probabilistic approach not only holds for the PCR and ShorelineS models, but also for the specific erosion model which will be implemented within the PCR method. Despite its high level of performance, advanced process-based models such as XBeach (Roelvink et al., 2009) are too computationally expensive for calculating storm erosion. Hence, more simplified models are to be used, with a sufficient level of accuracy for long-term purposes. Two models that would fit in this description are the CS-model (Larson et al., 2004) and the Dunerule model (Van Rijn (2013a), adjusted by Li (2014) and calibrated for the Dutch coast). Below, these two models are presented and a description is given of how they are implemented in this research.

CS-model
The CS-model is an analytical wave impact dune erosion model, based on the assumption that there is a linear relationship between the wave impact and the weight of sand eroded from the dune (Larson et al., 2016). It simulates cross-shore sediment transport and long-term beach and dune evolution in individual transects; multiple transects can be modelled to represent a coastal stretch. Included processes are dune erosion and overwash, dune build-up by aeolian transport, beach-bar exchange, and sea level rise. The model is based on a set of semi-empirical, physics-based sand transport

equations, which require site-specific data for calibration and validation in order to achieve a good model performance. One of the limitations of the CS-model is the fact that the incoming wave direction is not taken into account as a parameter in the formulations.

The cross-shore profile as used in this MSc research can be schematized as depicted in Figure 3.5:

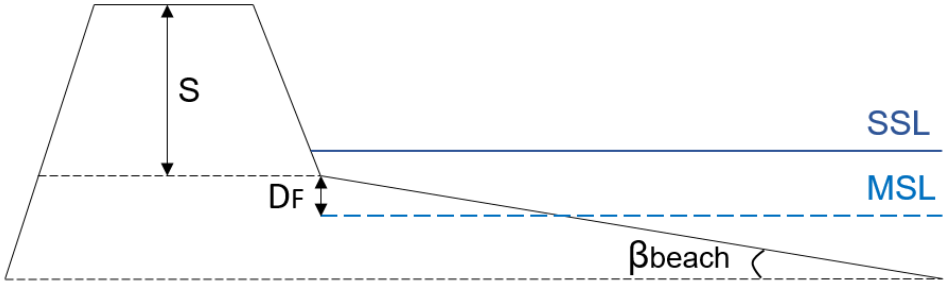

Figure 3.5: Profile schematization for the use of the CS-model.

This research focuses on the dune erosion component of the CS-model. The dune erosion is based on the wave run-up height R and the deep-water root-mean-square wave height H_{rms}, where the run-up height is estimated as follows:

$$R = 0.158\sqrt{H_{rms}L_0} \tag{3.1}$$

In which L_0 is the average deep-water wavelength (Holthuijsen, 2007):

$$L_0 = \frac{g \cdot {T_P}^2}{2\pi} \tag{3.2}$$

In order to account for the friction over the beach, the run-up height is adjusted by including the travel distance of the uprushing wave x_t [m] (Hanson et al., 2010). This distance is equal to the horizontal distance from the still water line to the dune foot, for a beach that is schematized as a right-angled triangle with a height equal to the dune foot height D_F (Hallin, 2019). c_f is an empirical friction coefficient.

$$R'_i = R \cdot \exp\left(-2 \cdot c_f \cdot x_t\right) + (D_F - SWL_i) \cdot (1 - \exp\left(-2 \cdot c_f \cdot x_t\right)) \tag{3.3}$$

$$x_t = \frac{(D_F - SWL_i)}{\beta_{beach}} \tag{3.4}$$

Note that the SWL changes for every time step (as described in Section 3.2.3), so the travel distance varies within a single storm event. Hence, this also holds for the adjusted run-up height. The CS-model can also account for varying wave conditions during a storm event, but in this research only the maximum Hs during a storm event is considered, as introduced in Section 3.2.3.

In the case that no overwash over the dunes occurs, i.e. if $D_F < R' + SWL < D_F + S$ with S being the dune height, the eroded volume from the dune face, q_D [m^3/m], is calculated per time step as:

$$q_{D,i} = 4 \cdot C_S \cdot \frac{(R'_i + SWL_i - D_F)^2}{T_P} \tag{3.5}$$

Here, C_S is an empirical dune erosion impact coefficient, which was found to be in between the values of $1.7 \cdot 10^{-4}$ and $1.4 \cdot 10^{-3}$ after calibration against data from field and laboratory experiments (Larson et al., 2004).

Eventually, the final coastline displacement Δy [m] can be determined by summing up the eroded volumes per time step for the total duration of a storm event, and dividing it by the dune height S. So, for a storm event of, e.g., 9 hours, and a 3-hour time step, three different dune erosion volumes are summed up as follows:

$$\Delta y = \frac{\sum q_{D,i}}{S} \tag{3.6}$$

It must be noted that in this research it is assumed that the eroded dune above the dune foot volume is directly translated to a retreat of the coastline - as described by Equation 3.6, since in this study with the PCR model, only severe storm erosion events are considered (Caroline Hallin, personal communication, November 15, 2022). The model only calculates storm erosion when the adjusted run-up height at least reaches the dune foot (see Equation 3.5 and description above it).

Dunerule model

The Dunerule model is an empirical function which was proposed by Van Rijn (2013a) and originates from the cross-shore model CROSMOR, which is based on a 'wave by wave' modelling approach solving the wave energy equation for each individual wave. The key difference between the Dunerule model and the CS-model is that Dunerule does include the wave direction in the calculations, which could be useful for modelling changes in coastline orientation, and the effects of these changes.

Dunerule was developed by studying the effects of various key parameters on the computed dune erosion for a reference case that is defined by Vellinga (1982, as cited in Li (2014)). Li calibrated and validated the model for a specific coastal profile along the Holland coast with the use of XBeach. To achieve this, Li used 298 storm events with different combinations of wave conditions to estimate the DUNERULE model coefficients. The result is the adjusted Dunerule formula (in which the coastal slope is assumed to be 0.02 and the median bed material diameter (d_{50}) is 0.2 mm):

$$R = 153 \cdot A_{dir} \cdot \left(\frac{h}{5}\right)^{\alpha_1} \cdot \left(\frac{H_{s,max}}{7.6}\right)^{\alpha_2} \cdot \left(\frac{D}{5}\right)^{\alpha_3} \cdot \left(\frac{T_p}{12}\right)^{\alpha_4} \tag{3.7}$$

In which R is the dune erosion volume [m^3/m] - not to be confused with the parameter R of the CS-model - and h is the maximum water level during a storm event [m]. Further, $H_{s,max}$ is the significant offshore wave height [m], T_p is the peak wave period [s] and D is the duration of a storm event [h].

Regarding the model coefficients, $\alpha_1 = 1.5$ for $h \leq 5$ and $\alpha_1 = 0.2$ for $h > 5$, $\alpha_2 = 0.3$ for $H_{s,max} \leq 7.6$ and $\alpha_2 = 0.9$ for $H_{s,max} > 7.6$, $\alpha_3 = 0.3$, $\alpha_4 = 1.3$ for $T_p \leq 12$ and $\alpha_4 = 0.9$ for $T_p > 12$.

The coefficient A_{dir}, which indicates the impact of the wave direction θ, is described with an empirical function as well:

$$A_{dir} = \begin{cases} 1 - 0.01 \cdot (270 - \theta) & for\ \theta \leq 270; \\ 1 - 0.01 \cdot (\theta - 326) & for\ \theta \geq 326; \\ 1 - 0.0107 \cdot (26 - |\theta - 298|) & for\ 270 < \theta < 326. \end{cases} \tag{3.8}$$

In this study, the calculated eroded volume R is assumed to be translated to the coastline retreat Δy [m] according to:

$$\Delta y = \frac{R}{h_D - h} \tag{3.9}$$

In which h_D is the dune crest height above MSL [m] and h is the maximum water level during a storm event [m].

Decreasing wave impact during storm

In this study it is assumed that all eroded sediment will be deposited on the beach, and no eroded sediment will be transported to the landward side of the dune (i.e. no overwash occurs). Due to this deposited sediment and the post-storm cross-shore profile as was introduced in Section 2.3.1 and Figure 2.6, uprushing waves will experience increased friction during a storm event. Hence, more wave dissipation occurs and the wave impact on the dune decreases as the storm proceeds. In this research, this phenomenon is not included in the erosion models, which may result in slightly conservative estimates of dune erosion and coastline retreat.

3.2.5. Coastline recovery rate

During calm periods in between storm events, the dune and coastline tend to recover due to wave-driven (onshore) sediment transport and aeolian transport, as described in Section 2.3.1. To describe realistic and accurate long-term effects of coastline erosion, it is highly important to take this recovery into account when using a storm time series. The rate of recovery is influenced by multiple factors such as wind speed, beach slope and vegetation. However, in this study, those processes are not considered and the coastline recovery rate is assumed to be constant. This has been implemented by previous PCR applications (e.g. Dastgheib et al. (2022)). In order to obtain the recovery rate based on the local wave and storm conditions, a trial and error application is implemented, as was done in Li (2014) and Ranasinghe et al. (2012). The following steps are to be performed (in which SLR is not taken into account):

1. Generate a time series of storm events;
2. Calculate the final coastline erosion after a certain simulation period based on this time series, taking no SLR into account;
3. Repeat these two steps for thousands of times (e.g. 100,000 times), with a new storm time series for every simulation;
4. Generate a CDF curve from all the calculated final coastline recession values and take the value with a 50% exceedance probability (i.e. the p50 value);
5. The recovery rate is derived based on the assumption that the coastline would fully recover from this p50 value.

It is known that the actual recovery rate of a specific coastal area is highly influenced by not only the beach width and dune height, but also by parameters which are not considered in the present study, such as obstacles on the beach (e.g. beach houses), sand bars, wind velocity, grain size and precipitation. Hallin et al. (2019) showed sensitivity of the CS-model to some of those parameters.

3.2.6. Sea level rise

SLR effects
One of the main consequences of climate change is sea level rise (SLR), which has two clearly distinguishable effects on coastline evolution:

1. SLR causes an extra retreat of the coastline as eroded sediment from the dune and beach is deposited on the more offshore located sea bed (Bruun, 1962). See also Section 2.4.4;
2. Next to that, the larger water depth might enhance dune erosion as storm waves and storm surges will act on the new elevated sea level. Hence, waves will reach higher ground and will break closer to the coastline during a storm event, inducing more severe erosion (Ranasinghe, 2016).

In this study, the first described SLR effect is implemented in the PCR model by including an extra (horizontal) retreat during the gap of time between two storm events. This retreat is calculated based on the water level difference between the previous storm and the next one, as follows:

$$R_{SLR} = \frac{WL(next\ storm) - WL(previous\ storm)}{slope} \tag{3.10}$$

It is noted that the slope of the beach around MSL is an important, influential factor here. It was taken as 0.025 (i.e. 1:40) in this study, according to JARKUS measurements and also in line with literature (Rijkswaterstaat, 2022; Stolk, 1989). This value can be varied to check the PCR model's sensitivity to it. In addition, also here it is assumed that the shape of the profile remains constant and only moves landwards (see Section 2.3.2); the new MSL is at the same point on the profile as it was before.

Secondly, the increased (storm) erosion due to rising water and surge levels is taken into account by using the increased water level in the dune erosion calculations. Evidently, this highly depends on the type of erosion model that is implemented. One of the important things to keep in mind here, is the fact that the coastal profile will most probably adapt to the SLR, which is not incorporated in the erosion function. This effect, as well as the sensitivity of the erosion models to the water level parameter, will be discussed more thoroughly in Chapter 5 on model application.

3.2.7. Modelling strategy

After all individual components have been established, the PCR modelling loop is started (Figure 3.2). The initial coastline position is set to be at x = 0 m. The coastline position indicator is defined to be the mean sea level (MSL). The first generated storm event is modelled to occur on the first day of the simulation period (January 1, 2023). The new coastline position after the storm event is determined by the erosion model, after which the time until the next storm event is generated from the non-homogeneous Poisson distribution, dependent on the current month. During this period of time, the coastline recovers according to the determined recovery rate. In addition to the coastline recovery, the extra retreat due to SLR is also implemented to the coastline, to finally obtain the coastline position before the next storm event. This loop is continued until the end date of the simulation period (January 1, 2100) is reached. Figure 3.6 shows an example of a time series derived from one single PCR model simulation.

The described procedure can be repeated thousands of times to generate a large number of time series of coastline positions for the period between 2023 and 2100. The tracked coastline position of each time series is decided to be the most landward position (i.e. maximum retreat) that is measured during every single PCR simulation. In Figure 3.6 the most landward position over time is highlighted with a red circle. The most landward position is chosen as indicator due to its applicability to coastal zone management purposes. The computed coastline positions are depicted relative to the initial coastline position.

Consequently, all obtained most landward coastline positions can be statistically analysed to obtain the cumulative distribution function (CDF) of coastline evolution for the simulated period. In this study, it is aimed to achieve convergence at the 0.01% probability of exceedance level. This means that the number of Monte Carlo simulations needs to be sufficiently large, in order to ensure that the value of recession for the specific 0.01% probability of exceedance does not change for a larger number of simulations. Then, this particular probability of exceedance has converged.

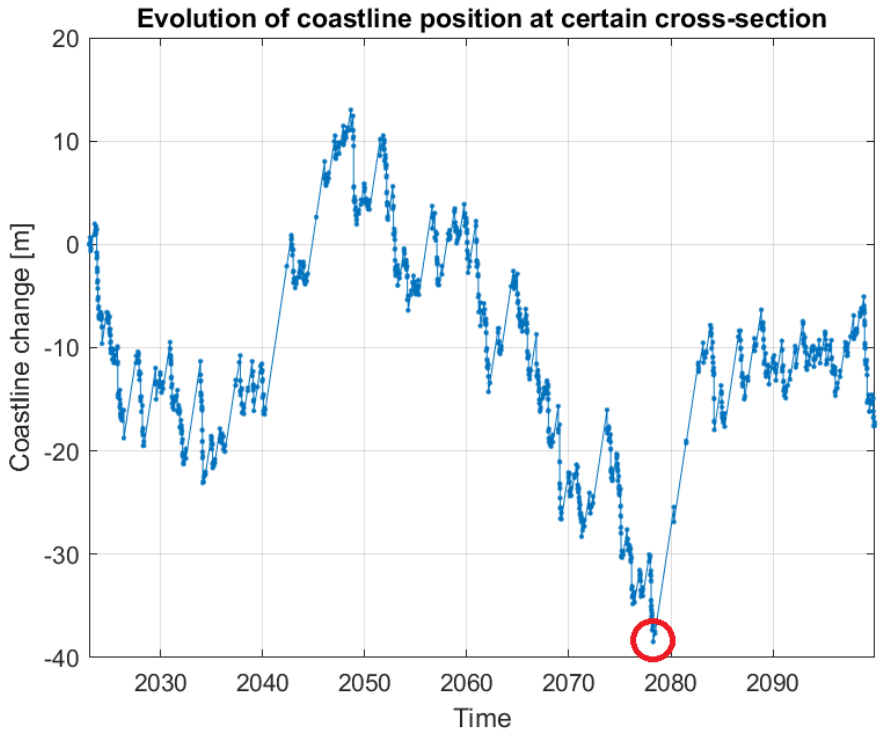

Figure 3.6: Temporal evolution of the coastline position at a certain cross-section, for an example case, modelled with PCR.

3.3. ShorelineS model

3.3.1. Introduction

The ShorelineS model (Roelvink et al., 2020) is a free-form coastline model which can describe long-term, alongshore coastal transformations based on longshore transport gradients. The origin of the ShorelineS model is the fact that at timescales beyond events and seasons, coastline changes along sandy beaches are often dominated by gradients in wave-driven longshore sediment transport (LST). Event-scale and seasonal variations, which are mostly due to cross-shore transport, are not (yet) considered in this model.

The model describes the coastline as a chain of grid points that can move, expand and shrink freely, i.e. a flexible grid (see Figure 3.7). It also allows for an arbitrary number of coastal sections, which can be open or closed and can interact with each other. The model is very well able to describe splitting and merging of coastlines, disturbances by hard structures and sediment bypassing around those structures, as well as the growing of spits, salients, tombolos and other forms. The modelled coastline points are situated at the MSL contour, to represent the profile's movement.

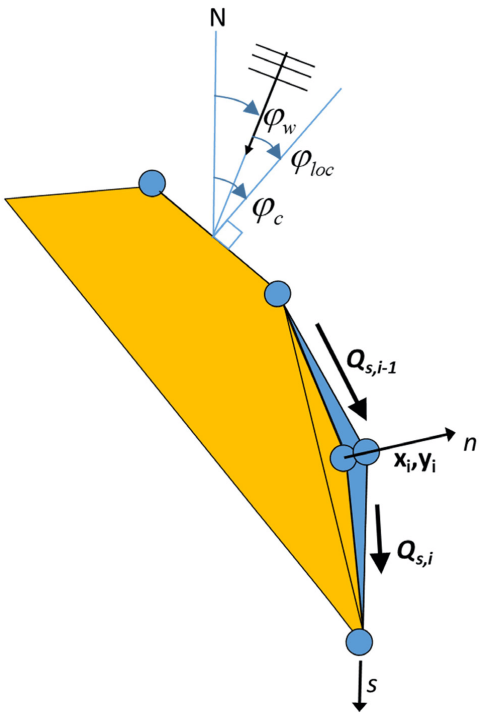

Figure 3.7: Schematic view of the free movement of grid points in ShorelineS (Roelvink et al., 2020).

Computational efficiency
The evaluation of coastline development on timescales of decades or centuries requires computationally intensive 2D/3D models. However, as for the PCR model, the ShorelineS model is able to describe the same coastal deformations as detailed 2DH morphodynamic models, but at considerably smaller computational expense. As expected, this comes with a few assumptions. For instance, the active profile depth is fixed, although it might vary in reality (see also Section 3.4). For coastlines with uniform cross-shore profiles, this would not raise problems, but this can not be assumed globally. Also, long-term retreat due to storms is not taken into account.

It is noted that the ShorelineS model is still in development; multiple studies to the model issues and shortcomings are being performed at the moment (Roelvink et al., 2020). The coupling with 2DH models such as Delft3D (Lesser et al., 2004) and XBeach (Roelvink et al., 2009) is highly promising: nearshore sink/source terms can be provided by the 2DH models and the corresponding two-dimensional changes in bathymetry are updated by ShorelineS.

3.3.2. Implementation

The ShorelineS model is implemented in Matlab. The flow diagram of its framework is given in Figure D.1 in Appendix D. Below, the basic equation for the coastline position updates is presented, which is based on the conservation of sediment:

$$\frac{\delta n}{\delta t} = -\frac{1}{D_c}\frac{\delta Q_s}{\delta s} - \frac{RSLR}{\tan\beta} + \frac{1}{D_c}\sum q_i \tag{3.11}$$

in which:

n	cross-shore coordinate
s	longshore coordinate
t	time
D_c	active profile height
Q_s	longshore transport [m^3/yr]
$\tan\beta$	average profile slope between dune crest and depth of closure
$RSLR$	relative sea level rise [m/yr]
q_i	source/sink term [m^3/m/yr]

Model input
As input data, the ShorelineS model requires the coordinates of the initial coastline position and of the hard coastal structures (if applicable). In addition, wave data is needed as input to the sediment transport formulations which calculate the wave-driven LST. Eventually, this LST determines the coastline changes. The wave data can be a time series of wave conditions, a representative wave climate with fewer wave conditions or a simple wave climate with predefined values for the significant wave height, wave period, incoming wave angle, etc.

Furthermore, it is necessary to define the (constant) active profile height as an input parameter. The active profile height defines the domain of the coastal zone in which morphological changes occur and the bed is very dynamic, hence the name ”active profile”. It is the sum of the closure depth and the dune toe elevation. The depth of closure (DoC) can be defined according to the Hallermeier equations (Hallermeier, 1978), who made a distinction between the inner and outer closure depths. Seaward of the outer DoC the influence of wave action on cross-shore sediment transport is said to be insignificant. It is therefore also sometimes called the Depth of Transport (DoT). Landward of the outer DoC the coastal profile is dynamic, but the bed dynamics occur mostly at depths smaller than the inner DoC. See also Figure 2.1. The calculation of the inner and outer closure depths are based on the local wave conditions (both closure depths refer to mean low water (MLW) conditions):

$$h_{in} = 2.28 \cdot H_{12h/y} - 68.5 \cdot \left(\frac{H_{12h/y}^2}{g \cdot T_{12h/y}^2}\right) \tag{3.12}$$

In which $H_{12h/y}$ is the wave height that is exceeded for 12 hours per year, i.e. the significant wave height with a probability of yearly exceedance of 0.137%, $T_{12h/y}$ is the wave period associated with $H_{12h/y}$, and g is the acceleration of gravity.

$$h_{out} = 0.013 \cdot H_s \cdot T_s \cdot \sqrt{\frac{g}{d_{50} \cdot (s-1)}} \tag{3.13}$$

In which H_s and T_s are the significant wave height and period respectively, d_{50} is the median sediment diameter and s is the ratio of specific gravity of sand to that of fluid (about 2.65).

Longshore sediment transport
The transport formulations implemented in ShorelineS are CERC formulas (USACE, 1984), the Kamphuis formula (Kamphuis, 1991, as cited in Roelvink et al. (2009)), and formulations by Mil-Homens (2016) and Van Rijn (2013b). These formulations vary in complexity since multiple assumptions have been implemented. For instance, the simplified CERC1 formula does not take refraction into account as it is solely based on deep water wave height and direction. Hence, wave breaking, the wave period and the sediment grain size are not considered. The formulations can be calibrated to match local transport rates by adjusting specific physical parameter settings (dependent on the used transport formula). The complexity and the number of input parameters varies significantly per transport formulation, hence it is evident that the sediment transport magnitudes will differ based on the implemented method.

Model simulation
Prior to the model simulation, boundary conditions can be implemented, such as the sediment transport rate at the start and end of the boundaries of the domain. Moreover, nourishments and other types of sinks and sources can be added in this phase as well. Next to that, the initial grid size and time step are to be defined. When necessary, new grid points are added or existing grid points are removed by the model itself. It is possible to include adaptability of the time step as well, in order to keep a reasonable balance between the spatial and temporal scales according to the Neumann criterion. This prevents the model from becoming unstable.

Finally, at each grid point, the local coastline orientation is determined from the two adjacent points, from which the LST is calculated for each segment. A difference between the transport of two segments (i.e. a gradient) causes the coastline points to build out or to shrink. Also, the model can account for wave shadowing (i.e. blocking of LST) behind structures or other sections of the coast. Moreover, diffraction of the waves around structures can be included as well. Therefore, it is possible to implement ShorelineS in coastal areas where groynes or rocky headlands are present.

3.4. Relevant assumptions

In this section, the most important assumptions implemented in this research are summarized. The assumptions are made mostly to reduce complexity and computational time, but are also based on previous research in which the simplifications have been shown to lead to comparable results, as discussed in Section 2.4.6.

Cross-shore profile shape
Following the one-line theory (Section 2.3.2, Figure 2.10), a constant cross-shore beach profile is assumed by multiple models such as the discussed CoSMoS-COAST, LX-shore and GenCade models (see Section 2.4.6). This also holds for the PCR and ShorelineS simulations. The main reason for implementing this assumption is to achieve higher computational efficiency. The assumption means that during the entire simulated period, the cross-shore profile maintains an average shape and only moves landward or seaward as a whole. It thus neglects seasonal changes in shape and slope of the profile (although they occur at almost every site). Moreover, extreme episodic (storm-induced) changes in the beach profile are also not considered. Lastly, material exchange between dune, beach and bar(s) is neglected as well. However, this concept has been supported by many field investigations (Bruun, 1954 and Dean, 1977, as cited in Hallin (2019)). The assumption is particularly valid for long-term modelling purposes, where deviations on the smaller scales are less important and where seasonal profile variations are averaged out.

Active profile height
One of the major assumptions within the ShorelineS framework is the constant active profile height. The active profile height is the vertical distance between the closure depth (see Section 2.2.1) and the dune toe elevation. As can be seen in the governing ShorelineS equation (Section 3.3) and in the formulations of other discussed models (Section 2.3.4), the depth of closure is often highly important for the calculation of the coastline displacement. To reduce model complexity and computational time, the active profile depth is typically fixed in coastline models. However, in practice, they can vary spatially and temporally depending on the wave conditions and the previous bathymetry (Roelvink et al., 2020). Hence, implementing this assumption will result in a considerable simplification of reality.

Cross-shore recovery rate
As discussed in Section 2.3.1, an episodically eroded shoreline recovers in between storms due to the calm wave conditions transporting sediment in onshore direction and by wind-induced (aeolian) transport of sand to rebuild the dunes. A lot of factors and processes (such as wind speed, fetch, beach slope, sediment availability, vegetation, etc.) play a role in this so-called cross-shore recovery. However, in the PCR model, these processes are not further studied and a constant recovery rate is assumed (Dastgheib et al., 2018; Dastgheib et al., 2022; Li, 2014; Ranasinghe et al., 2012). The recovery rate is defined such that the probability of exceedance for the coastline to be in equilibrium should be 50%, while neglecting SLR (see Section 3.2.5).

Other assumptions
Furthermore, some other assumptions are made to simplify reality and to reduce computational time and effort:

- The sediment grain size is assumed to be constant (i.e. 0.2 mm) for each modelled cross-section in this study. In further, more advanced research, varying sediment characteristics can be implemented for different cross-sections along the coast, to study the influence on storm-induced coastline erosion;
- In this research, it is assumed that no overwash over the dunes occurs. This means that no sand is lost to the landward side of the dune, and all eroded sand from the dune is deposited on the beach or further in the sea or offshore;
- Also, no beach-bar migration, i.e. material exchange between beach and sandbar(s), is assumed in the calculations of the coastline erosion.

3.5. Key points of Chapter 3

- The cross-shore processes storm erosion, coastline recovery in between storm events and sea level rise can be modelled with the Probabilistic Coastline Recession (PCR) model.
- Due to its low computational time, the PCR model can run thousands of simulations of a coastline's response to the impact of storms and sea level rise for a certain simulation period. As a result, the model outcome can be statistically analysed to obtain stochastic estimates of long-term coastline evolution.
- Within the PCR model, a synthetic storm time series is generated based on fitted distributions of the wave and water level forcing variates. This storm time series is used as input into an erosion model, which simulates the storm-induced coastline retreat.
- The PCR model implements an approach that the coastline is in equilibrium with the median calculated storm-induced retreat (for a case without sea level rise). This results in a constant rate for the coastline recovery in the period between consecutive storm events.
- Consequently, the coastline recession as a result of sea level rise is modelled, after which a certain coastline indicator can be analysed, such as the most landward coastline position during the simulated period.
- The long-term development of a coastline induced by gradients in longshore sediment transport can be simulated with the ShorelineS model. It is a free-form coastline model which is computationally efficient, making it highly suitable for long-term modelling purposes. Multiple sediment transport formulas can be implemented in the ShorelineS model.
- The main relevant assumptions implemented in this study are the assumption of a constant shape of the cross-shore profile and a constant active profile height, which is a significant simplification of the reality.

4

Frameworks

This chapter discusses the process towards developing a probabilistic framework to combine cross-shore and longshore processes in long-term coastline modelling. It presents the defined framework alternatives and for each framework, the advantages and limitations are discussed.

4.1. Framework 1: separate modelling

In the first framework, the studied coastline is modelled for the total simulation period with the PCR model and with the ShorelineS model, separately. Time series of shoreline positions can be obtained from both models. Figures 3.6 and 4.3 show examples of time series derived from one single PCR model run and one ShorelineS simulation, respectively. If these time series are combined, the evolution of the coastline position induced by both cross-shore and longshore impacts can be depicted. This defines the first developed framework, which can be schematised as shown below in Figure 4.1.

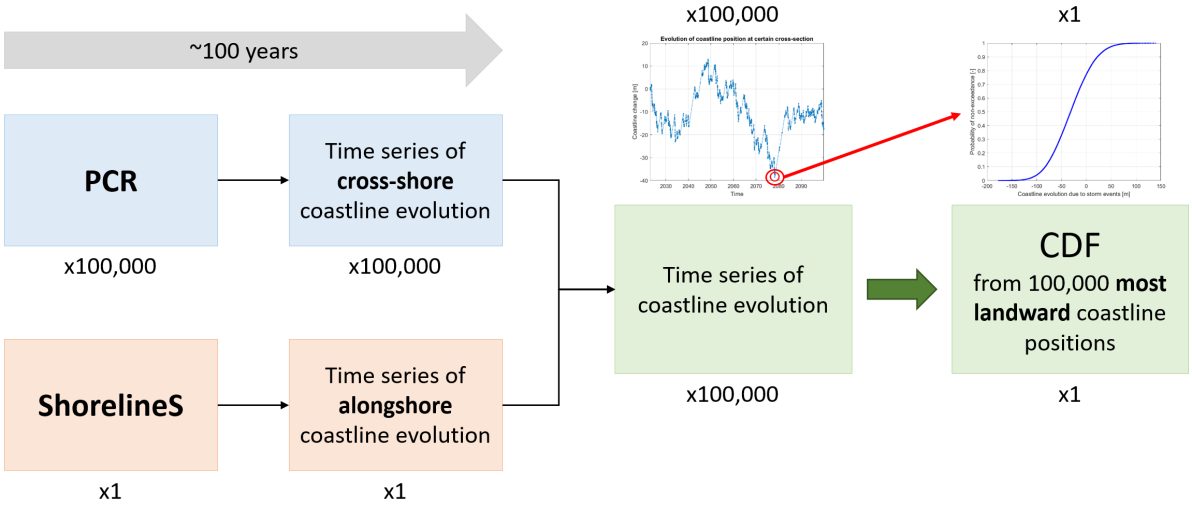

Figure 4.1: Schematic to combine modelled time series: Framework 1.

Advantages

This framework is the most simple one and is quick to implement, which can be useful to obtain first insights in long-term coastline evolution. The computational time of implementing this method is limited. Also, the full PCR cycle is run uninterrupted, enabling a probabilistic projection of coastline development.

Limitations

On the other hand, the result of this framework can not be expected to be entirely accurate, since no interaction between cross-shore and longshore processes is taken into account. In addition, the framework can result in larger uncertainties than usual due to the fact that two separate models are used - instead of one single model. Another important element of this framework is how the time series are combined in a probabilistic way: are all PCR time series combined with one ShorelineS time series, or is one specific CDF value from PCR used to combine with ShorelineS? Or, would it be possible to obtain a probabilistic output out of ShorelineS? These questions are further discussed in the next paragraphs.

Probabilistic component

As can be seen in Figure 4.1, only the PCR model is studied probabilistically, where the simulation is run for thousands of times to generate a CDF curve. For ShorelineS, this is assumed not to be possible in the proposed framework. It is evident that it is still desired to obtain the final prediction of the coastline evolution in a probabilistic way, thus including a bandwidth representing the uncertainty in the projections. This bandwidth can help with optimizing designs in projects in coastal areas. Hence, a decision has to be made between one of the two following options:

1. **Only PCR model probabilistic**

   The PCR model can be implemented as originally intended, meaning that thousands of simulations and thus thousands of time series of the shoreline position are modelled. Regarding ShorelineS, only one simulation is run and the obtained time series is added to each of the time series from PCR. A final CDF curve is generated which comprises a probabilistic estimate of cross-shore coastline development and a deterministic estimate of the longshore part.

2. **Both models probabilistic**

   The second option is that the ShorelineS model is also simulated thousands of times, with different (simplified) wave climates as input. To enable this, some assumptions have to be implemented, as discussed in Section 2.4.3. From this, the coastline changes induced by gradients in LST can be derived in a probabilistic way as well. The time series of both models can be added in each possible combination to generate a final CDF curve of coastline development. It is noted that this option is only viable if it is feasible to run the ShorelineS model for multiple times, considering the large computational time it might require.

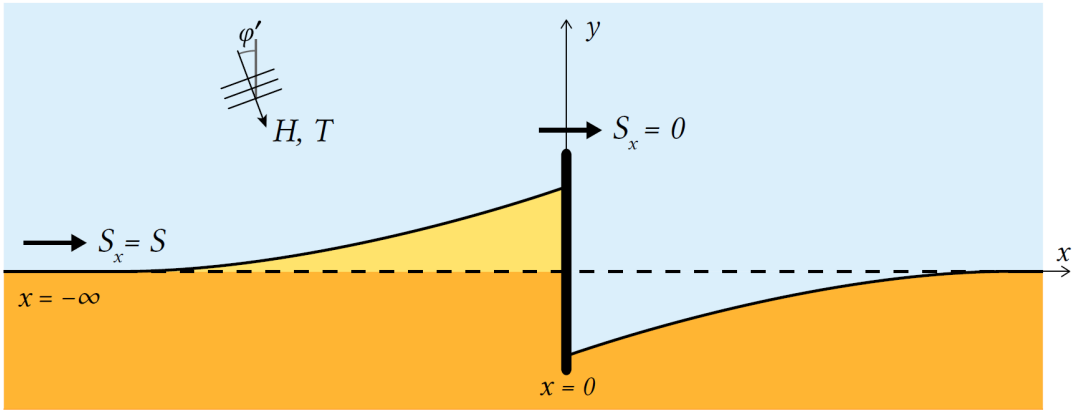

Figure 4.2: Principle of the shoreline response after interruption by a structure (Bosboom & Stive, 2021).

Cross-sections of interest

The origin of this framework is based on the concept of coastline behaviour after interruption by a coastal structure, as significant coastline displacement can occur: see Figure 4.2. An important point of attention for combining PCR and ShorelineS is that multiple cross-shore profiles at multiple locations along the coast will have to be modelled, since the PCR model only simulates the displacement of a single cross-shore profile at a specific point on the coastline. ShorelineS models the full coastline. From the Shorelines output, it is important that the coastline evolution at certain transects is obtained carefully.

An indication of the transects of interest is given by the red dashed lines in Figure 4.3, for the example case of a coastline interrupted by a structure (Figure 4.2). In addition, the coastline evolution at these particular transects is also depicted. For coastal zone management purposes, special attention is most likely paid to the erosive side of the breakwater. The land use of that specific coastal zone determines the design requirements.

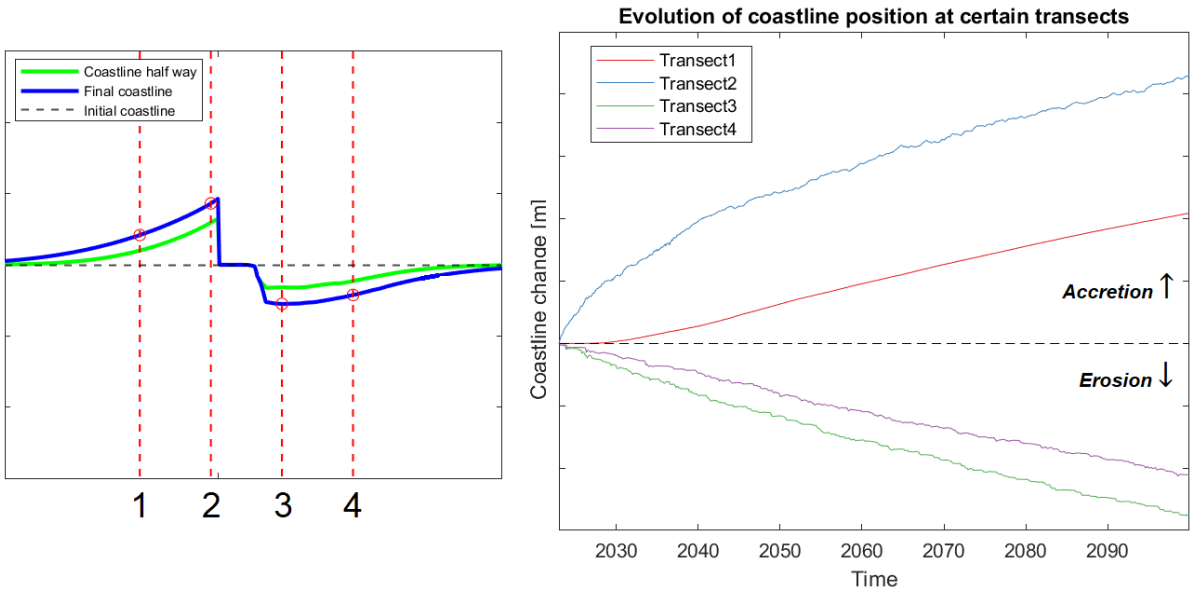

Figure 4.3: Example case showing coastline evolution of transects of interest, modelled in ShorelineS.

4.2. Framework 2: longshore response

Varying coastline orientation due to storm erosion induces changes in the LST rates and thus in LST gradients. To implement this, ShorelineS is used as the main model in Framework 2. The cross-shore erosion - obtained from the PCR model - is implemented as a sink during the regular ShorelineS simulation. Herein, the coastline evolution due to storms, subsequent recovery and SLR is simulated with the PCR model as usual. These probabilistically obtained changes are stored in a large data set, from which random samples are taken as a ”sink” within the ShorelineS simulation. This sink element is translated to an extra change in coastline in the ShorelineS model, after which the regular ShorelineS simulation continues. An important point of attention is the frequency with which the sink is applied: the sampling can be done yearly, or a few times per year (corresponding to the occurrence storm events). A schematic of the framework is presented in Figure 4.4.

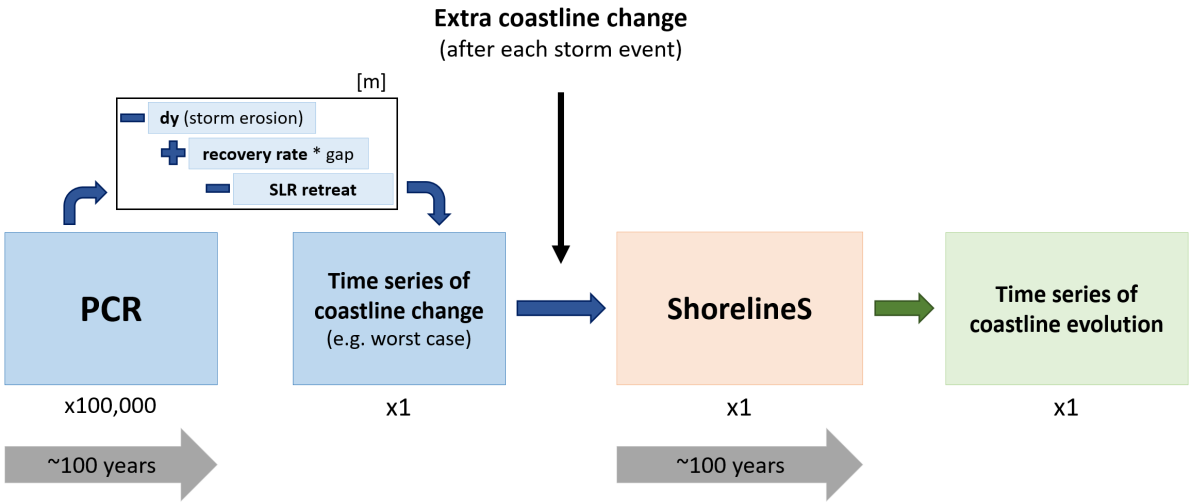

Figure 4.4: Cross-shore shoreline change (from PCR) added as a sink in the ShorelineS simulation: Framework 2.

Advantages

This method is also quick and easy to use, since PCR and ShorelineS are still implemented separately. In addition, cross-shore erosion is taken into account in the computations of LST-gradient-driven shoreline evolution, even during the simulation period. Therefore, this approach involves both cross-shore and longshore processes.

Limitations

The reason why this framework might be inapplicable for some specific purposes is the fact that the final output is not probabilistic. Although the data set with cross-shore storm erosion is obtained in a probabilistic way, the sampling of erosion values as a sink in only one ShorelineS simulation will result in only one final prediction of the coastline evolution. Moreover, it is difficult to determine when and how often the ”sink” element is implemented in ShorelineS for a realistic representation. Lastly, with this approach it is still assumed that changes in orientation (due to LST gradients) do not affect cross-shore storm erosion and more importantly, that no changes in coastline orientation are induced by a storm event.

4.3. Framework 3: cross-shore response

Framework 3 includes the response of storm erosion to changes in coastline orientation, which were induced by gradients in LST. In other words, different storm erosion occurs for different incoming wave directions. The eroded beach/dune volume and coastline retreat during a storm is calculated with a specific erosion function which is applicable for the studied site. This erosion function can include the direction of the incoming waves, i.e. the wave angles. If so, the amount of erosion and coastline retreat changes with varying coastline orientation. It is thus important that this effect is accounted for when modelling long-term shoreline evolution. More information on such an erosion function is presented in Section 3.2.4.

The implementation of this framework, as depicted in Figure 4.5, means that actual changes in shoreline orientation have to be incorporated in the erosion function and thus within the PCR simulation cycle. Those actual changes can be derived by the time series of shoreline position obtained from ShorelineS. The main challenge is to decide how often this ”feedback” from ShorelineS is needed to be given to the PCR model; this can be for every storm event, or just for every simulated year, or even less often.

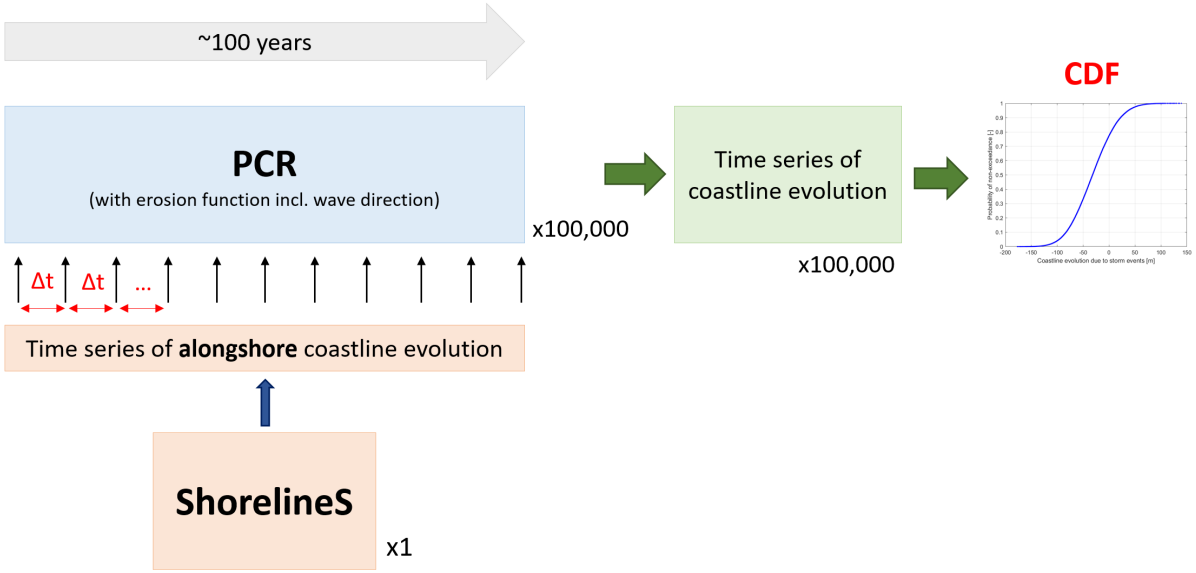

Figure 4.5: Schematic to incorporate cross-shore and longshore interaction in the PCR model: Framework 3.

Advantages
It is highly useful that both models can still be used individually, significantly reducing computational time. Furthermore, using this approach, interacting effects between cross-shore and longshore processes are taken into account due to the fact that the calculation of storm erosion does not neglect (changes in) coastline orientation. This is expected to result in more accurate projections of shoreline evolution.

Limitations
As already mentioned above, a point of concern is the frequency with which the coastline orientation changes are implemented in PCR, i.e. how large Δt is. This will largely influence the computational effort and time of this framework. Hence, it is crucial to find an acceptable balance between the desired resolution (spatial and temporal scales) of the modelled case and the required calculation time. Also, in order to detect the changes in coastline orientation, at least three cross-sections have to be modelled in PCR. Otherwise, only the cross-shore displacement of the coastline is taken into account. This introduces more modelling work and thus time. Lastly, in this framework, the long-term ShorelineS simulation of coastline evolution induced by LST gradients neglects potential influences of (cross-shore) storm erosion.

4.4. Framework 4: coupled modelling

The last framework intends to fully implement the interaction between cross-shore and longshore processes. It is based on the method used by Krijnen (2021), which was introduced in Section 2.4.6. This method couples a cross-shore and longshore model, by enabling feedback between the models during both their simulation periods.

The described method forms the base for Framework 4 and is described as follows (see also Figure 4.6):

1. First, a coastline is modelled with the longshore model, resulting in a coastline change for a particular time step;
2. This result is used as the initial coastline position for the cross-shore model, which models the coastline change for the same time step (multiple time steps might be needed to ”catch up” with the longshore time step);
3. The output of the cross-shore model is then used for the next modelling step of the longshore model, and so on;
4. This feedback loop is repeated until the desired simulation period is modelled.

The key challenge for this framework is to determine the length of the modelled time steps, i.e. to decide how frequently the coupling takes place and how frequently the models provide feedback to each other. Evidently, this depends on the desired simulation period. It must be taken into account that this approach requires considerable computational time and effort.

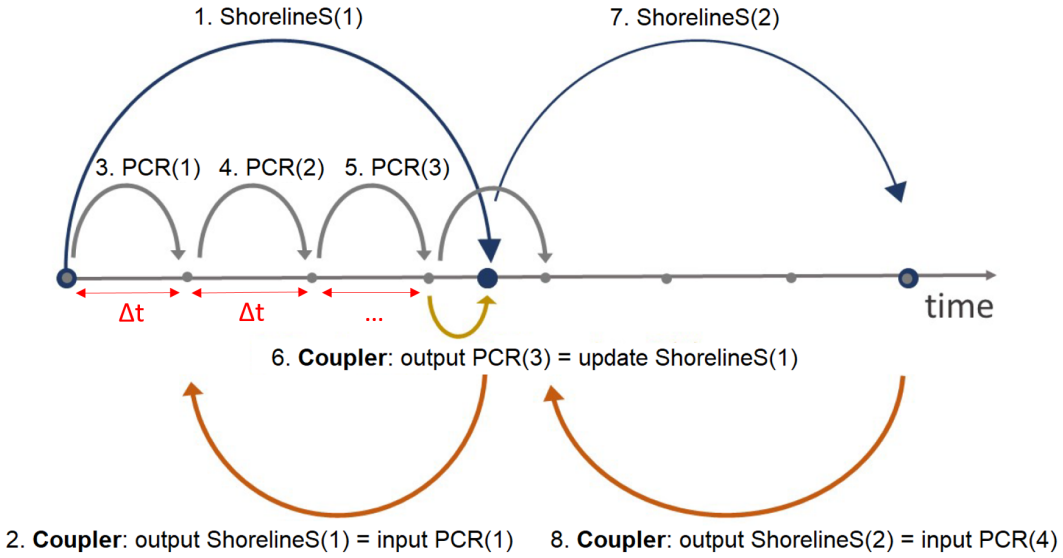

Figure 4.6: Schematic overview to couple PCR and ShorelineS: Framework 4 (modified from Krijnen (2021)).

Advantages
Although dependent on the frequency with which the models are coupled, this framework enables full coupling of cross-shore and longshore processes. It is expected to result in a highly accurate output. To let those processes fully interact, ideally, both models are coupled after each storm event or even every hour of the day. However, even by coupling the models every year or after 10 or 20 years, a significant increase in prediction accuracy is expected for this method.

Limitations
A major drawback of this framework is the considerable computational time and effort, since both models have to be used multiple times. It is also very difficult to determine when and how often the models are coupled (for a balance between efficient modelling and realistic representation). It is advised to only implement this approach if highly accurate predictions are required and, more importantly, if it is certain that cross-shore and longshore interactions are present at, and important for, the studied site.

4.5. Key points of Chapter 4

- This chapter proposes four different frameworks to combine cross-shore and longshore processes in long-term coastline modelling in a stochastic way.
- Framework 1 combines the individual results of the predicted cross-shore and alongshore coastline evolution. Special attention has to be paid to the combination of the probabilistic character of the cross-shore estimates and the deterministic projections of the longshore component. An advantage is that this is a very quick method.
- Framework 2 models the response of the longshore coastline displacement to the storm-induced retreat by implementing the cross-shore-induced coastline change as a sink during the regular ShorelineS simulation. An important element is the frequency with which the sink is applied.
- Framework 3 incorporates the longshore-induced changes in coastline orientation into the calculation of the storm-induced coastline retreat. For this method it is required that the implemented erosion model includes the incoming wave direction as an input parameter.
- Framework 4 proposes a fully coupled model, in which the individual cross-shore and longshore model provide feedback to each other after a certain defined time step.

5

Model application: IJmuiden

As introduced in Section 1.4, the research framework is applied to a case study of the coastline near IJmuiden. In this chapter, the implementation of the models for the IJmuiden case study is presented and discussed.

The developed Framework 1 is tested for a real case: the coastline near IJmuiden. This coastline is particularly interesting due to the presence of a port entrance channel including large breakwaters (see Figure 5.1). These breakwaters completely block the longshore sediment transport (LST) and as a result, gradients in LST exist. The response of the coastline to these gradients is aimed to be modelled in this case study. The full IJmuiden coastline is implemented in ShorelineS (see Figure 5.13). Moreover, the long-term evolution of this coastline under influence of storm events and sea level rise (SLR) is studied with the PCR model.

Figure 5.1: Aerial photograph of the Port of IJmuiden (by Rob van Zeist, obtained from Krijnen (2021)).

5.1. PCR model implementation

The PCR model is applied to the IJmuiden coastline. In this section, all relevant input data and the PCR model components are presented and discussed. First, in Table 5.1, an overview is given of the determined input for the PCR model implementation.

Table 5.1: PCR model: input conditions for the IJmuiden application.

Input	Value
Wave data	Offshore data (YM6, depth 23.2 m MSL)
Water level data	Deep water data (depth 8 m MSL)
Dune crest height	19 m +MSL
Dune toe elevation	3 m +MSL
Beach slope	0.025 (1:40)
Erosion model	Dunerule model
Recovery rate approach	Equilibrium with median retreat
SLR scenarios	No SLR; RCP2.6; RCP6.0; RCP8.5

5.1.1. Wave and water level data

For the wave and water level data, data sets are used from measurement stations in front of the Dutch coastline as indicated in Figure 5.1. The data is provided by Deltares (Bas Huisman, personal communication, November 15, 2022). These data are 3-hourly measurements for the period of 1994 to 2021. From these data, individual storm events can be identified and their characteristics can be analysed, as was introduced in Section 3.2.3.

For the PCR model, the offshore wave climate is used as input, since the implemented erosion model (i.e. Dunerule) is based on offshore wave conditions (see also Section 5.1.3). The wave data were also transformed to a nearshore wave climate at 8 m depth using the SWAN wave model (Booij et al., 1999, as cited in (Hallin et al., 2019)). These conditions are used as input for the ShorelineS model. This will be elaborated in Section 5.2.

In Figure 5.2, the wave rose of the used offshore wave data in the PCR model is depicted. The wave data were measured at the YM6 wave buoy (IJmuiden Munitiestortplaats, 52.55°N, 4.058°E, see red circle in Figure 5.1) in front of the IJmuiden coastline at a depth of 23.2 m MSL. The simulated wave climate is dominated by waves from WSW to N. The average wave height during the simulation period is 1.06 m and the maximum wave height is 6.94 m. The average peak wave period is 5.74 s and the peak period is 22.97 s. The maximum observed still water level is 2.74 m +MSL.

5.1.2. Synthetic storm time series

Storm identification
In order to generate the synthetic storm time series (SSTS), first the storm events are detected from the data set according to Figure 3.3. Here, a storm event is defined to be the period in which the measured wave height is above the threshold of the 97th-percentile value of the wave height data: 3.32 m. In addition, the minimum water level to be identified as a storm event is 0.50 m +MSL. In this case, from this definition and the used data, the total number of storms per year is calculated to be 9.45, which seems to be reasonable for its location (i.e. the Dutch coast). The wave data is provided in time steps of 3 hours, so a duration of 1.5 hours is added to both ”sides” of a detected storm event (so 3 hours added in total). In other words: if two successive measurements show a wave height above the threshold, with a 3-hour time step in between them, the duration of the detected storm event is taken as 6 hours, not as 3 hours.

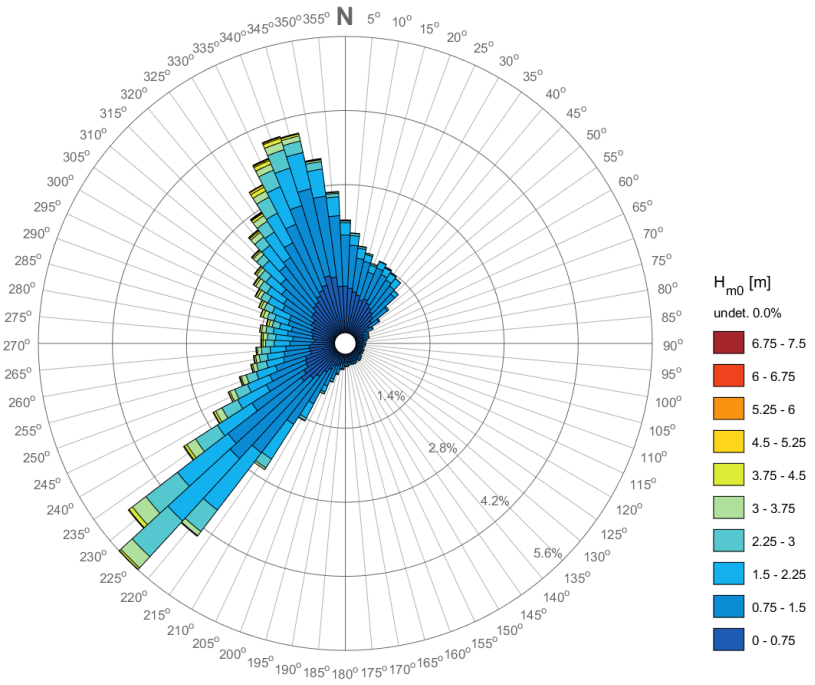

Figure 5.2: Wave rose of offshore significant wave height at 23.2 m depth, from wave buoy YM6 in front of the IJmuiden coastline.

Statistical analysis

For the statistical analysis of the identified storm events, first, the significant wave height and storm duration are analysed. Based on the optimum of the Curve Fitter function in Matlab, the maximum significant wave height per storm event and the storm duration are both fitted with a Gamma distribution (see Figure 5.3). Note that in Figure 5.3b only 3-hourly duration values are visible due to the 3-hourly wave data; each plotted dot represents multiple detected storm event durations. More importantly, a dependency is seen between the maximum significant wave height and the storm duration, with the higher waves occurring during the longer storms. In order to describe this relationship, a dependency distribution is generated using a copula method. A copula is a multivariate probability distribution which is able to correlate two (or more) variables without changing their marginal distributions (Li, van Gelder, Ranasinghe, et al., 2014). A joint cumulative distribution function (CDF) is fitted between the two variables, as shown in Figure 5.4a.

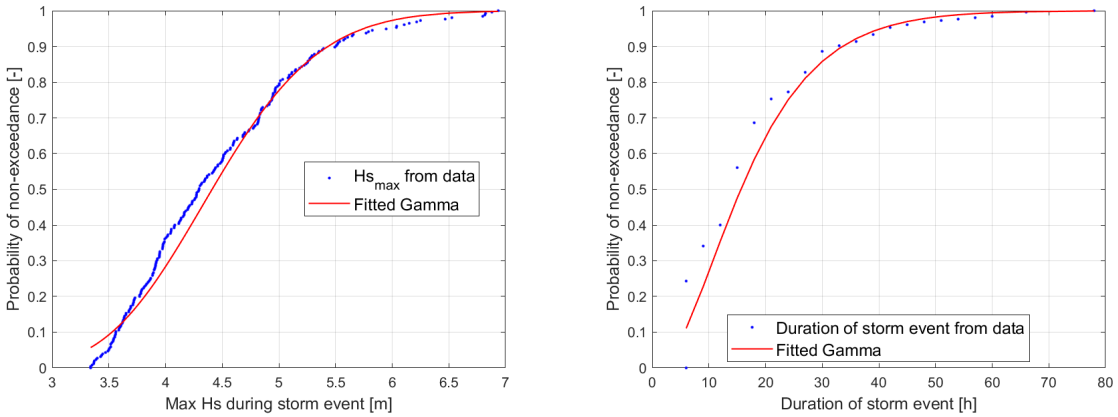

(a) CDF fitted to maximum Hs during storm event.

(b) CDF fitted to duration of storm events.

Figure 5.3: Fitted distributions for wave height and storm duration.

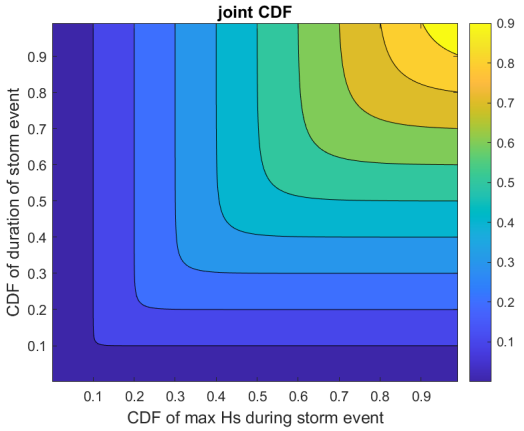

(a) Joint CDF of maximum Hs and storm duration using Clayton copula method.

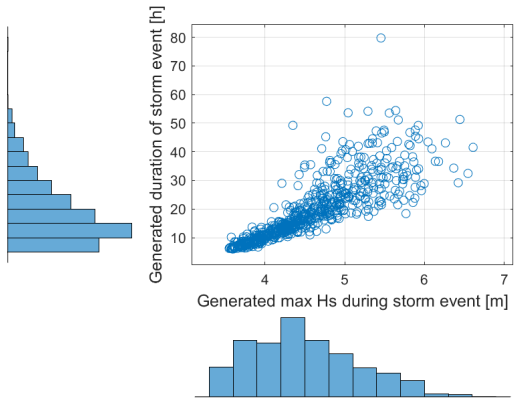

(b) Generated values of maximum Hs during storm event and storm duration.

Figure 5.4: Dependency distribution and sampled values of maximum Hs during storm event and storm duration.

In this study, the Clayton copula method is chosen for creating the joint CDF between max Hs during a storm event and the storm duration. This decision is based on the correlation coefficient, which is a measure of the linear dependence between two random variables. The criterion is that the correlation coefficient of the generated samples is closest to the correlation coefficient of the initial pair of data sets of the variables (which is 0.4509). Different copula families such as Gumbel, Clayton and Frank are tested, and Clayton gives the best fit. Eventually, Figure 5.4b shows the generated values of the max Hs during a storm event and the storm duration for the SSTS.

Regarding the water level, it was also studied if a dependency between the max Hs during a storm event and the water level exists. From the analysis as shown in Figure 5.5a and the correlation coefficient being very low (i.e. 0.2082), it was concluded that no noteworthy dependence is present between the variates. Hence, in this study, only the joint probability between the maximum significant wave height during a storm event and the storm duration is considered. For the water level, eventually, also a Gamma distribution is fitted to the observed water level data (Figure 5.5b). For each storm event, a value is sampled from this fitted distribution.

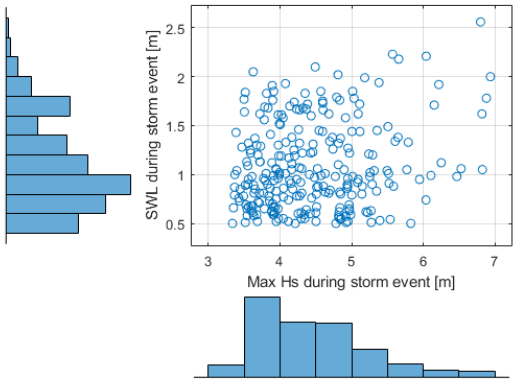

(a) Observed values of maximum Hs during storm event and water level.

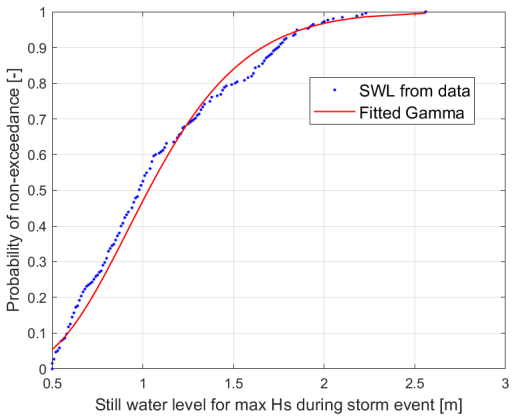

(b) CDF fitted to water level parameter.

Figure 5.5: Fitted distribution for water level and observation of max Hs and water level.

Furthermore, a linear function is fitted to link the wave height and wave period (Figure 5.6a). For each maximum wave height that is drawn when generating the synthetic storm time series, the corresponding value for the peak wave period is drawn from this fitted linear function.

Lastly, the wave direction is not related with any variable. It has a weak correlation with the other variates. An empirical distribution function is fitted for the wave direction. This is shown in Figure 5.6b, in which the weak dependency between wave direction and the detected max Hs is visible as well. So, for the wave direction, it is seen that its extreme values have little impacts on the consequences induced by the extreme storm events. Therefore, the empirical distribution is an acceptable option to account for the wave direction in the generation of the synthetic storm time series.

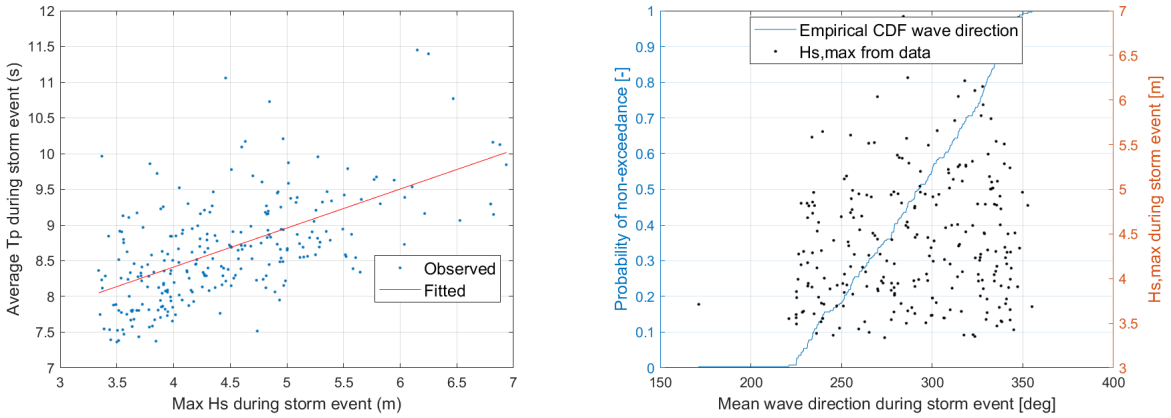

(a) Fitted linear function for maximum Hs during storm event and peak wave period.

(b) Empirical CDF of wave direction and observation of wave direction vs. max Hs.

Figure 5.6: Fitted distributions for peak wave period and wave direction.

Spacing in between storm events

Regarding the gaps between storm events, the storm event frequency is analysed from the wave data set for the period of 1994 to 2021, according to the established storm definition. It was derived that the number of observed storm events varies per month, hence the gaps in between storm events vary monthly as well. This is shown in Figure 5.7. A very clear seasonality effect is observed: between September and March, the average number of storms is considerably larger than in the summer months.

From this observation, it was decided to fit a non-homogeneous Poisson distribution to the gaps between storm events. This means a monthly varying λ parameter is implemented, to reproduce the storm seasonality. The generated gap after a storm event directly depends on the specific month in which the storm event takes place. By manually calibrating this λ parameter, eventually the total number of storms was modelled successfully (see Section 6.1.1 for the validation).

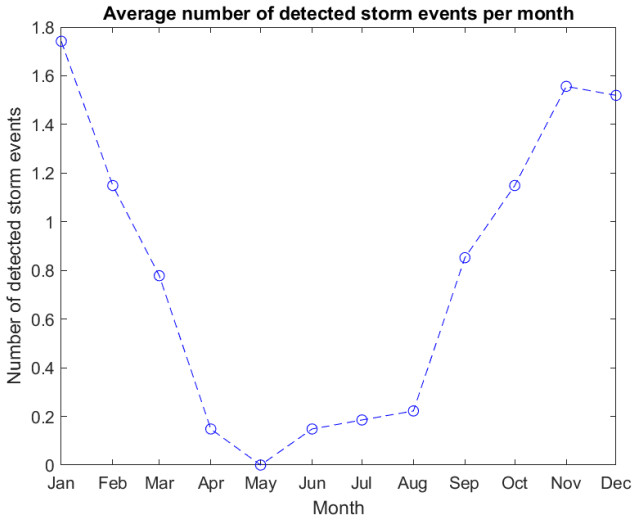

Figure 5.7: Average number of observed storm events per month in the period of 1994-2021.

Generation of the storm time series
Finally, to generate the storm event time series, it is decided to simulate the period from 01/01/2023 to 01/01/2100, so 77 years. Taking into account 10 storms per year (as was obtained from the data earlier), this means a total number of 770 generated storms. The generation process is as follows:

1. First, two random numbers are generated from the joint CDF of max Hs during storm event and the storm duration using the fitted copula (Figure 5.4a): one for the probability of exceedance of the max Hs, one for the probability of exceedance of the storm duration;
2. Consequently, the values for the generated Hs and duration are obtained from their individual cumulative distributions using the generated probabilities (Figure 5.4b);
3. The water level is derived from the fitted Gamma distribution (Figure 5.5b);
4. Next, the Tp is retrieved from the fitted Hs-Tp linear function (Figure 5.6a) corresponding to the generated Hs;
5. Then, the wave direction is sampled from its empirical distribution (Figure 5.6b).
6. Lastly, after each generated storm event, the gap between the generated storms is sampled from the non-homogeneous Poisson distribution, based on the month in which the storm occurs.

This way, a database of storm characteristics is obtained for the total simulation period of 77 years with 10 storms per year. Each storm event consists of a wave height, a duration, a water level, a peak wave period and a mean wave direction (see also Figure 3.4).

5.1.3. Erosion model

For the IJmuiden case, it is decided to use the Dunerule model to simulate the storm erosion. The reason for this is the calibration and validation with measured and observed dune erosion volumes during storm events from literature (de Vries et al., 2012). The Dunerule erosion model is based on the significant offshore wave height, as was introduced in Section 3.2.4. The eroded dune volume R is calculated according to:

$$R = 153 \cdot A_{dir} \cdot \left(\frac{h}{5}\right)^{\alpha_1} \cdot \left(\frac{H_{s,max}}{7.6}\right)^{\alpha_2} \cdot \left(\frac{D}{5}\right)^{\alpha_3} \cdot \left(\frac{T_p}{12}\right)^{\alpha_4} \tag{5.1}$$

in which $\alpha_1 = 1.5$ for $h \leq 5$ and $\alpha_1 = 0.2$ for $h > 5$, $\alpha_2 = 0.3$ for $H_{s,max} \leq 7.6$ and $\alpha_2 = 0.9$ for $H_{s,max} > 7.6$, $\alpha_3 = 0.3$, $\alpha_4 = 1.3$ for $T_p \leq 12$ and $\alpha_4 = 0.9$ for $T_p > 12$.

Moreover, the coefficient A_{dir} is expressed as:

$$A_{dir} = \begin{cases} 1 - 0.01 \cdot (270 - \theta) & for\ \theta \leq 270; \\ 1 - 0.01 \cdot (\theta - 326) & for\ \theta \geq 326; \\ 1 - 0.0107 \cdot (26 - |\theta - 298|) & for\ 270 < \theta < 326. \end{cases} \tag{5.2}$$

Finally, the calculated eroded volume R is converted to the coastline retreat Δy [m] as follows:

$$\Delta y = \frac{R}{h_D - h} \tag{5.3}$$

The dune crest height h_D is set to 19 m +MSL. This was derived from JARKUS data (Rijkswaterstaat, 2022), which is depicted in Appendix A, and it is also in line with previous studies to the IJmuiden coastline (Hallin et al., 2019; Krijnen, 2021). h is the maximum water level during the particular storm event [m].

5.1.4. Coastline recovery

Following the method as described in Section 3.2.5, a constant recovery rate for the specific site of IJmuiden is computed. The dune erosion model is used to model the final coastline erosion after the 2023-2100 simulation period, assuming that no SLR occurs. This process is repeated 100,000 times, with a new synthetic storm time series for every new simulation. In this study, consequently, it is assumed that the probability of exceedance for the initial coastline to remain as it is should be 50%; i.e. an equal probability of accretion or erosion. This was also observed by de Vries et al. (2012), who concluded for the Dutch coast that the total erosion of storm events is of similar order as the measured beach growth.

Eventually, the coastline recovery rate is determined to be 6.6181 m/year. This is equal to approximately 0.34 m^3/m/day, taking into account a dune crest height of 19 m +MSL, which was assumed for the IJmuiden case study. This value is in line with the findings of Li, van Gelder, Vrijling, et al. (2014), who adopted the same method for the Dutch coastline near Noordwijk and found a constant recovery rate of 0.3 m^3/m/day. Taking into account a dune height of 18 m +MSL (representative for Noordwijk coastal profile), this would be equal to approximately 6.0875 m/year. It can thus be concluded that the calculated recovery rate in this study is of the same order of magnitude.

5.1.5. Sea level rise

In order to include the large uncertainty of SLR into the coastline evolution projections, multiple SLR scenarios are implemented in this study. As was introduced in Section 3.2.6, two processes are induced by rising sea levels: an extra coastline retreat due to the elevated water level and an increased storm erosion due to larger water depth (i.e. waves breaking closer to the shoreline). These effects were studied for four scenarios: one scenario without SLR and three including SLR, of which the SLR rate depends on the specific RCP as defined by IPCC (Wong et al., 2014). See also Figure 5.8. In this research, RCP2.6, RCP6.0 and RCP8.5 are implemented and the corresponding SLR curves are derived by using the intermediate assessment method of Nicholls et al. (2011) according to Equation 5.7. The obtained SLR curves for RCP2.6 and RCP8.5 were shown in Figure 5.9.

The first described process is implemented by superimposing an additional coastline retreat due to SLR on the retreat caused by a storm event. This happens right before each new storm event occurs. The SLR-induced coastline retreat is based on the water level at that specific date and is calculated according to Equation 5.4, in which the slope for the IJmuiden coastline is determined to be 0.025 (i.e. 1:40) according to JARKUS data (Rijkswaterstaat, 2022):

$$R_{SLR} = \frac{WL(next\ storm) - WL(previous\ storm)}{slope} \tag{5.4}$$

Next, the second described process is implemented in the PCR model by increasing the water level parameter in the Dunerule erosion model. The increased water level can be implemented in the calculation of the erosion volume as well as in the corresponding calculation of the coastline retreat, as can be seen in Equations 5.5 and 5.6:

$$R = 153 \cdot A_{dir} \cdot \left(\frac{h + SLR}{5}\right)^{\alpha_1} \cdot \left(\frac{H_{s,max}}{7.6}\right)^{\alpha_2} \cdot \left(\frac{D}{5}\right)^{\alpha_3} \cdot \left(\frac{T_p}{12}\right)^{\alpha_4} \tag{5.5}$$

$$\Delta y = \frac{R}{h_D - (h + SLR)} \tag{5.6}$$

However, it is found that the calculated erosion volume in Equation 5.5 is extremely sensitive to the increased water level. This is further discussed in Appendix B, in which is shown that this process leads to unrealistic values of coastline retreat. This sensitivity was already discussed by Van Rijn (2013a), who concluded that the water level is actually one of the two most influential parameters of the Dunerule model. The same phenomenon was also found by Bitaki (2019).

An explanation for this remarkable sensitivity could be that the coastal profile will most probably adapt to the SLR. The newly formed coastal profile will be significantly more resistant to the increased storm intensities, just like the post-storm coastal profile can withstand storm impact much better (see also Section 2.3.1). This adaptation process is not incorporated in the erosion function, hence the peculiar results.

As a result, it is decided to only include the increased water level in the final calculation of the coastline retreat in Equation 5.6, additional to the separately determined SLR-induced coastline retreat in Equation 5.4. The elevated water level is not taken into account in the calculation of the dune erosion volume (Equation 5.5); the eroded volume is still calculated with Equation 5.1. So, in summary, both described effects of SLR on coastline erosion are considered in this study, albeit in an adjusted way.

SLR projections

For the exact values of the changes in MSL, different scenarios are considered, based on the Representative Concentration Pathways (RCP) of sea level change determined in the Fifth Assessment Report (AR5) of IPCC (Church et al., 2013). The corresponding SLR projections include large uncertainty due to the difficulty of predicting future emission scenarios, see Figure 5.8. Global SLR projections are assumed to be relevant in this research, and multiple RCPs are studied. It is assumed that the SLR at January 1, 2023 is zero, since the modelled projections of coastline change are relative to the coastline position of that reference date. In addition, no land subsidence is considered. The median values of the IPCC SLR scenarios are directly used.

Emission scenario	Representative Concentration Pathway (RCP)	Mean sea level rise (m)	
		2046–2065	2100
Low	2.6	0.24 [0.17–0.32]	0.44 [0.28–0.61]
Medium low	4.5	0.26 [0.19–0.33]	0.53 [0.36–0.71]
Medium high	6.0	0.25 [0.18–0.32]	0.55 [0.38–0.73]
High	8.5	0.29 [0.22–0.38]	0.74 [0.52–0.98]

Figure 5.8: Projections of global mean SLR relative to 1986–2005 (modified from Wong et al. (2014)): the median values as well as the 5-95% range.

In order to obtain SLR time series and curves, the method of Nicholls et al. (2011) is used, which has also been implemented in previous PCR studies (Dastgheib et al., 2022). In this method, the SLR over time is obtained by fitting the following equation to the available SLR data from AR5L:

$$SLR = a_1 \cdot t + a_2 \cdot t^2 \tag{5.7}$$

in which:

SLR	mean sea level rise [m]
t	number of years starting from 2023 [y]
a_1	rate of sea level rise at year 2023 [m/year]
a_2	factor of the change in rate of sea level rise [m/year^2]

See Figure 5.9 for the derived curves of sea level rise.

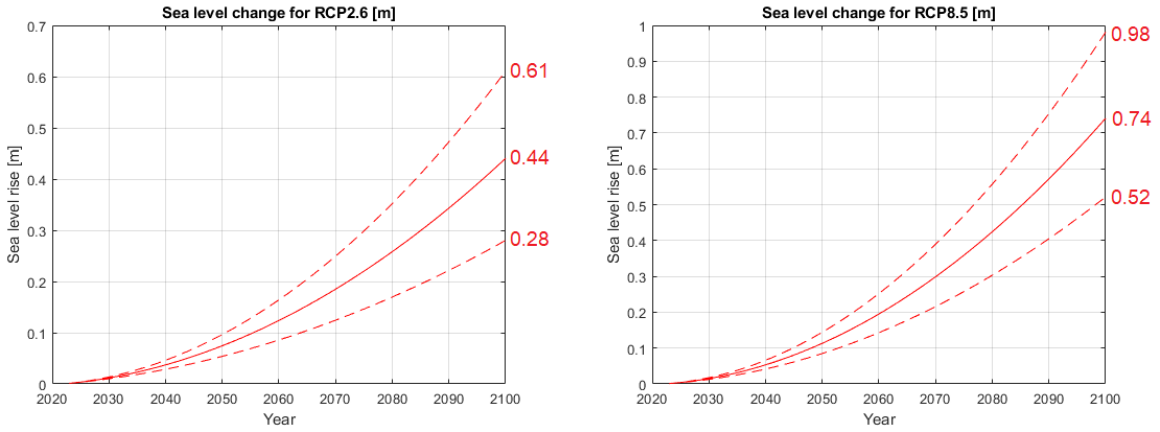

(a) Sea level rise curve for RCP2.6.

(b) Sea level rise curve for RCP8.5.

Figure 5.9: Sea level rise curves obtained by Equation 5.7: median value and 5-95% ranges.

5.1.6. PCR modelling loop

After every single component of the PCR model has been defined, the modelling cycle is initiated, as described in Section 3.2.7 and Figure 3.2. In this IJmuiden case study, the PCR model is simulated 100,000 times, resulting in 100,000 time series of coastline evolution for the 77-year period of 2023 to 2100. From these time series, 100,000 most landward coastline positions over time (relative to the initial coastline position of x = 0 m) are detected and statistically analysed into a cumulative distribution function (CDF). The convergence at the 0.01% probability of exceedance level is achieved, which was expected for the large number of simulations. This is further visualised and explained in Chapter 6, in which the results of the PCR model are presented.

5.2. ShorelineS model implementation

For the alongshore coastal dynamics, the ShorelineS model is applied to the IJmuiden coastline. In this section, all relevant input data are presented and discussed. First, in Table 5.3, an overview is given of the determined model input.

Table 5.3: ShorelineS model: input conditions for the IJmuiden application.

Variable	Input
Wave data	Representative wave climate (-7.8 m MSL)
Active profile height	8.3 m
Depth of closure	-5.3 m MSL
Dune toe elevation	+3 m MSL
Sediment transport formula	CERC1, calibration factor b = $1 \cdot 10^6$
Diffraction method	Kamphuis
Initial space step	100 m

5.2.1. Wave data

For the ShorelineS model, wave data at a depth of 7.8 m is used. The location of the wave climate is depicted in Figure 5.10 in green (i.e. Transect 12). In Figure 5.11, the wave rose of the used wave data is shown. The data is based on measured offshore wave data at 23.2 m depth MSL (see Section 5.1.1) and is transformed to a nearshore wave climate at 7.8 m depth. The simulated wave climate is dominated by waves from WSW to WNW. The average wave height during the simulation period is 0.75 m and the maximum wave height is 4.08 m. The average peak wave period is 5.29 s and the peak period is 14.56 s. The maximum observed still water level is 3.06 m +MSL.

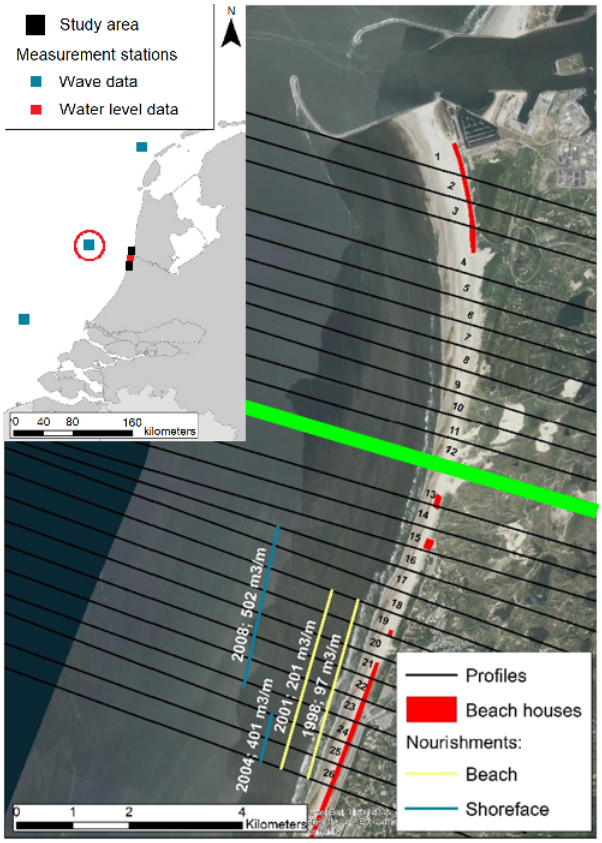

Figure 5.10: Location of extracted wave climate: Transect 12 in green (from Hallin et al. (2019)).

Representative wave climate
As input into the ShorelineS model, a representative wave climate is generated, in order to reduce computational time. Due to the long-term focus of this study, it is acceptable to use a reduced wave climate, as was discussed in Section 2.4.3. The reduced wave climate is derived based on the wave energy flux by dividing the wave energy into 50 separate bins. This is depicted in Figure 5.12. The black dots represent the 50 obtained wave conditions which form the representative wave climate. The magnitude of the black dot corresponds to the relative contribution of that particular wave condition within the representative wave climate. In the ShorelineS simulation, every time step a wave condition is sampled from the reduced wave climate according to this relative contribution. Hence, in this application, the wave condition with a wave height of approximately 0.5 meter and a wave direction of 330°N (i.e. the largest black dot) is sampled more often than one of the wave conditions with a wave direction between 250-300°N.

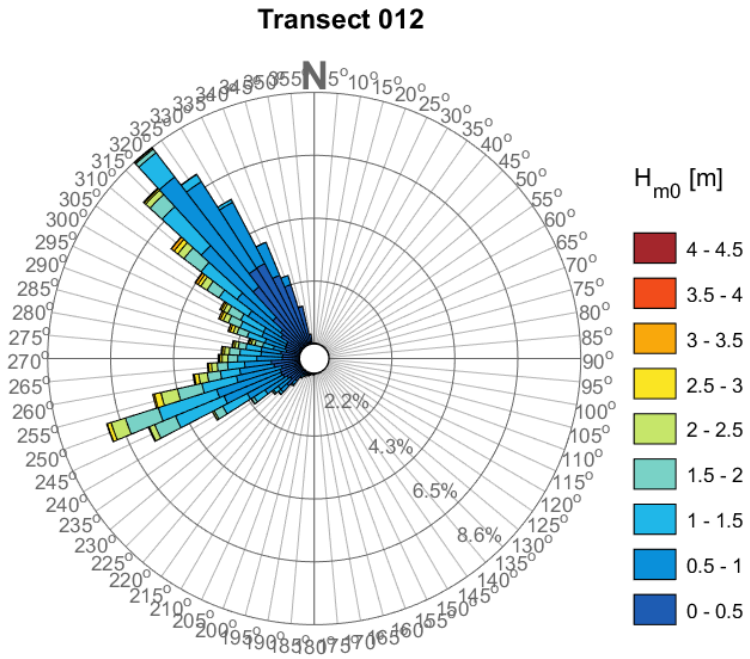

Figure 5.11: Wave rose of significant wave height at 7.8 m depth for Transect 12.

5.2.2. Coastline and structure positions

The positions of the IJmuiden coastline, as well as the breakwaters, were implemented in the ShorelineS model as depicted in Figure 5.13. Here, the (initial) coastline position in 1967 is visible, as well as the observed positions of the coastline in 1985 and in 2007. The implemented coordinate system is Amersfoort / RD New (EPSG 28992), which is a projected Cartesian (metric) system applicable for The Netherlands.

5.2.3. Active profile height

The active profile height is assumed constant in the ShorelineS model (see Sections 3.3 and 3.4). The active profile height is the sum of the closure depth and the dune toe elevation. The dune toe elevation is assumed to be 3 m +MSL according to JARKUS measurements (Appendix A) as well as other field measurements found in literature (de Vries et al., 2012; Rijkswaterstaat, 2022). The depth of closure (DoC) depends on local wave conditions and can be calculated by the Hallermeier equations (see Equations 3.12 and 3.13 in Section 3.3). However, the used wave data in the ShorelineS model is specifically extracted for a certain transect (Figure 5.10). Hence, to ensure uniformity over the total modelled coastline, a constant value of -5.3 m MSL is used. This value is based on the research of Hallin et al. (2019), who used this closure depth along the full coastline of IJmuiden based on field measurements and literature. Eventually, the total active profile height is 8.3 meters.

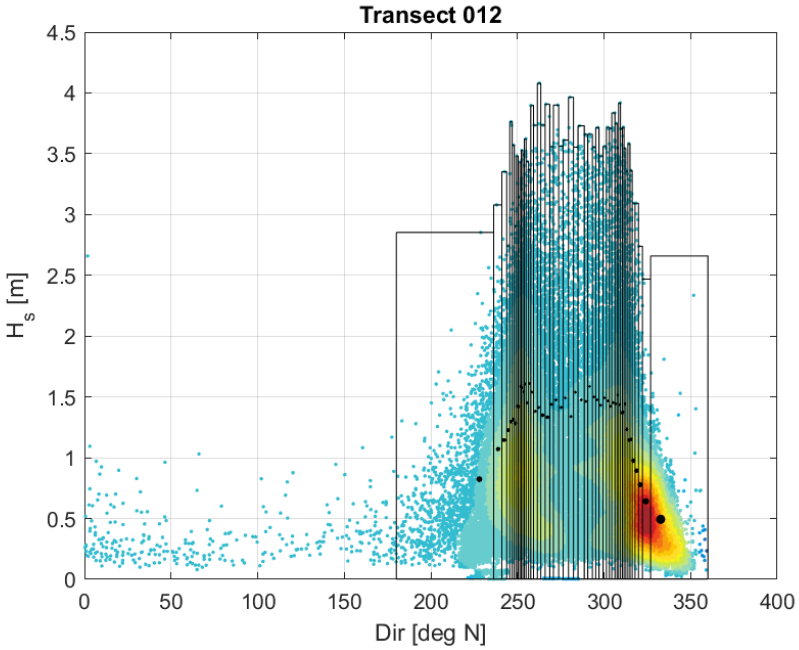

Figure 5.12: Representative wave climate based on wave energy flux (final wave conditions indicated by black dots).

5.2.4. Transport formulation

Regarding the calculation of the sediment transport volumes, it is chosen to implement the simplified CERC1 formula of USACE (1984). The formula is depicted in Equation 5.8. The main reason for this decision is the computational time and the model stability. Multiple transport formulations were implemented, leading to extremely large simulation time and/or numerical instabilities in which the coastline formed unrealistic spikes. The latter was most likely caused by too large spatial steps, leading to incorrect longshore transport volumes and gradients, and thus to incorrect coastline change.

$$Q_s = b \cdot H_{S0}^{5/2} \cdot \sin 2(\phi_{loc}) \tag{5.8}$$

One of the drawbacks of the CERC1 formula is that it is solely based on deep water wave height and direction. Hence, wave breaking and refraction is not taken into account. In this study, it is assumed that no significant inaccuracies will be caused by that, since the wave data is located at a depth of 7.8 m MSL (which is not far offshore).

5.2.5. Diffraction

Since a large structure is present on the coastline to be simulated, the process of wave diffraction can not be neglected. Diffraction is the process when a wave turns as a result of a (sudden) change in boundary conditions due to coastal structures or rocky headlands. Mainly due to a local gradient in wave height, waves will turn around the tip of the structure into the so-called shadow zone behind the structure. It changes the wave height and direction. Hence, the wave energy is spread differently and also wave breaking is influenced. It is therefore important to include wave diffraction when calculating longshore transport and corresponding gradients in the vicinity of a coastal structure. The diffracted breaking wave height $H_{diff,br}$ is calculated using the wave height at the tip of the structure H_{tip} and the diffraction coefficient K_d according to:

$$H_{diff,br} = H_{tip} \cdot K_d \tag{5.9}$$

In ShorelineS, different (simplified) methods to account for diffraction are implemented, which have been thoroughly studied (Elghandour, 2018; Overgaauw, 2021). The methods are named by their founders, i.e. Roelvink and Kamphuis. In this study, both methods are tested. After the calibration

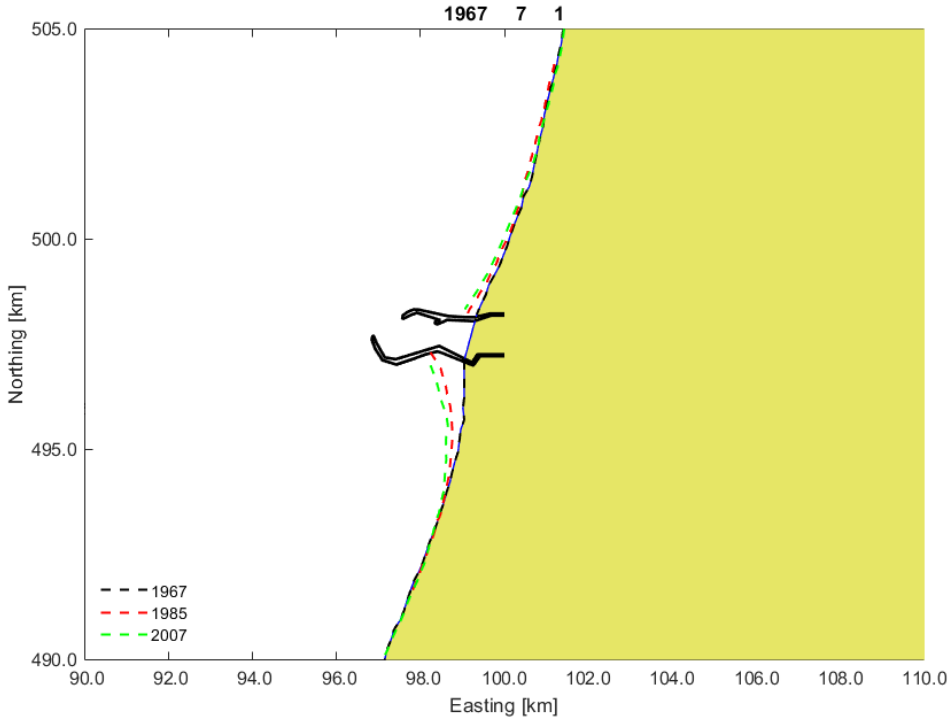

Figure 5.13: Implementation of IJmuiden coastline and structures in ShorelineS.

process, it is decided to use the Kamphuis method (Kamphuis (1992), as cited in Overgaauw (2021)). Simple equations were derived by Kamphuis to compute the diffraction coefficient in the shadowed zone of a coastal structure (Equation 5.10). Finally, a rotation factor was included to determine how severe the wave direction is influenced by the diffraction. This value was set to be 2.0 according to Hurst et al. (2015, as cited in Overgaauw (2021)).

$$K_d = \begin{cases} 0.69 + 0.008\theta & for\ 0 \geq \theta > -90; \\ 0.71 + 0.37 \sin\theta & for\ 40 \geq \theta > 0; \\ 0.83 + 0.17 \sin\theta & for\ 90 \geq \theta > 40. \end{cases} \tag{5.10}$$

5.2.6. Sediment bypassing

When a non-permeable structure interrupts a coastline, the longshore sediment transport is usually completely blocked. However, after a certain amount of time, the beach might have experienced so much accretion that sediment will be transported around the breakwater tip: sediment bypassing. In the specific IJmuiden application, the length of the structure is sufficiently long to prevent this form of sediment bypassing.

A second process that can occur, is sub-aqueous sediment bypassing (i.e. under the water level). This happens when the depth at the structure head is smaller than the so-called depth of active longshore transport (D_{LT}), meaning that sediment transport is still active there. D_{LT} can be seen equal to the depth of the highest 1/10 waves at the updrift side of the structure (Hanson & Kraus, 1989) and is usually less than the closure depth. In order to assess if sub-aqueous bypassing of sediment around the breakwaters will occur, the water depth at the tip of the structure (D_s) and the depth of active longshore transport (D_{LT}) have to be known. The amount of sediment that is transported around the breakwater is determined by the bypassing factor as follows (Roelvink et al., 2020):

$$BPF = 1 - \frac{D_s}{D_{LT}} \tag{5.11}$$

The bypassing ratio varies between 0 and 1. In this study, D_{LT} is assumed to be equal to the defined outer depth of closure of 5.3 m MSL (see Section 5.2.3). After analysis of the length of the structure

in the Port of IJmuiden (which is at least 1800 meters) and JARKUS data (see Appendix A), it was determined that the water depth at the tip of the structure was at least larger than 10 meters. Hence, it is concluded that no sub-aqueous sediment bypassing occurs around the port breakwaters at this site.

5.2.7. Other input conditions

Further input conditions are the initial space step, which is set to 100 meters in order to detect coastline changes on a sufficiently small grid. The time step was set to be adaptive, meaning that it can adjust to the required balance between temporal and spatial scales. One of the consequences of this decision was a large increase in computational time. However, for a larger spatial step, the model became unstable and not all coastline changes on smaller spatial scales were detected, leading to an inaccurate representation of the coastline. Lastly, regarding the boundary conditions, the Neumann settings were implemented. This means that no gradient in LST can be present at the boundary of the modelled domain. Hence, no coastline displacement at the boundaries occurs.

5.3. Key points of Chapter 5

- Chapter 5 presents the implementation of the PCR model and the ShorelineS model for a case study of the coastline near IJmuiden.
- For the PCR model, the Dunerule model is used as the erosion function. It is an empirical model which is calibrated for the Dutch coastline. The model uses offshore wave data as input. Statistical analysis of the measured wave conditions in front of the IJmuiden coast resulted in an average of 9.45 detected storm events per year.
- To account for the (uncertain) effects of climate change, a range of sea level rise scenarios as defined by IPCC is studied: no SLR, RCP2.6, RCP6.0 and RCP8.5.
- Finally, 100,000 time series of coastline evolution for the 77-year period of 2023 to 2100 are obtained, from which 100,000 most landward coastline positions over time (relative to the initial coastline position) are detected and statistically analysed into a cumulative distribution function (CDF).
- To reduce computational time, the ShorelineS model uses a representative wave climate based on the wave energy flux. A constant active profile height of 8.3 m is implemented (a depth of closure of -5.3 m MSL and a dune toe elevation of +3 m MSL).
- For the sediment transport formula, the simplified CERC1 formula is used in order to minimize the computational time. Hence, no refraction effects are included in the simulation.
- To account for the effects of the breakwaters near the coast of IJmuiden, diffraction is included in the ShorelineS model.

6

Results

In this chapter, the results of the model validations and the final obtained projections of coastline evolution for the IJmuiden case study are presented. The individual results of the PCR model and the ShorelineS model are analysed and discussed, as well as the combined results after the implementation of Framework 1.

6.1. Validation

6.1.1. PCR model

This section presents the validation of the PCR model. First, the implemented Dunerule erosion model is discussed, after which the full PCR model simulation of the coastline evolution is analysed.

Validation erosion model
In order to check the performance of the Dunerule erosion model and its applicability to the IJmuiden case study, it is necessary to validate the calculated erosion volumes with historical measurements of storm erosion. This is done as follows:

- First, historical observations of eroded dune volumes after storm events are studied. Unfortunately, there is limited storm event data available for the Dutch coast, mainly because the JARKUS data consists of yearly measurements only. As a result, the impact of single storm events can not be detected in these measurements. However, de Vries et al. (2012) studied the storm impact on the Dutch coast and discussed three measured erosion events: storm events in 1953, 1976 and 1983 with corresponding erosion volumes of 80-100 m^3/m, 15-80 m^3/m and 1.45-55.13 m^3/m, respectively. The return periods of these storm events are estimated to be around 10-50 years. These measured erosion events are helpful in assessing whether the calculated erosion volumes with the Dunerule model are representative or not.
- Consequently, the Dunerule model is used to model the erosion volumes of the detected storm events in the wave and water level data for the period of 1994-2022. This way, the actual wave conditions are used to model storm erosion, instead of the generated synthetic storm time series (SSTS). This resulted in 255 detected storm events. The hindcasted erosion volumes are shown in Figure 6.1. Also, the maximum erosion volumes of the measured historical events are depicted in the figure, which show that the hindcasted erosion volumes are representative for the Dutch coastline. This conclusion has to be handled carefully, since a longer, more representative wave data set is unfortunately not available.
- Lastly, the Dunerule erosion model is used to model random erosion events based on the generated SSTS, also for the period of 1994-2022. This simulation is run for 10,000 times and for each simulation, the maximum modelled erosion volume is stored. These maximum modelled erosion volumes thus have a return period of 28 years - equal to the return period of the maximum *detected* storm erosion event (here: 99.79 m^3/m, see Figures 6.1 and 6.2). In order to check whether the modelled maximum erosion volumes are representative for the measured data, the

10,000 maximum erosion volumes are statistically analysed and compared to the hindcasted erosion volumes.

In Figure 6.2, these hindcasted erosion volumes (based on actual measured data) are again depicted by the blue dots, whereas the red dashed lines represent the exceedance probabilities of the maximum modelled erosion volumes (based on the SSTS). In this case, the P99 value means that 99% of the modelled erosion volumes is smaller than this value, and the same goes for the P1 value, and so on. From the figure and the analysis it can be concluded that the largest values of the detected hindcasted erosion volumes are in the probability range of the maximum modelled erosion volumes by the Dunerule model. Hence, despite the limited data availability, this analysis shows that the Dunerule erosion model performs adequately in simulating the erosion volumes - although it still has to be implemented with caution.

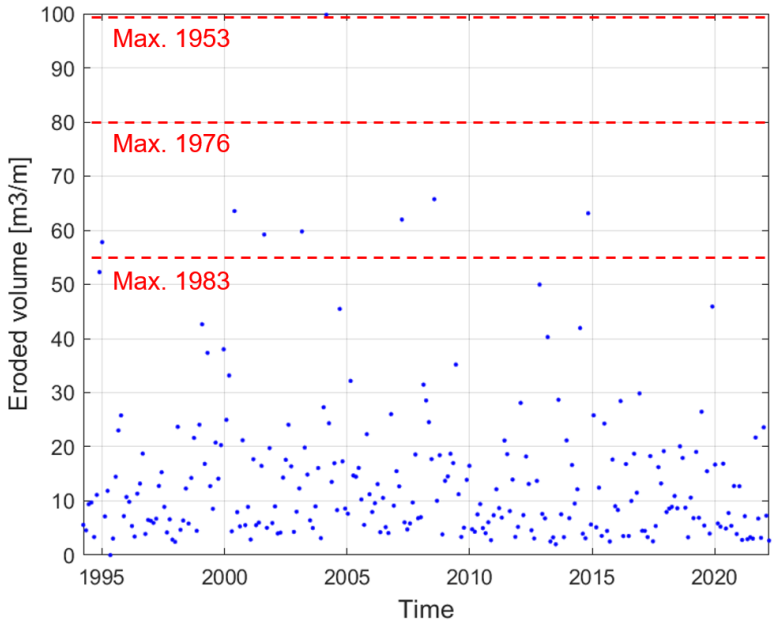

Figure 6.1: Hindcasted erosion volumes with Dunerule model using actual measured wave conditions.

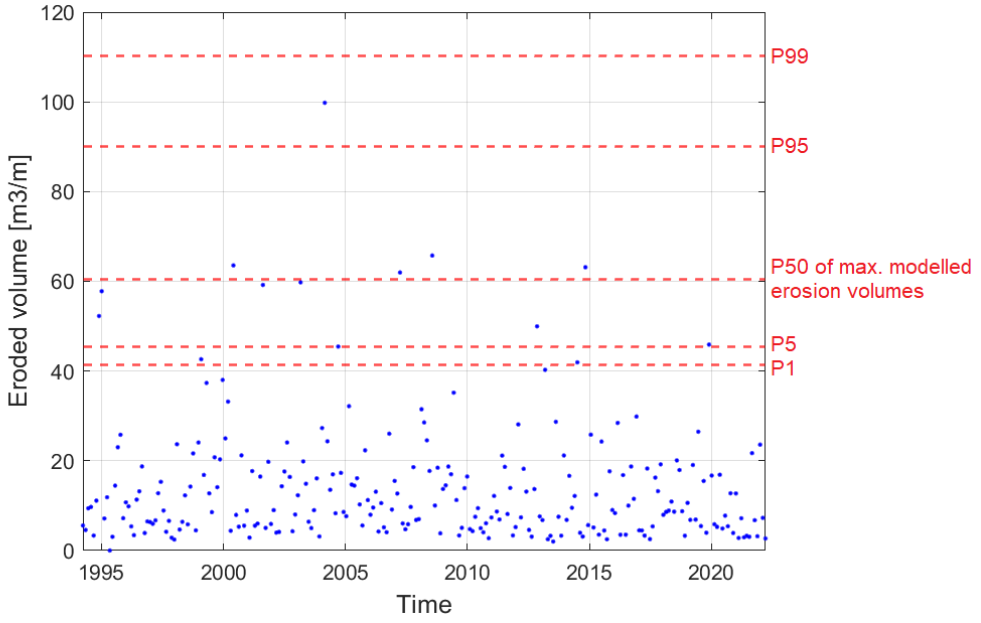

Figure 6.2: Hindcasted erosion volumes and probability range of maximum generated erosion events.

Validation hindcast period

In the previous section the modelled erosion volumes were validated, but it is also necessary to analyse the translation of these erosion volumes to the evolution of the coastline position. In order to assess the performance of the PCR model framework, the full PCR model is used to simulate the period of 1994-2022 (i.e. a hindcast) with the actual measured wave conditions as input. This results in one single time series of coastline evolution. It is noted that this does not cover the full probabilistic PCR framework as it is intended; it only considers the simulation loop of storm events followed by the subsequent recovery (i.e. the circled elements in Figure 3.2 on the PCR framework as a whole).

The historical wave data is analysed and a storm definition is determined, resulting in a storm time series which represents the actual storm events - and the actual gaps between them - that have occurred in the period of 1994-2022. This simulation does not include SLR effects since it considers a historical period. The coastline evolution of 1994-2022 as modelled by the PCR model is presented in Figure 6.3. The detected most landward coastline position over the simulated period is 5.89 meter landward of the original coastline position.

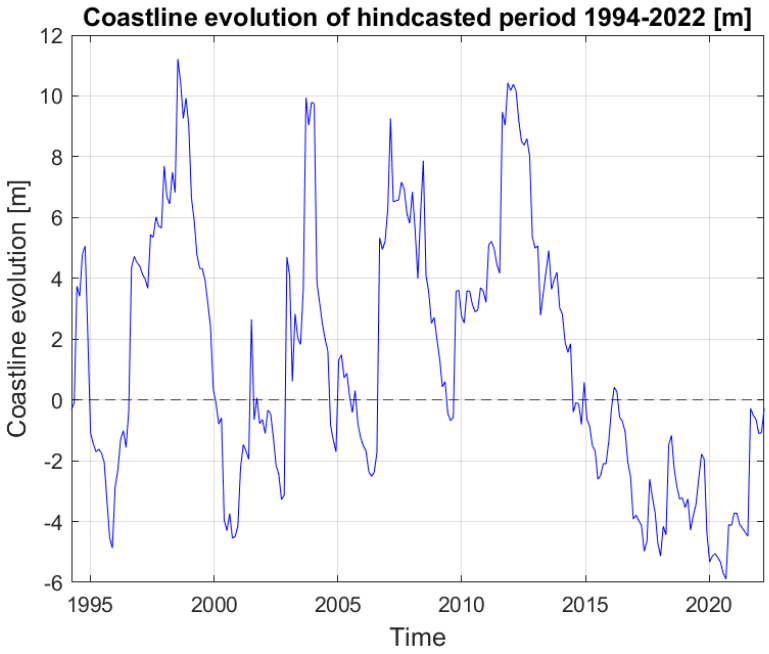

Figure 6.3: Coastline evolution modelled by the PCR model for the period 1994-2022.

It is important to assess if the PCR simulation is able to run adequately. It is crucial that the gaps between the storm events and thus the total number of storms are simulated correctly in the PCR model. In Figure 6.3 it is seen that the PCR model is capable of realistically simulating the evolution of a coastline which is in equilibrium for the cross-shore processes, i.e. in simulating storm-induced erosion and subsequent recovery. Again, it is mentioned that no SLR effects are taken into account as only a hindcast period is considered.

Regarding the PCR model validation for a specific case study, it is noted that the PCR model is developed for prediction purposes and not for hindcasts. The main reason for this is the applied approach for the coastline recovery process, which basically ”forces” the coastline to return towards its original position. This makes the historical validation of the PCR model for the IJmuiden coastline highly complex, since the longshore processes, which are dominant for the IJmuiden coastline, are not considered in the PCR model.

Validation forecast period
Regarding the projections of future coastline evolution, it is also important to assess whether the PCR model correctly simulates the storm impact and the coastline recovery in the calm periods between storm events. The number of detected storms for the studied coastline was found to be 9.45 storms per year (Section 5.1.2). A clear seasonality effect was seen, with significantly more storms occurring in the winter months than in summer. In order to simulate this correctly in the PCR model, a non-homogeneous Poisson distribution was fitted to the gaps between storms (see Section 5.1.2). As a first check if the model succeeded in modelling the right amount of storms, the mean generated number of storms per year was analysed for the 100,000 simulations for each of the SLR scenarios. It was found that the model successfully modelled the total number of storms and that the non-homogeneous Poisson distribution simulated the storm spacing correctly: see Table 6.1.

Table 6.1: Mean number of generated storms per year for the different PCR simulations.

Detected (from data)	No SLR	RCP2.6	RCP6.0	RCP8.5
9.4501	9.4536	9.4523	9.4529	9.4523

Validation recovery rate
The recovery rate is determined such that the coastline is in equilibrium with the median calculated storm retreat (for a case without SLR). This was also observed by de Vries et al. (2012), who concluded for the Dutch coast that the total erosion of storm events is of similar order as the measured beach growth. For the projections of future coastline evolution, the coastline recovery rate is determined to be 6.6181 m/year. This is equal to approximately 0.34 m^3/m/day, taking into account a dune crest height of 19 m +MSL, which was assumed for the IJmuiden case study. This value is in line with the findings of Li, van Gelder, Vrijling, et al. (2014), who adopted the same method for future projections of the Dutch coastline near Noordwijk and found a constant recovery rate of 0.3 m^3/m/day. Taking into account a dune height of 18 m +MSL (representative for Noordwijk coastal profile), this would be equal to approximately 6.0875 m/year. It can thus be concluded that the calculated recovery rate in this study is of similar magnitude.

For the hindcast period (Figure 6.3), the obtained constant recovery rate is 0.029 m^3/m/day. This is a factor 10 smaller than the recovery rate found for the long-term, future projections as found in this study and by Li, van Gelder, Vrijling, et al. (2014). This difference is most probably caused by the fact that this validation is confined to a relatively short period of 28 years, in which no extremely large events have occurred. Hence, a smaller recovery rate is required for the coastline to remain in equilibrium. The mentioned larger rates were derived for a long-term prediction with the PCR model based on the generated synthetic storm time series, which may include extreme (extrapolated) wave conditions and thus extreme erosion events.

Conclusion PCR model validation
From the analyses in this section, it is concluded that the PCR model performs adequately. The implemented erosion model is capable of modelling synthetic erosion volumes which are representative for historical erosion events. Moreover, the implemented approach for the constant recovery rate and the final obtained value of this recovery rate are both in line with findings in literature. Lastly, the PCR model is able to simulate storm events and subsequent coastline recovery for a coast which is in equilibrium for the cross-shore processes.

6.1.2. ShorelineS model

The alongshore evolution of the IJmuiden coastline is modelled with the ShorelineS model. The main driver for the longshore coastline changes is the presence of gradients in longshore sediment transport (LST) induced by the port breakwaters. In Section 5.2 all input conditions for the ShorelineS model are presented and discussed. The most important elements are the fact that a representative wave climate is used, that the active profile height is assumed to be constant (here: 8.3 meter) and that the used sediment transport formulation is the simplified CERC1 formula. in order to reduce computational time. The representative wave climate is based on real measured wave conditions along the IJmuiden coastline represented by the wave rose in Figure 5.11.

In order to test the performance of the ShorelineS model, validation with measured morphological data is necessary. To this end, the observed positions of the IJmuiden coastline in 1967, 1985 and 2007 were implemented to calibrate the model with the actual, observed coastline displacement (see Figure 5.13). Regarding the calculation of sediment transport volumes, the calibration coefficient 'b' of the CERC1 transport formula can be adjusted. After several calibration iterations, the b-factor is determined to be $1{\cdot}10^6$. Together with all the defined input conditions of the ShorelineS model as presented in this section, the final result of the model calibration is presented in Figure 6.4. The underlying satellite image represents the coastline of today (i.e. 2023), which is important to take into account when validating the ShorelineS model based on satellite imagery.

Analysis of calibration
Overall, the result of the calibration as presented in Figure 6.4 is satisfactory. There are, however, some important points of attention:

- The first one is the overestimation of the accretion on the southern side of the breakwaters, between 492.0 and 495.0 km Northing. The model simulates coastline accretion in that region, whereas in reality this has not occurred. What is remarkable, is the fact that in 1985, the overestimated accretion by the ShorelineS model is not visible (yet).

  A process that is not considered in the ShorelineS model is wind-driven flow. In the nearshore zone, not only waves, but also wind determines the currents and thus the (longshore) sediment transport. Wind-induced currents drive longshore sediment transport. Krijnen (2021) also studied the coastline of IJmuiden and found that including wind- and tide-induced LST gradients significantly stimulates the curvature of the coastline, with the wind component being the main driver (compared to tide-induced LST). This effect could be an important reason for the estimated accretion in the discussed region by the ShorelineS model, which is only based on wave-driven processes.

  Furthermore, another potential cause is the fact that ShorelineS does not account for aeolian transport, which could have led to a redistribution of sediment over the coastal profile, i.e. wind-blown transport of sediment from the beach to the dunes. As a result, the position of the MSL would have shifted.
- Secondly, the model did not correctly simulate the accretion on the northern side of the breakwaters between 499.0 and 501.0 km Northing. This could be caused by the specific sampling of the representative wave climate, which might have missed important wave directions. In addition, the omission of refraction effects and uncertainties in the bathymetry could play a significant role.

  It could also be the case that the sheltering of the waves due to the presence of the breakwaters has incorrectly influenced the LST rates to being too small in that region. More importantly, it was found while performing this research that the ShorelineS model does not perform well in simulating structure-coastline interactions. This often results in model instabilities, which might be the reason for the modelled erosion on the northern side of the breakwaters.
- It is also noted that the maintenance nourishments performed by the Dutch authorities have not been taken into account in this calibration. Between 1998 and 2008, multiple beach and shoreface nourishments have been carried out. Evidently, this is of large importance for the studied coastline. It is therefore a significant simplification that these nourishments are not incorporated in the ShorelineS model.

- Finally, another influential process in this region is the sea level rise (SLR), which is not considered in this calibration of the ShorelineS model. SLR is currently mainly projected relative to the period of 1985-2005 (Wong et al., 2014), hence no significant effect on coastline development can be distinguished. However, it must be mentioned that climate change and SLR will definitely play a large role in the coming decades, so it is highly important to include this process in the ShorelineS model.

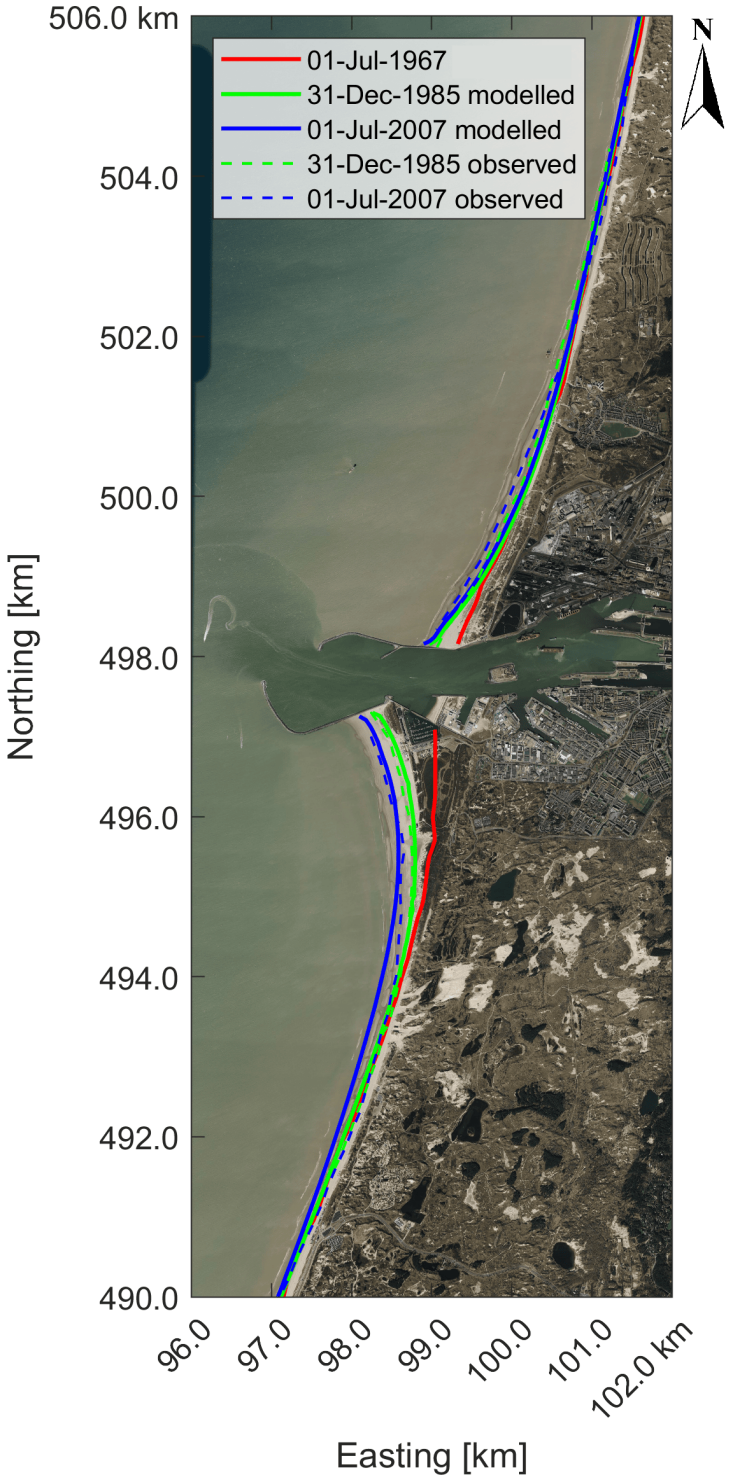

Figure 6.4: Result of ShorelineS calibration for the IJmuiden coastline application.

Quantitative analysis
If specific coastline transects are studied according to the method as described in Section 4.1 on Framework 1, the coastline evolution can be quantified. See Figure 6.5. In addition to the ShorelineS model validation with the observed coastline displacement of IJmuiden as presented in Figure 6.4, the model is also compared with JARKUS data (Rijkswaterstaat, 2022). For multiple coastline transects, the measured position of the Mean Sea Level (MSL) in cross-shore direction is derived and analysed from the JARKUS data. The evolution of the MSL position of JARKUS transect 5700 is shown in Figure 6.6. For the location of this transect, it is referred to Figure A.1 in Appendix A.

In both Transect 1 and 2 in Figure 6.5, it is visible that the rate of the coastline displacement decreases over time; an equilibrium situation slowly develops. When the coastline evolution of Transect 1 is compared to the JARKUS data, it is seen that the ShorelineS model slightly overestimates the accretion w.r.t. the measured position of JARKUS, with approximately 250 meters. This also holds for other coastline transects that have been studied. The reason for this observed difference is most likely one of the above mentioned processes, namely the fact that ShorelineS does not consider wind-induced currents driving longshore transport, as well as wind-driven (aeolian) cross-shore transport which potentially transports sediment from the beach to the dunes. It is noted that the described difference between the JARKUS data and the ShorelineS result is not visible in Figure 6.4. This is most probably caused by the fact that the satellite imagery represents one particular, instantaneous moment in time, which could differ from the yearly JARKUS measurements.

Additionally, the deviation between ShorelineS and JARKUS can also be caused by the fact that storm-induced coastline erosion is not included in the ShorelineS model. This storm-induced coastline evolution as modelled by the PCR model is depicted in Figure 6.3. Although this is modelled for a different period, it still represents the phenomenon that a coastline is not always stable. Most often, a coastline recovers from this storm-induced retreat, but it can be the case that over the years, eroded sediment is transported away from the coastal region in alongshore direction (i.e. structural erosion) - even though the overall trend is coastline accretion. See Section 2.3.4 for elaboration on these cross-shore and longshore interaction processes.

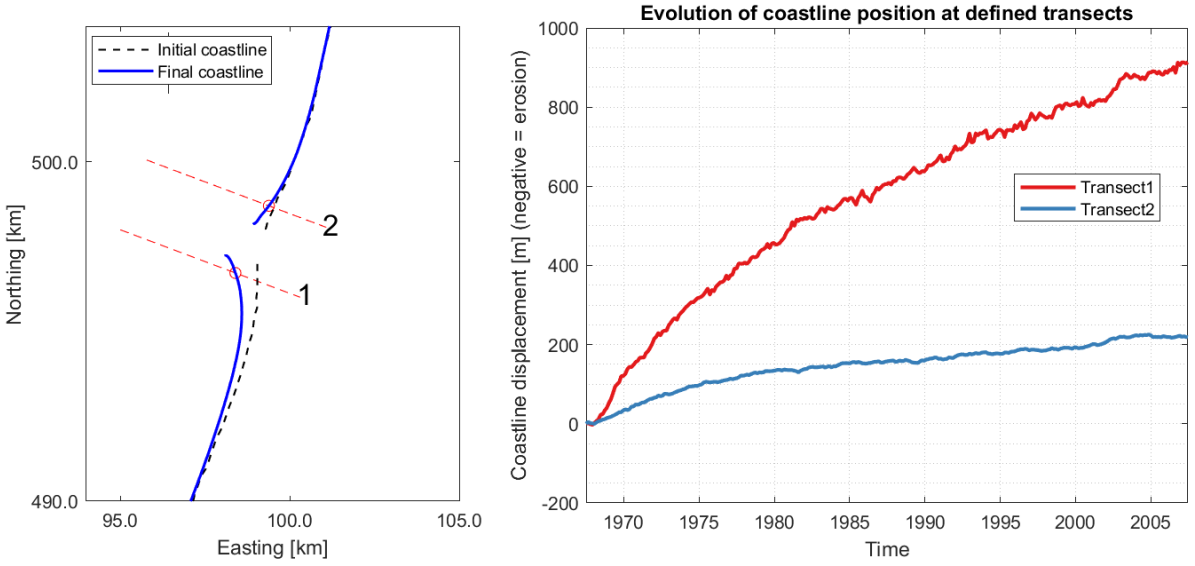

Figure 6.5: Result of ShorelineS model: coastline evolution for selected transects for 1967-2007.

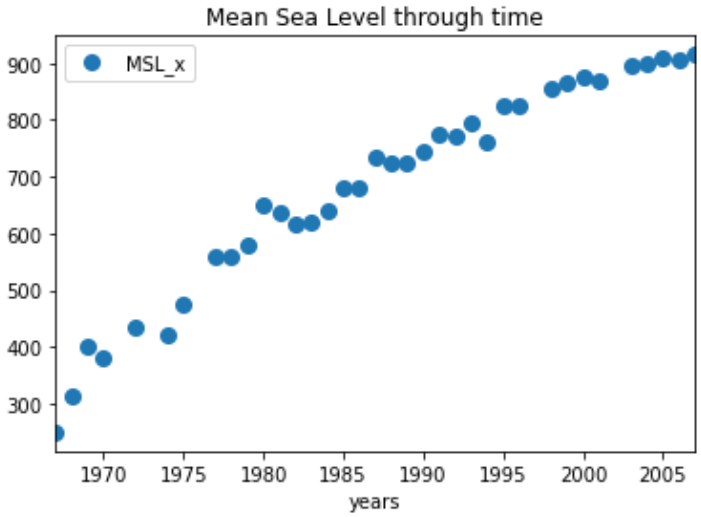

Figure 6.6: Yearly measured position of MSL over time: JARKUS transect 5700.

Comparison with previous research

The result of the ShorelineS calibration for the IJmuiden case study is also compared with previous research that has been conducted for the IJmuiden coastline, namely by Hallin et al. (2019) and Krijnen (2021). Hallin et al. (2019) used measured data of gradients in LST derived from observed beach and dune volume changes, whereas Krijnen (2021) also modelled LST gradients with a self-developed model: see Figure 6.7. What is clearly visible is the fact that both studies indicate negative LST gradients in the coastal region corresponding to 494.0 and 490.0 km Northing (for the numbers of the coastal profiles see also Figure 5.10). This indicates that this coastal region is naturally eroding, which is also seen from historical satellite imagery. Nowadays, this erosion is not visible anymore as nourishments have been applied. However, in Figure 6.4 it was seen that the ShorelineS model estimates accretion - even though ShorelineS does not take into account any nourishments. This model inaccuracy is important to consider when other case studies are modelled with this calibrated ShorelineS model. It is therefore recommended to further study the discussed processes that the ShorelineS model does not consider and to further calibrate the ShorelineS model with more advanced sediment transport formulas. This is not investigated in this study.

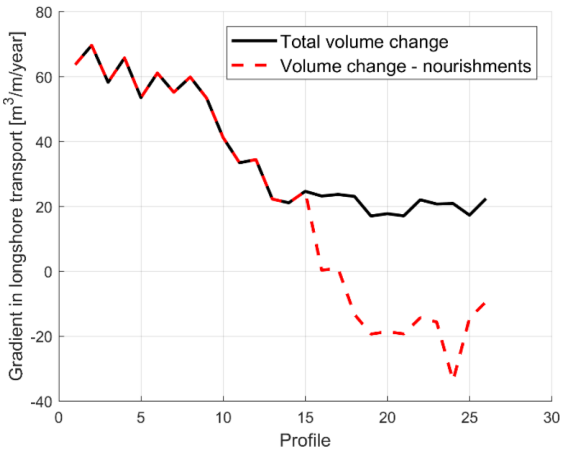

(a) Observed gradients in LST (Hallin et al., 2018).

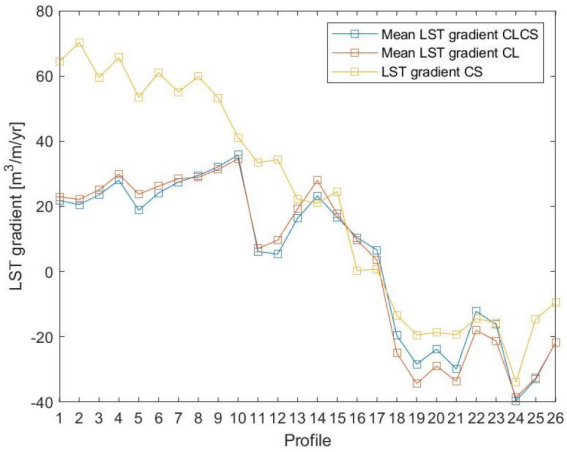

(b) Gradients in LST: modelled and observed (Krijnen, 2021).

Figure 6.7: Observed and modelled gradients in LST for the IJmuiden coastline profiles.

6.1.3. Framework 1

This section discusses the validation of the Framework 1 implementation, in which the obtained results of PCR and ShorelineS are combined for a hindcasted period. The PCR and ShorelineS models are validated for different hindcast periods as a result of specific data availability. Figure 6.8 presents the implementation of Framework 1 for the mutual hindcasted period: March 29, 1994 to July 1, 2007.

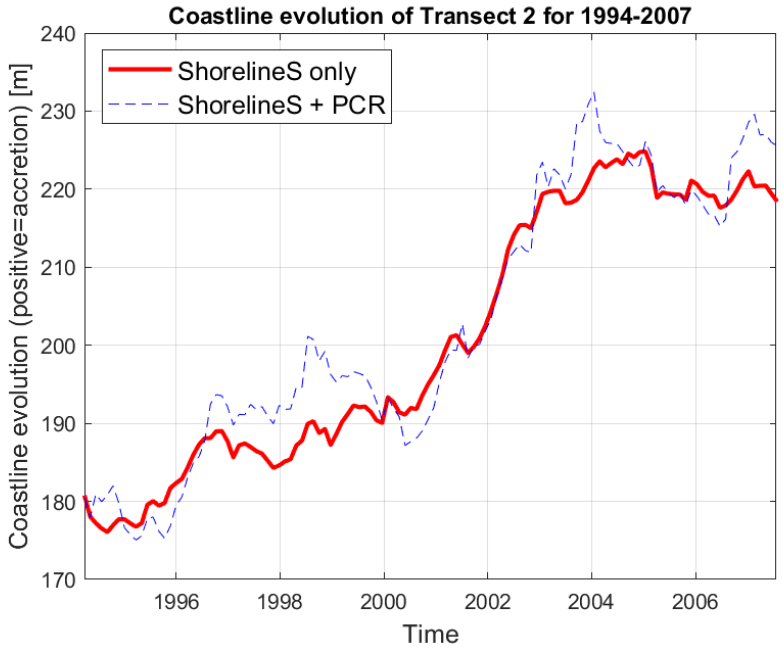

Figure 6.8: Result of Framework 1: coastline evolution for selected transects for 1994-2007.

Dominant processes
In Sections 6.1.1 and 6.1.2 it is introduced and highlighted that the PCR model and the ShorelineS model are developed for completely different processes: modelling cross-shore and longshore processes, respectively. In these sections it is concluded that the longshore processes are dominant for the IJmuiden case study. As a result, the ShorelineS simulation is validated in a quantitative way with historical measurements of the IJmuiden coastline. Regarding the PCR model, the validation is based on historical erosion volumes for the Dutch coastline and on the model's capability to simulate the cycle of storm events and subsequent recovery. The PCR model is not validated for the IJmuiden coastline in particular, as a result of the implemented approach for the recovery process in between storm events.

The result of implementing Framework 1 for coastline Transect 2 (see Figure 6.5 for its location) consists of the longshore-induced coastline displacement representing accretion, along with the cross-shore-induced coastline evolution representing the cross-shore variability of the coastline position. As mentioned in Section 6.1.1, this cross-shore variability, which represents the storm retreat and subsequent recovery, is not quantitatively validated for the specific IJmuiden case study due to the dominance of longshore coastline displacement and due to the fact that only yearly measurements are available.

Relevance cross-shore variability
On the other hand, Figure 6.8 emphasises the added value of Framework 1 with respect to considering only cross-shore or longshore processes. It is highly useful to detect and to predict the (potential) cross-shore-induced variability of a coastline, even when the coastline is mainly accreting. For the IJmuiden coastline, for example, Figure 6.8 shows that neglecting cross-shore processes could lead to a miscalculation of the coastline position of more than 10 meters - even for a case without SLR. Analysis of this variability is especially relevant for coastal zone management purposes regarding coastal structures or buildings, in which not only the long-term trend of a coastline is important, but also the most landward position that a coastline might reach during a certain period. This is further discussed in Section 6.2.3.

6.2. Projections

6.2.1. PCR model

In order to model the cross-shore coastline development for the IJmuiden coastline under the influence of storm erosion and sea level rise (SLR), the PCR model is implemented. As was described in Sections 3.2.7 and 5.1.6, the PCR model is simulated 100,000 times, resulting in 100,000 time series of coastline evolution for the 77-year period of 2023 to 2100. From these time series, 100,000 most landward coastline positions over time (relative to the initial coastline position of x = 0 m) are detected and statistically analysed into a cumulative distribution function (CDF). In addition, the most landward coastline positions in the years 2040, 2070 and 2100 are analysed, in order to gain knowledge on the long-term coastline evolution over the years - and to study the impact of SLR over time.

Sea level rise scenarios
The PCR model was used to predict the cross-shore coastline evolution for the period of 2023 to 2100 using multiple SLR scenarios as defined by IPCC: no SLR, RCP2.6, RCP6.0 and RCP8.5 (Wong et al., 2014). The reason for implementing multiple scenarios is the large uncertainty of the magnitude of SLR and the fact that projections for the long-term are studied. The obtained CDF curves for the multiple SLR scenarios are presented in Figure 6.9. It is clearly visible that the more severe the rate of SLR, the larger the probabilities for more severe coastline displacement. This outcome highlights the importance of including the impact of climate change and SLR in the prediction of coastline changes. Furthermore, it can be seen that a good representation of the 0.01% probability of exceedance is achieved, according to the modelling objective as described in Section 3.2.7.

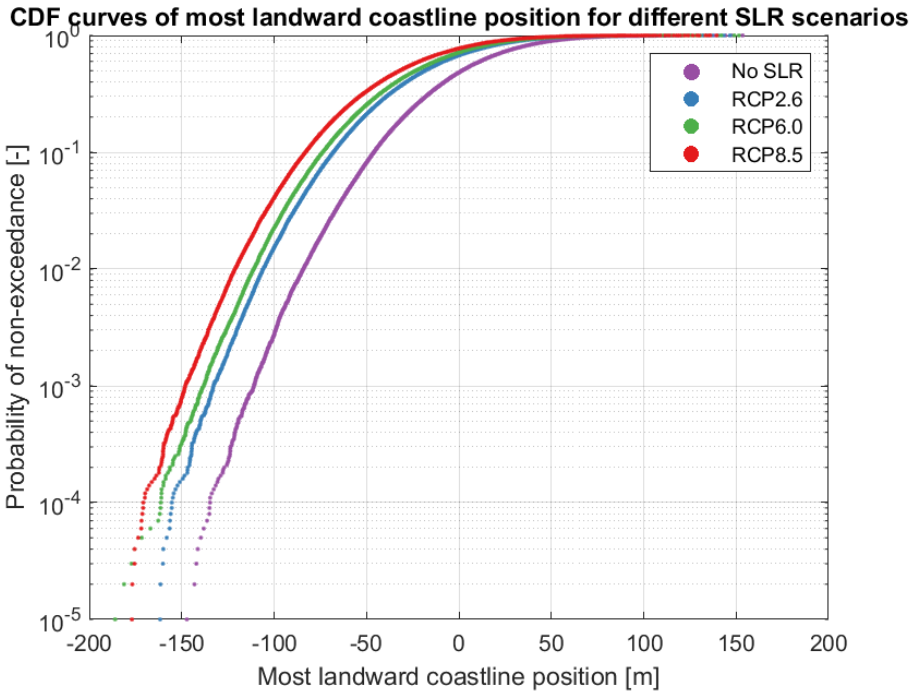

Figure 6.9: PCR model: CDF curves of the modelled most landward positions for different SLR scenarios.

The CDF curves are presented on a logarithmic y-axis in order to have a good understanding of the low non-exceedance probabilities. Moreover, the y-axis is defined as the probability of non-exceedance, since exceedance means that a value is larger, with positive values being larger than negative values. The negative values on the x-axis represent the PCR model's predictions that the modelled most landward position is *landward* of the original coastline position, whereas positive values indicate that the most landward position is *seaward* of the original coastline position. In Figure 6.9, a very low non-exceedance probability means that the most landward position is most likely to be more seaward than the modelled value corresponding to this low non-exceedance probability. To illustrate, for the RCP8.5 scenario, a most landward position of approximately -175 meters is modelled for one of the 100,000 simulations. This means that the probability is very large that the coastline evolution positively exceeds this value, for instance that the coastline evolution is -50 meters.

Recovery rate

It is noted that for each of the implemented SLR scenarios, the applied recovery rate is equal. This means that it is assumed that the coastline will recover with the same pace for different scenarios with different magnitudes of coastline erosion. This might have influenced the severeness of the coastline displacement for the more severe SLR scenarios, as presented in this section. The reason for implementing this assumption is the fact that it is unknown how coastlines and cross-shore profiles will respond to elevated sea levels. This is further elaborated in Section 5.1.5. It is expected that this will significantly influence the recovery rate, however this is not further studied in this research.

Median coastline changes

Next to the CDF curves, also the median (i.e. P50) values of the most landward coastline position for the different SLR scenarios are presented in Figure 6.10. It can be seen that for the case with no SLR, the coastline is almost in equilibrium (but slightly accreting), which is in line with the applied method for coastline recovery as explained in Sections 3.2.5 and 5.1.4. For the RCP8.5 scenario, it is found that the median coastline retreat lies around 32 meters.

Figure 6.10: PCR model: P50 values of most landward coastline position over time for different SLR scenarios.

These observations are also presented in Figures 6.11a and 6.11b, in which the uncertainty ranges of the most landward position for the two discussed SLR scenarios (no SLR and RCP8.5) are visualised. The uncertainty ranges of the RCP2.6 and RCP6.0 scenarios are presented in Appendix C. From these figures it can be seen that the uncertainty range of the PCR projections is considerable; even for a case without SLR, the PCR model predicts coastline recessions of approximately 60 meters for 5% of the time. It is therefore of large importance to study the results thoroughly and with common sense. It is crucial to statistically analyse the obtained results by applying a sufficiently large number of simulations, and to have the limitations and risks of the PCR model in mind.

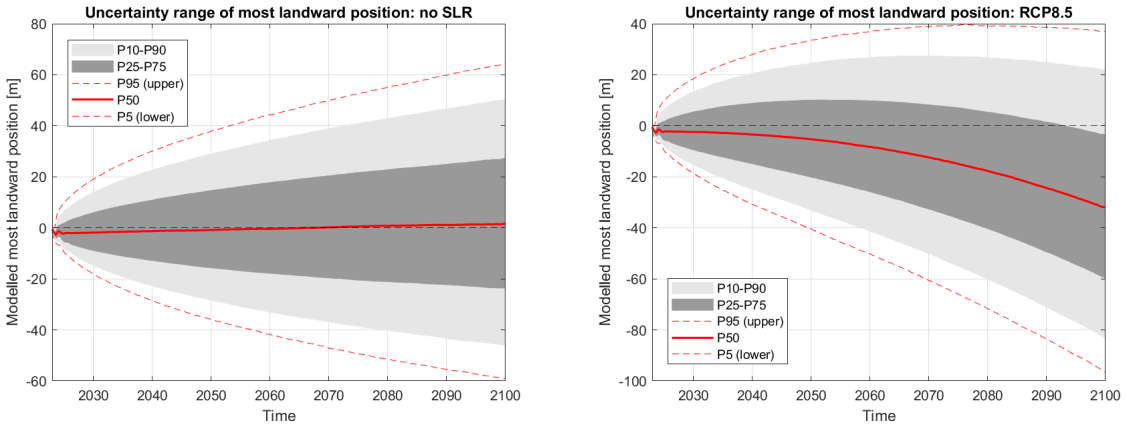

(a) Uncertainty range of most landward position for the case without SLR.

(b) Uncertainty range of most landward position for SLR scenario RCP8.5.

Figure 6.11: Uncertainty ranges of most landward coastline position for two SLR scenarios.

Temporal evolution of probabilities of exceedance

The currently observed average beach width in the coastal area of IJmuiden is found to be approximately 100 meters (Rijkswaterstaat, 2022). See Appendix A. In Figure 6.9 it is clearly visible that for certain probabilities the modelled most landward position is more landward than the average current beach width. This means that (at least temporarily) the full beach could be eroded, or even overwash over the dunes would occur. The probability that the most landward position is more landward than the beach width is 1.53% and 4.07% for the RCP2.6 and RCP8.5 scenario, respectively. Even for the case with no SLR, this probability is 0.27%. These observations highlight the necessity for beach maintenance by applying nourishments or other interventions.

To study the temporal evolution of the potential most landward coastline positions more thoroughly, the CDF curves of the projected coastline evolution for the years 2040, 2070 and 2100 are depicted in Figure 6.12. It is illustrated for the SLR scenarios RCP2.6 and RCP8.5. The CDFs clearly show that the impact of SLR becomes more important over time. In addition, the probability of exceedance of specific most landward coastline positions are presented in Figures 6.13a and 6.13b and Table 6.2. Moreover, Table 6.3 presents the modelled most landward positions for several specific probabilities of exceedance.

From Figure 6.13 and Table 6.2, it is especially relevant to study the probabilities of exceedance over time for a most landward coastline position being more landward than 100 meter of the original position, since this is is the currently observed average beach width. To this end, the temporal evolution of this probability of exceedance is depicted in Figure 6.14 for the RCP2.6 and RCP8.5 scenarios (on a non-logarithmic scale).

These types of observations and statistics are highly relevant and useful for risk-based coastal zone management strategies. Multiple values for exceedance probabilities as well as for most landward coastline positions can be studied, according to defined safety standards or other relevant regulations for decision-makers. Also, risks can be quantified and/or recommendations can be given regarding potential damage to specific coastal structures or buildings that are present on a certain distance from the mean water line.

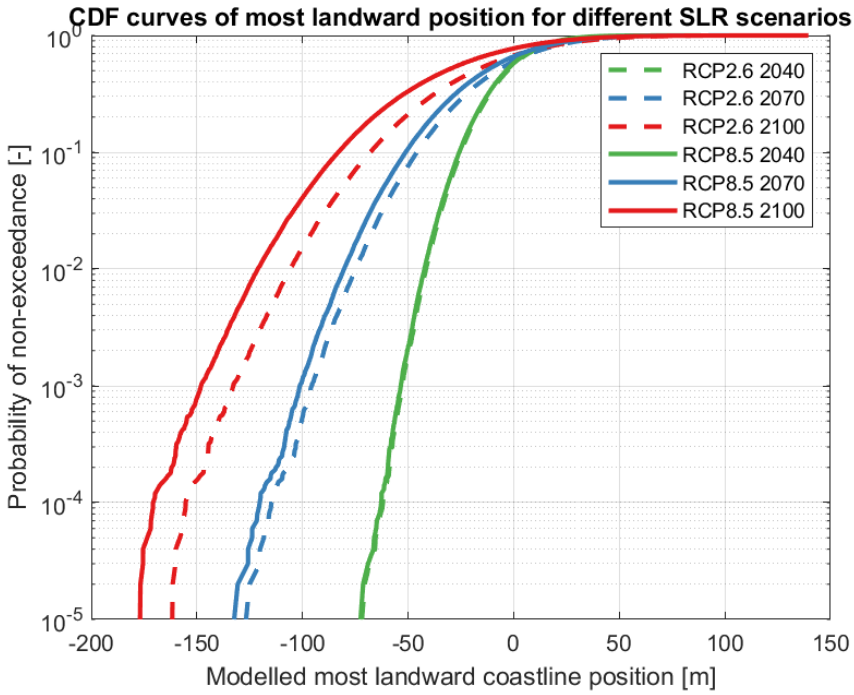

Figure 6.12: CDF curves of most landward coastline position for the selected years (RCP2.6 and RCP8.5).

Table 6.2: Probabilities of exceedance [%] for most landward positions (RCP2.6 and RCP8.5).

	RCP2.6			RCP8.5		
Coastline recession [m]	**2040**	**2070**	**2100**	**2040**	**2070**	**2100**
0	56.27	60.39	67.51	57.81	66.23	77.43
50	0.18	7.64	21.15	0.21	10.74	33.26
75	-	0.98	7.07	-	1.66	14.34
100	-	0.05	1.53	-	0.11	4.07
150	-	-	0.015	-	-	0.078

Table 6.3: Most landward positions [m] corresponding to specific probabilities of exceedance (RCP2.6 and RCP8.5).

	RCP2.6			RCP8.5		
Prob. of exceedance [%]	**2040**	**2070**	**2100**	**2040**	**2070**	**2100**
50	2.86	7.94	18.26	3.53	12.92	31.94
10	25.06	45.83	67.98	25.76	51.21	83.11
1	41.52	74.82	105.89	42.23	80.33	121.19
0.1	52.69	95.62	132.78	53.44	101.15	148.03
0.01	61.88	114.51	155.06	62.63	120.06	170.34

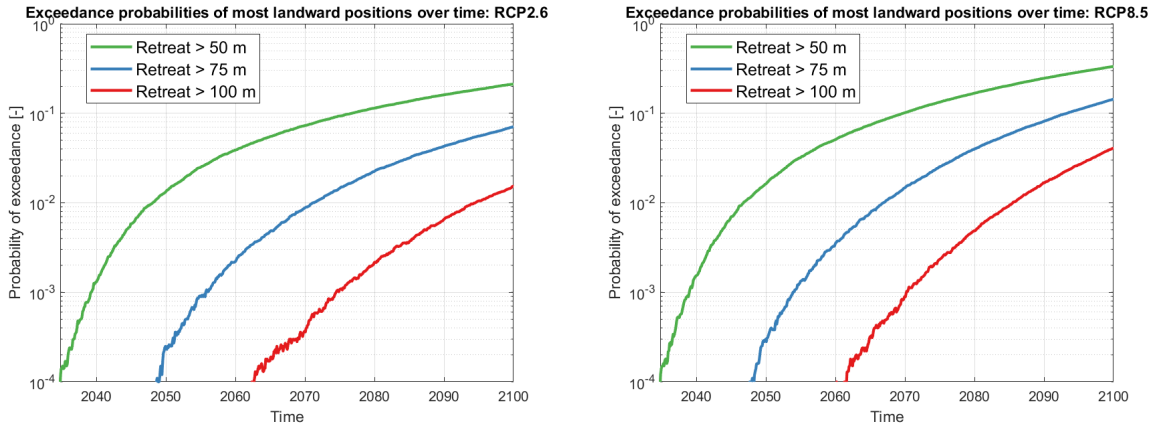

(a) Specific most landward positions exceedance probabilities for RCP2.6.

(b) Specific most landward positions exceedance probabilities for RCP8.5.

Figure 6.13: Exceedance probabilities of specific most landward positions over time (RCP2.6 and RCP8.5).

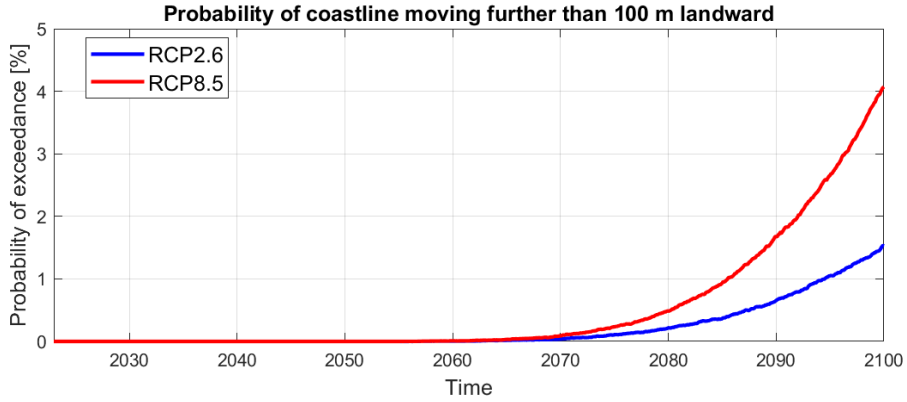

Figure 6.14: Temporal evolution of the probability of the coastline moving - at least temporarily - further than 100 meter landward (RCP2.6 and RCP8.5).

Predicted coastline accretion

As can be seen in Figures 6.9 and 6.12, the PCR model predicts most landward coastline positions being seaward of the original position for some simulations. This means that - although for a low probability - it can occur that no coastline recession occurs, but on the contrary, the coastline will experience accretion. This can also be observed in Table 6.2, where it is seen that a most landward coastline position landward of the original position is not certain at all. The reason for this outcome of the PCR model is the fact that the adopted non-homogeneous Poisson distribution for the gaps between storms can result in long periods of recovery in between storm events. As a result, the coastline experiences accretion before a new storm event occurs - essentially due to ”too much” recovery. The storm-induced erosion is consequently not large enough to cause coastline recession.

For the IJmuiden case specifically, this observation is not unrealistic. Namely, dune growth by aeolian transport has been observed as a result of the sediment availability by the applied nourishments (Hallin et al., 2019). This process evidently influences the recovery rate, but it is not taken into account in the PCR application of this study. This might have influenced the final results of the PCR model. However, since the predicted cases of coastline accretion form no threat for coastal erosion or even coastal flooding, the discussed accretion projections are not further considered in this study.

Comparison with Bruun rule

The obtained PCR projections are also compared to the Bruun rule principle, as was introduced in Section 2.4.4. The Bruun rule is often used as a quick and simple tool to predict coastline displacement due to SLR, but it is said to be rather conservative. In Figure 6.15 it is seen that the most landward coastline position modelled by PCR (the median value) is smaller than predicted by the Bruun rule, for

each implemented SLR scenario. It is therefore interesting to check the probabilities of exceedance of the PCR model projections that correspond to the computed retreats using the Bruun rule.

In Table 6.4 this is shown for the RCP2.6 and RCP8.5 scenarios, again for the selected years 2040, 2070 and 2100. In addition, in Figure 6.16, the temporal evolution of the PCR model's exceedance probabilities corresponding to the calculated Bruun rule estimates is shown (for RCP2.6 and RCP8.5). From these observations, it can be concluded that the Bruun rule becomes more conservative over time, relative to the PCR model.

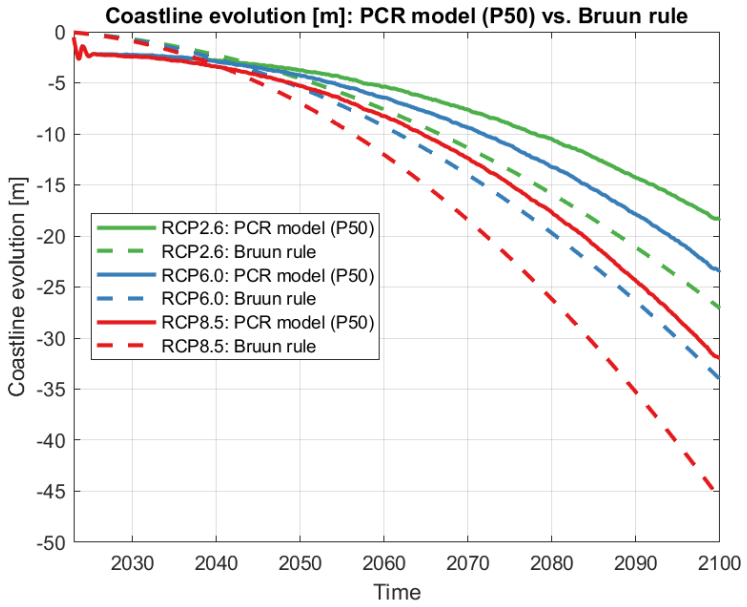

Figure 6.15: Projected coastline evolution over time: PCR model (median value) vs. Bruun rule.

Table 6.4: Calculated retreats using Bruun rule and corresponding probabilities of exceedance for the PCR model's predicted most landward position (RCP2.6 and RCP8.5).

	RCP2.6			RCP8.5		
	2040	**2070**	**2100**	**2040**	**2070**	**2100**
Recession (Bruun rule) [m]	2.47	11.78	27.08	3.57	19.14	45.74
Corresponding prob. of exceedance (PCR model) [%]	50.86	44.98	41.27	49.92	41.97	37.09

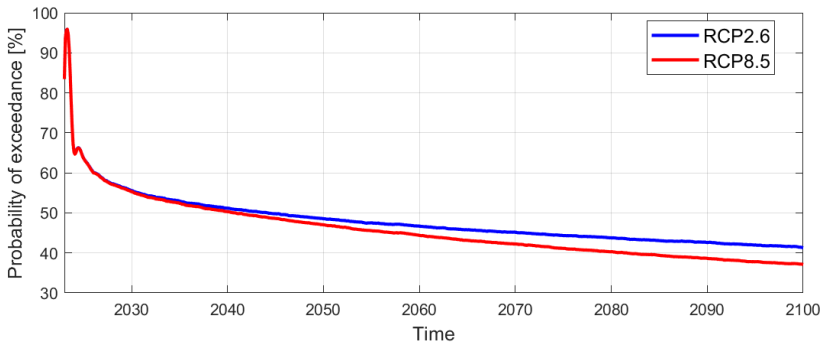

Figure 6.16: Temporal evolution of PCR model's exceedance probabilities corresponding to the Bruun rule estimates.

Physical reasoning behind observed difference
Both described methods are known to have their simplifications and limitations. For instance, in both cases a constant cross-shore coastal profile shape is assumed. Hence, it is not considered that the coastal profile might adapt to the elevated water level due to SLR and that it might become more resistant against the increased impacts. Also, the sediment grain size is assumed uniform for both methods and they both ignore influences of longshore sediment transport (LST).

Despite the mutual assumptions, a clear difference is observed between the Bruun rule estimates and the median most landward coastline positions as projected by the PCR model (Figures 6.15 and 6.16). The reason for this is the underlying physical processes that are modelled in both methods. The Bruun rule only considers the response of a coastal profile to SLR, whereas the PCR model also includes the impact of storm erosion. Consequently, the applied formulations for cross-shore sediment transport are totally different for both methods. Eventually, this resulted in the Bruun rule estimating larger coastline recessions than the PCR model's most landward coastline positions. However, the PCR model projections show a wide uncertainty range of coastline evolution, which include the predicted Bruun rule values (for lower probabilities of exceedance - see Table 6.4).

It must be mentioned that the PCR model is highly dependent on the implemented erosion function within the model framework. A different erosion function to calculate the coastline retreat after a storm could have lead to completely different results than observed and discussed above.

Sensitivity Bruun rule
The computation of SLR-induced coastline retreat using the Bruun rule is highly dependent on several input parameters. As explained in Section 2.4.4, the retreat is calculated according to:

$$R = \frac{L \cdot SLR}{B + h} \tag{6.1}$$

in which:

h	depth of closure
L	horizontal distance from the shoreline to depth h
B	berm or dune elevation estimate for the eroded area

The dune elevation B is taken as 19 meter, which is implemented for the coastal profile in this research. The rates of SLR for the different scenarios are obtained from the SLR curves as defined in Section 5.1.5 (Figure 5.9).

More importantly, it can be seen that the computed coastline retreat is highly sensitive to L, which is related to the closure depth h. In this research, it is decided to assume a depth of closure (DoC) of 5.3 meter (see Section 5.2.3), which is in line with literature findings (Hallin et al., 2019). When analysing the cross-shore coastal profiles of the IJmuiden coastline from JARKUS data (see Appendix A), L is taken to be equal to 1500 meters for the defined DoC. This value is used in the Bruun rule for calculating the SLR-induced coastline recessions as shown in Figure 6.15.

It must be noted, however, that the coastal profile is highly dynamic, leading to a large variety in the cross-shore location of the DoC, i.e. in the values for L. It is also found in the data that this cross-shore location varies significantly along the coastline transects defined by JARKUS. A larger or smaller value of L would have a large influence on the Bruun rule prediction. Therefore, using the Bruun rule to calculate coastline recession comes with large uncertainty and has to be handled with care. This is especially relevant when comparisons with other cross-shore models are made, e.g., the PCR model.

6.2.2. ShorelineS model

After the ShorelineS model has been calibrated to match the historically observed coastline change of the IJmuiden coastal area, it is used to further predict the long-term coastline evolution under influence of gradients in LST for the same period as the PCR model application: January 1, 2023 to January 1, 2100. All input conditions are similar to the input that has been used for the calibration of the model, except for the initial coastline position. It is assumed that the initial coastline position in 2023 is equal to the observed coastline position for July 2007. It is evident that this is not an accurate representation of the coastline, hence this must be taken in mind when analysing the results. Moreover, no nourishments are taken into account in this simulation as well, while the Dutch government has a strict beach maintenance policy. However, as the long-term projection of the ShorelineS model is mainly used for illustration purposes, in combination with a lack of data availability, this is assumed acceptable.

Furthermore, since all other input conditions are kept equal, it also means that the same representative wave climate is used. Hence, no climate change effects on the wave conditions are considered in this long-term projection of coastline change. The main reason for this is a) the large uncertainty regarding the impact of climate change, and b) the fact that sea level rise (SLR) is already accounted for as a separate physical process in the PCR model projection. This way, no double counting for this effect occurs.

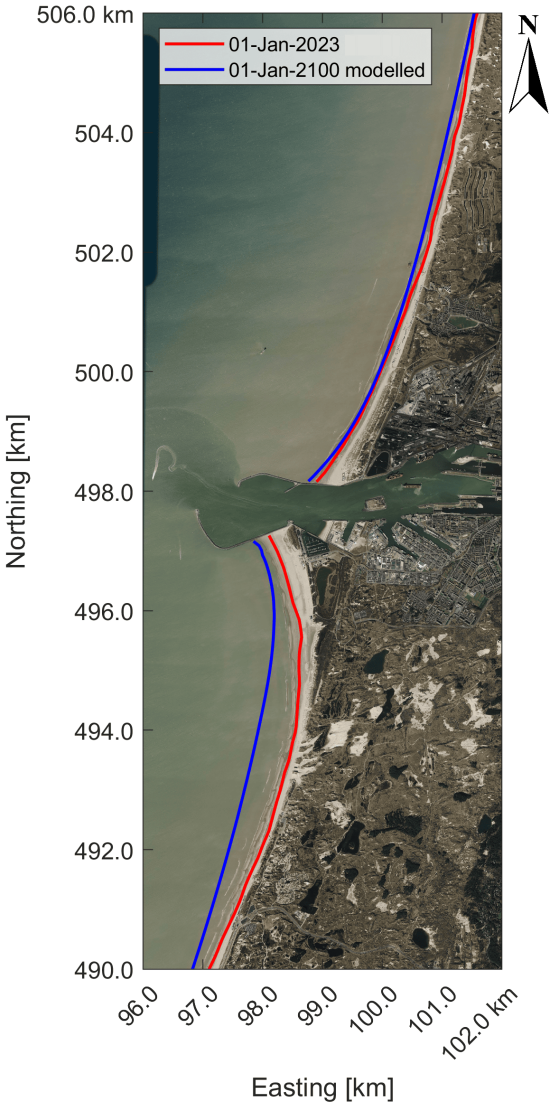

Figure 6.17: Result of ShorelineS model: prediction for the IJmuiden coastline for 2023-2100.

The final result of the long-term projection of the ShorelineS model is depicted in Figure 6.17. It is immediately visible that the large rate of coastline accretion on the southern side of the breakwater, as discussed in the Validation section (Section 6.1.2), is still present. The modelled accretion of that specific region is at least disputable. The same processes as discussed in the previous section can be the cause, namely the omission of wind-driven currents, aeolian transport and/or wave-driven sediment bypassing around the breakwaters in the ShorelineS model. However, it is debatable if these processes are the only reason for the (over)estimated coastline accretion, or if it is caused by the shortcomings of the model related to structure-coastline interaction.

Quantitative analysis

To study the specific coastline displacement predicted by the ShorelineS model quantitatively, certain transects are selected from which the temporal evolution of that specific coastline point is determined. These transects can be of any location, but it is most likely to study a coastline transect in which the modelled coastline change is the largest. For coastal zone management purposes, it is useful to study the transects in which potential coastline erosion occurs.

In the example as presented in Figure 6.18, it is clearly visible that significant coastline accretion has occurred in Transect 1, whereas Transect 2 seems to have been rather stable. It is interesting to evaluate the ”wiggles” in the evolution of the coastline position for the selected transects. A small variability in coastline position is common, but the variation of the position in Transect 1 seems rather large. Moreover, the modelled erosion in the first decades of the simulation do not look reliable as well. These observations are most likely caused by shortcomings of the ShorelineS model, such as the simplification of the active profile height and the interaction between the coastline and the structures. In addition, more importantly, the model inaccuracies probably origin from incorrectly simulated coastline displacement as a result of how ShorelineS threats the incoming wave angles. Hence, the used wave climate and the initial positions of the coastline and the potential structures have to be carefully considered.

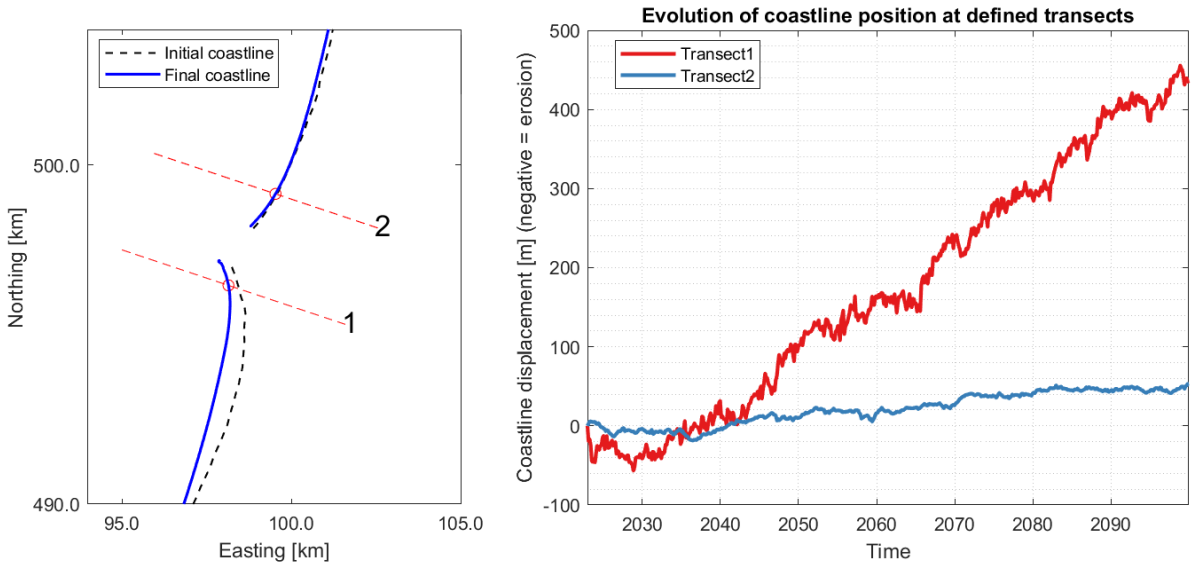

Figure 6.18: Result of ShorelineS model: coastline evolution for selected transects for 2023-2100.

Model limitations

To further illustrate potential ShorelineS limitations, an example is discussed. See Figure 6.19. If a small spit is formed on the coastline, this influences the longshore transport on both sides of this spit. Namely, the spit starts to accrete due to a (small) gradient in LST. The longshore transport at the front side of the spit is very large due to an incoming wave angle of around 45°. The LST gradient has developed because in the grid point behind the spit, the longshore transport is determined to be (almost) zero by the model. Consequently, the spit starts to grow further, resulting in an actual wiggle in the coastline. Fortunately, the model is often capable of recovering from these instabilities (if not too large), but the temporal evolution of a certain position on the coastline will show this process.

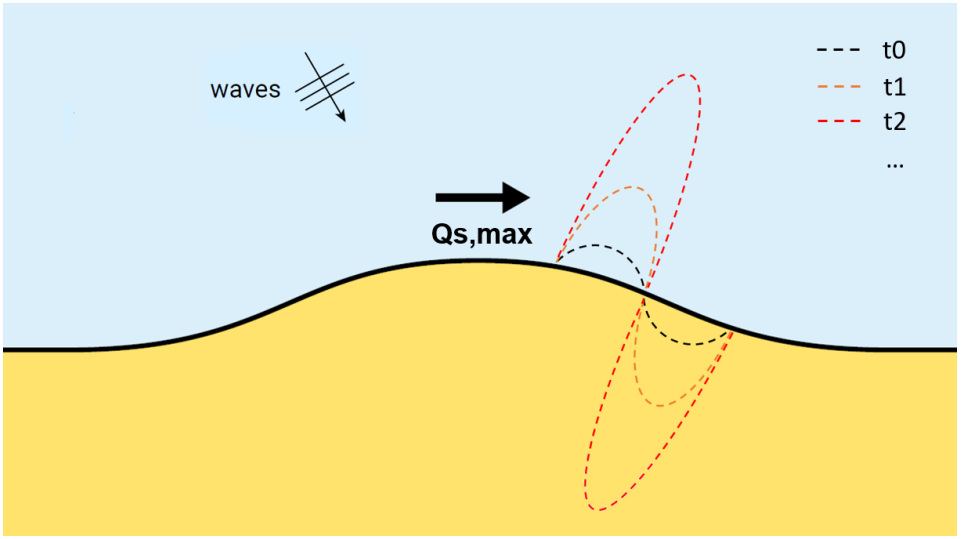

Figure 6.19: Schematic example of incorrectly simulated coastline displacement by the ShorelineS model.

6.2.3. Framework 1

In this section, the results of the implementation of the developed Framework 1 are presented. This is essentially the combination of the results from the PCR model and the ShorelineS model, visualised in one projection of coastline evolution. The results are shown in Figures 6.20 and 6.21 for the SLR scenario RCP8.5. The projections of the other SLR scenarios are presented in Appendix C.2. For illustration purposes, the same coastline transects are presented as in the ShorelineS results, see Figure 6.18 (left). Once again, it is mentioned that a wide range of transects can be studied by the user, dependent on the particular purpose.

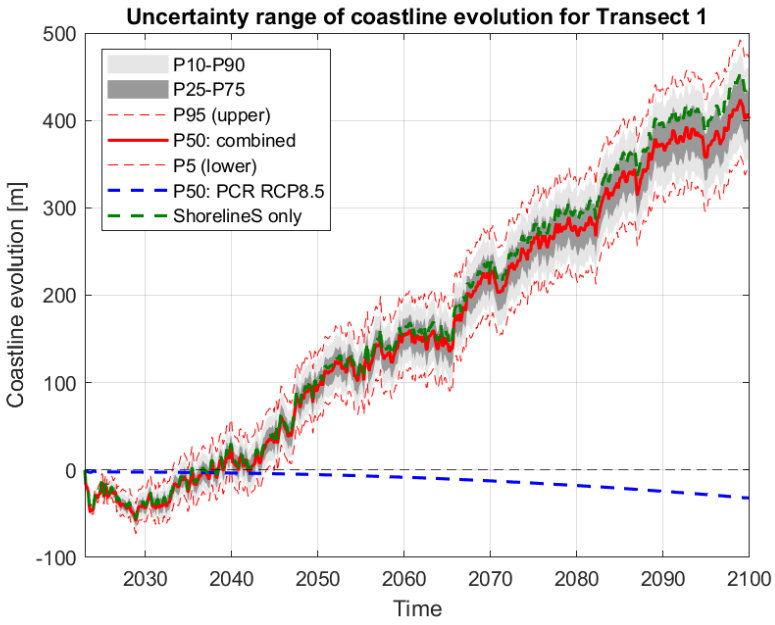

Figure 6.20: Result Framework 1: projection for IJmuiden coastline Transect 1 for 2023-2100 (RCP8.5).

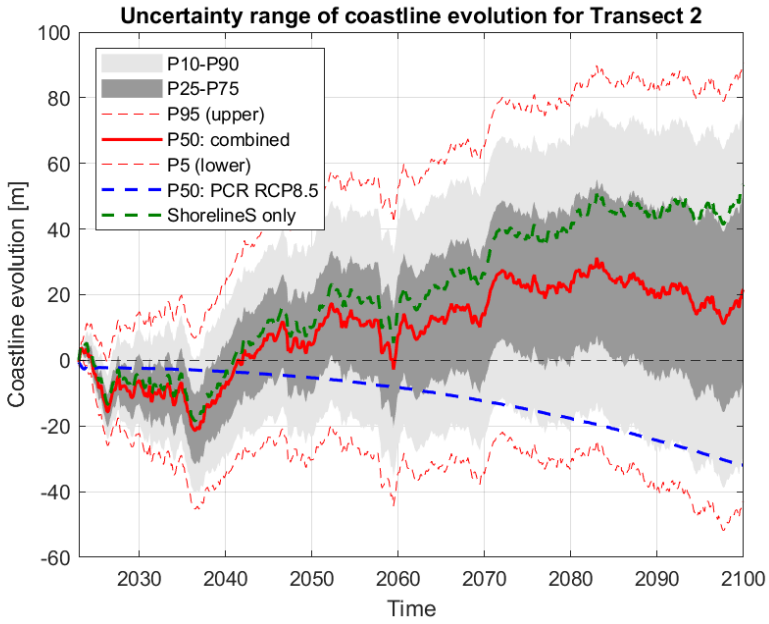

Figure 6.21: Result Framework 1: projection for IJmuiden coastline Transect 2 for 2023-2100 (RCP8.5).

Interpretation and analysis of results
Figures 6.20 and 6.21 show that the combined projections include an uncertainty range in the estimations of coastline change. This uncertainty range is solely based on the stochastic estimates of the cross-shore-induced coastline variability as modelled with the PCR model. Hence, no uncertainty in longshore-induced coastline development is included. It is interesting to see that the final combined median coastline evolution (i.e. the P50 value, thick red line) differs significantly from both the individual ShorelineS prediction and the individual PCR model prediction (the latter is presented for the most extreme SLR scenario RCP8.5).

A large difference between the plots of Transect 1 and 2 is observed. When compared to the separate results of the models presented in Sections 6.1.1 and 6.1.2, it can be concluded that for a coastline transect experiencing considerable coastline displacement due to longshore processes, the uncertainty range in cross-shore coastline change is less significant. This is the case for Transect 1 (Figure 6.20). Here, the P95-P5 uncertainty range of the coastline evolution, which is 69.08 meters on the upper and 64.51 meters on the lower side of the median predicted coastline evolution (i.e. a total range of 133.59 meters), is relatively small compared to the predicted median value (i.e. 404.34 meters of accretion).

In Figure 6.21, however, it is clearly visible that for Transect 2 the presented uncertainty in coastline evolution is highly significant due to the different order of magnitude than for Transect 1. Namely, the P95-P5 uncertainty range (i.e. 133.59 meters, equal to the uncertainty range of Transect 1) is considerably larger than the median value (i.e. 21.58 meters). As a result, it can be concluded that the calculated uncertainty range representing cross-shore-induced coastline variability is more relevant for Transect 2 than for Transect 1. This analysis of the ratio of cross-shore and longshore contributions on coastline evolution is relevant for every coastline transect in the world.

Comparison with previous research
It is stated that it is difficult to compare the obtained combined results of this study quantitatively with previous research. The main reason for this is the fact that previous studies to the IJmuiden coastline (Hallin et al. (2019) and Krijnen (2021)) only considered a historical validation period, and no predictions were modelled in these studies. Bitaki (2019) studied a prediction for the year 2100 for the Holland coastline evolution induced by cross-shore processes, using only the PCR model. For the coastline transects around the IJmuiden coastline (the northern side of the port), the modelled median retreat by Bitaki (2019) was 42 meters for the RCP8.5 SLR scenario. This is just slightly larger than the PCR model's predicted median retreat of 31.94 meters in the present study - also for RCP8.5.

No previous studies have been performed in which cross-shore and longshore impacts are predicted in a probabilistic way. However, regarding the individual models, it is seen that the PCR model is capable of stochastically generating storm wave conditions and simulating dune erosion volumes in accordance with field measurements and literature (Section 6.1.1). In addition, the projected cross-shore coastline evolution by the PCR model is found to be realistic when compared to other methods such as the Bruun rule (Section 6.2.1). For the ShorelineS model, it is concluded that the model could be satisfactorily calibrated to simulate the coastline accretion of the IJmuiden coastline, also in line with the presented results by Hallin et al. (2019) and Krijnen (2021). See Section 6.1.2. This provides confidence to assume that the predicted combined results of Framework 1 have a sufficient level of accuracy.

Relevance of stochastic cross-shore variability
Next to the relevance of the uncertainty range for certain transects as described above, it can also be detected that over time, when the rate of SLR accelerates, the combined median coastline change (red thick line) starts to deviate more and more from the individual ShorelineS projection. This is evidently caused by the increase in coastline recession induced by storm erosion and the increasing effect of SLR over time. Figure 6.21 shows that for Transect 2, the increasing median retreat as predicted by the PCR model is the reason that the final combined median coastline evolution is significantly smaller than the final predicted value of only ShorelineS (i.e. 21.58 versus 53.52 meters of accretion). The described difference is equal to the predicted median cross-shore-induced retreat of 31.94 meters for the year 2100. For Transect 1 (Figure 6.20), again this effect is less significant as the predicted 31.94 meters median cross-shore-induced retreat is relatively small compared to the final predicted accretion by ShorelineS (i.e. 436.28 meters).

This analysis confirms that for coastline transects such as Transect 2, where gradients in LST do not result in large coastline displacement, the coastline variability is mainly governed by cross-shore processes. It shows the added value of the developed Framework 1 with respect to existing methods in which only cross-shore or only longshore processes are considered. Moreover, the obtained stochastic projections of (cross-shore-induced) coastline change can be highly useful for coastal zone management purposes as the exceedance probabilities and the uncertainty ranges enable risk-based approaches. For instance, it is relevant for management strategies regarding coastal structures or buildings, in which not only the long-term trend of a coastline is important, but also the most landward position that a coastline might reach during a certain period.

Disclaimer of results
In the figures it is also seen that the ”wiggles” in the projections are still present. They origin from the ShorelineS model prediction (see Section 6.2.2) and not from the PCR model. It is noted that these wiggles most probably do not correctly simulate the real coastline evolution. Moreover, the coastline displacement in the first decades of the ShorelineS simulation does not look realistic, as discussed in Section 6.2.2. Therefore, it has to be noted that the final results of the combined projections of coastline evolution might not be reliable and have to be analysed carefully. It is thus decided not to present them in a statistical analysis as was done for the PCR results in Tables 6.2 and 6.3.

On the other hand, it must be stated that the qualitative temporal evolution of the coastline induced by both cross-shore and longshore processes is clearly visible, as well as the individual cross-shore and longshore impacts. This also holds for the relevance of the obtained stochastic estimates of cross-shore-induced coastline variability.

6.3. Key points of Chapter 6

- The PCR model is validated based on historical erosion events and on the simulation of storm events, storm spacing, coastline recovery and the total numbers of storm events. It is concluded that the model performs adequately and is capable of modelling synthetic erosion volumes which are representative for historical erosion events. Also, the PCR model is able to simulate storm events and subsequent coastline recovery for a coast which is in equilibrium for the cross-shore processes.
- For the projections of cross-shore-induced coastline evolution for a range of sea level rise scenarios, the PCR model clearly shows the increasing effects of sea level rise on coastline erosion over time, predicting a median retreat of 32 meters in the year 2100 for the most severe RCP8.5 scenario. When compared to the Bruun rule, it is found that the Bruun rule retreat estimates become more conservative over time, relative to the PCR model.
- Regarding the ShorelineS model, overall, the calibration for the IJmuiden coastline is found to be satisfactory. The model is capable of simulating the coastline accretion on both sides of the breakwaters and also (to a desired extent) the observed curvature of the coastline.
- Observed deviations with the real, measured coastline evolution are most likely caused by the fact that ShorelineS does not consider wind-induced currents driving longshore transport, as well as wind-driven (aeolian) cross-shore transport. In addition, the omission of refraction effects and uncertainties in the bathymetry could play a significant role. Lastly, the ShorelineS model does not perform well in simulating structure-coastline interactions, which poses a significant shortcoming of the model.
- The implementation of Framework 1 shows that a coastline is almost never stable for the cross-shore processes, even if a coastline is accreting. It can therefore be highly important to include the cross-shore processes when predicting the long-term evolution of such a coastline.
- The projected temporal evolution of the cross-shore-induced coastline retreat indicates that over time, the cross-shore-induced coastline evolution becomes more significant, relative to the longshore component. This highlights the added value of Framework 1 with respect to existing methods in which only cross-shore or only longshore processes are considered.
- Lastly, the obtained stochastic projections of cross-shore-induced coastline changes can be highly useful for coastal zone management purposes as the exceedance probabilities and the uncertainty ranges enable risk-based approaches.

7

Discussion

Based on the results of this research as presented in the previous chapter, this chapter provides a discussion on the performed study. First, the meaning, importance and relevance of the implemented framework and the obtained results are discussed. Secondly, a thorough discussion is presented on the simplifications and limitations of the applied research methods.

7.1. Relevance of the research

This research aimed to combine predictions of long-term coastline evolution induced by cross-shore and longshore processes. Previous studies to combine cross-shore and longshore components in long-term coastal modelling have been performed. Hallin et al. (2019) derived gradients in longshore sediment transport (LST) directly from field observations and implemented these in a cross-shore model as a constant value per studied transect. It was studied whether this improved the model performance, compared to a simulation in which only cross-shore processes are considered. The results showed that gradients in LST are a key factor for long-term dune evolution at the studied site. For some of the transects, the LST gradients are the only supply of sediment available for aeolian transport - except for dune erosion during storms. Moreover, for one specific transect, the simulation including the LST gradients shows an almost perfect fit to the measured data. However, it was also found that the relative importance of different transport processes varies with location and time. Hallin et al. (2019) recommended the coupling of the used cross-shore model with a LST model, to account for the variability in LST rates due to varying forcing conditions, climate change and evolution of the coastline shape.

Bitaki (2019) used a probabilistic approach for simulating cross-shore transport processes and accounted for gradients in LST in the coastline's recovery process after storm events. It was found that the omission of LST gradients leads to under- or overestimation of the recovery rate as these gradients were found to have a significant accreting or eroding effect on coastal profiles. As for Hallin et al. (2019), the LST gradients were assumed to be constant over time. Krijnen (2021) developed a coupled model to account for the interaction between cross-shore and longshore sediment transport. A reduced-complexity longshore coastline model was used to implement time-varying LST gradients into a cross-shore coastal profile model, instead of data-derived LST gradients. Despite the uncertainty this method induces, the coupled model was found to be capable of simulating the long-term beach and dune evolution. The interaction of cross-shore and longshore processes even allowed for the simulation of the alongshore and cross-shore redistribution of nourished sediment.

To predict long-term coastline evolution under influence of both longshore and cross-shore processes, among which the highly uncertain climate change effects, ideally the probabilistic character as well as the interaction effects are taken into account. To obtain stochastic projections of long-term coastline development, the present study uses computationally efficient models which implement the assumption of a constant cross-shore profile. Krijnen (2021) concluded that the interaction between cross-shore and longshore processes is mainly relevant for the redistribution of nourished and/or eroded sediment over the coastal profile, which is assumed constant in this research. Therefore, this study considers no

interaction effects and combines the separately modelled time series of the cross-shore and longshore processes to obtain a combined projection of coastline evolution. This way, the temporal variability of the longshore coastline changes is taken into account, instead of only using gradients in LST. Furthermore, the cross-shore model provided probabilistic estimates, enabled by the large number of simulations. This resulted in an uncertainty range for the projections of long-term coastline evolution which is highly relevant for risk-based coastal zone management purposes.

The contribution of the long-term coastline development resulting from longshore processes is only described by a single, deterministic projection. It is not common to combine a stochastic output with a deterministic prediction, as this can lead to difficulties in reading and understanding the final projections. However, it can be debated that uncertainties in future coastline evolution mainly arise from the large uncertainty in storm intensity and frequency, as well as in climate change effects such as sea level rise (SLR). In this research, these processes are incorporated in the probabilistic cross-shore model, so the described uncertainties are taken into account. Large gradients in LST as a result of the blockage of LST by coastal structures are found to be significantly less uncertain. Therefore, in this study, it is considered acceptable to use deterministic values for longshore-induced coastline changes.

7.2. Research limitations

The developed framework in this research performs satisfactory in modelling cross-shore erosion volumes as well as coastline changes induced by gradients in LST. It also satisfied the aim of being computationally efficient. As a result, this framework can be seen as a useful method to combine cross-shore and longshore predictions in long-term, probabilistic coastline modelling. However, in order to achieve the research objective, several assumptions and simplifications have been implemented.

7.2.1. Research methodology

This section discusses the limitations of the research related to the applied methodology and the corresponding assumptions that are implemented in this study.

Probabilistic approach
As indicated in the previous section, the obtained projections of coastline evolution only include probabilistic estimates (i.e. an uncertainty range) based on the cross-shore processes. The ShorelineS model, responsible for the prediction of coastline changes induced by longshore processes, is not used in a probabilistic way. In this study, the modelled projections show a large variety in coastline displacement, which only represents the cross-shore variability as modelled by the PCR model. Two completely different predicted coastline positions within this uncertainty range might influence the longshore coastline changes differently. As a result, it can be considered an important simplification that only one single, deterministic projection for the alongshore coastline evolution is implemented. It is therefore highly recommended to investigate the possibilities of obtaining probabilistic projections of coastline change induced by longshore processes. However, it is mentioned again that most uncertainty arises from the cross-shore storm erosion and SLR, hence it is debatable if stochastic longshore projections would add significant value.

Interaction cross-shore and longshore
The described interaction between cross-shore and longshore processes is not taken into account in this study, as only Framework 1 (see Chapter 4) is applied and analysed. This forms a limitation of the present study. One of the most important reasons for this decision is the fact that the PCR model is not able to model changes in coastline orientation and in the cross-shore profile after erosion of a storm event. The model purely focuses on cross-shore coastline displacement and assumes a constant cross-shore profile - and so does the ShorelineS model. In reality, severe storm erosion can induce a (local) change in coastline orientation and in the coastal profile. A changed coastline orientation influences the longshore transport due to a changed incoming wave angle. If sufficiently large and abrupt, it can even cause gradients in LST. Hence, the modelled longshore-induced coastline change might differ significantly if storm events are neglected. Furthermore, a change in the cross-shore profile after a storm event determines the sediment availability (to be transported) in the coastal zone. If this

change is not considered in a sediment transport model, the amount of transported sediment might be considerably over- or underestimated. These interaction processes, which are thoroughly described in Section 2.3.4, are not considered in the combined projections as obtained in this study. This limitation could be mitigated by modelling multiple coastline transects with the PCR model, with each transect having its own wave conditions and morphological properties (i.e. dune height, etc.).

7.2.2. Model implementation

In this section, it is described how specific limitations and assumptions of the used models are responsible for certain research limitations.

Neglected processes
The recovery of the coastline during calm periods in between storm events is assumed to be constant in this research (Sections 3.2.5 and 5.1.4). This means that time-varying processes such as dune build-up by aeolian transport are not studied as a separate process, while - for the IJmuiden case - it is found to be the main driver for the redistribution of (eroded) sediment over the coastal profile after a storm event or after nourishments have been applied (Hallin et al., 2019). This happens in both cross-shore and alongshore direction. Hallin et al. (2019) and Krijnen (2021) showed that aeolian transport rates can be modelled with, for instance, the CS-model. This is not further looked into in the present study. Moreover, human influences such as vegetation placement and/or removal, beach houses and maintenance activities are also not considered, while they can strongly hinder the alongshore and cross-shore distribution of sediment.

Climate change uncertainty
Another noteworthy limitation of this study is the large uncertainty of the coastal response to climate change effects. These effects can be implemented in coastline modelling in numerous ways. In this research, the impact of SLR on coastline erosion is studied. It is included as an extra retreat of the coastline and it is also taken into account in determining the coastline retreat from the calculated erosion volumes (Sections 3.2.6 and 5.1.5). It was found that the implemented erosion model within the PCR framework (i.e. the Dunerule model) is highly sensitive to an elevated water level, resulting in unrealistic predictions of coastline recession. The main reason for this is the fact that the calibrated Dunerule model does not include the adaptation of cross-shore coastal profile to rising sea levels. Therefore, in this study an adjusted method to account for SLR effects is implemented (Section 5.1.5), leading to large uncertainties. Evidently, these uncertainties can not be assessed as it concerns future estimates.

Model uncertainty
It is mentioned that the fact that this study uses two different coastline models, each having their own uncertainties, might have resulted in a larger total uncertainty for the final results. This must be considered when analysing the obtained projections. As described in Section 2.4.3, model uncertainty can arise from model inadequacy (when the model does not cover all relevant processes), parameter uncertainty (in case of limited knowledge on parameters like grain size or settling velocity) and numerical limitations (e.g. due to model resolution). Kroon et al. (2020) found that model uncertainty is highly relevant for studies with large temporal and spatial scales, as it can become dominant over wave climate uncertainty and variability. The reason for this is the fact that for a long simulation period, years with extreme wave conditions are compensated by calmer years, while on the other hand, model uncertainty is a cumulative effect which increases with each time step. The present study does not further investigate this model uncertainty.

Sediment transport formulas
The Dunerule model, which has been used to calculate the storm-induced coastline erosion in this research, is a formulation that is specifically calibrated for the Dutch coastline by Li (2014). The universal applicability of this erosion function is thus not guaranteed at all. This has to be taken into consideration when using the Dunerule model within the developed framework of the present study. For the IJmuiden coastline, the Dunerule model was able to satisfactory compute erosion volumes, provided that effects of SLR were excluded (as indicated in the previous paragraph). However, other erosion models can easily be implemented in the framework of this study.

Regarding the calculation of the longshore transport in the ShorelineS model, the simplified CERC1 formulation was used (Section 5.2). The CERC1 formula is based on deep water wave height and direction. This means that no refraction is included in the calculation, while the used wave climate represented deep water wave conditions before wave breaking. This might have led to inaccurate ShorelineS results due to inaccurate values of incoming wave direction, especially for the long-term projection of the 2023-2100 period. Also here, it is mentioned that other transport formulations can easily be implemented into the developed framework.

Model shortcomings

The breakwaters on the IJmuiden coastline cause a shadow zone behind the structures with reduced wave action. This sheltering effect is implemented in the ShorelineS model for longshore transport, but it is not included in the PCR model due to the fact that the PCR model only models a single transect. This has to be taken into account when using the PCR model results to study a transect in the lee side of a breakwater. Finally, it is noted that the used models are both still in the development phase. Regarding the PCR model, the assumption of the constant recovery rate and the used erosion function are important points of attention. For ShorelineS, the improvement of simulating structure-coastline interaction is currently being studied by its developers. Also, ShorelineS can experience difficulties with handling incoming wave angles with respect to the forming of spits: see Figure 6.19. Finally, the adaptive time step within the ShorelineS model (Section 3.3.2) is to be handled with care.

8

Conclusion

In this chapter, the conclusions and recommendations of the research are presented. First, the main research question and the sub-questions are answered. After this, the recommendations for further research are discussed.

8.1. Conclusions

The goal of this study was to investigate the possibilities to combine predictions of long-term coastline evolution induced by both cross-shore and longshore processes, using a stochastic approach. This section provides the answers to the main research question and the corresponding sub-questions. These answers form the final conclusion of this research.

8.1.1. Sub-questions

1. What are the relevant physical processes responsible for long-term coastline evolution?

Based on literature research and on available coastline models, it was found that the main physical processes relevant for long-term coastline modelling are: structural coastline erosion due to storm impact, coastline recovery in the periods between extreme storm events, sea level rise (SLR) and gradients in longshore sediment transport (LST). The first three processes occur perpendicular to the coastline, i.e. cross-shore, whereas the latter occurs parallel to the coastline, i.e. longshore. It is found that these processes can have a combined influence on long-term coastline evolution and can interact. For coastal areas dominated by LST, storm erosion could lead to amplified coastline displacement, since the eroded sediment might be transported away from the particular coastal section. Hence, the coastal profile can not recover to its initial state due to a lack of sediment availability.

Next to that, severe storm-induced erosion can cause a change in coastline orientation and in the cross-shore coastal profile, which influences the local LST rate since it depends on the angle of the incoming waves. In other words, cross-shore storm erosion might change or induce gradients in LST, which are responsible for the long-term evolution of the coastline. Moreover, it is found that the effect of storm erosion depends on the incoming wave angle (e.g., reduced wave heights due to refraction). Hence, a significant change in coastline orientation induced by longshore processes also influences the coastline's response to (cross-shore) storm impact. Finally, it was also found that accreting beaches respond faster to storm impact due to the sediment supply being close to the coastline, resulting in high sediment transport efficiencies.

It is found that nourishments can have a large influence on the sediment availability in a coastal zone and therefore on the long-term coastline evolution. The effects of nourishments, however, were not further studied in this research. This also holds for the process of wind-blown (aeolian) transport, which is found to have an important contribution to the recovery of the coastline in between storm events.

2. How can the relevant physical processes be modelled to obtain long-term projections of coastline evolution?

The response of a coastline to the impact of an extreme storm event can be modelled by implementing a dune erosion function, i.e. a sediment transport formula which translates the transported sediment from the dune to a retreat of the dune or coastline. To this end, analytical, (semi-)empirical or process-based models can be developed. These models can be one-dimensional (1D), two-dimensional depth-averaged (2DH) or three-dimensional (3D). The more detailed and complex the model, the higher the required computational time. Therefore, to approach the research objective of this study to model long-term coastline evolution, it is not possible to implement an advanced, process-based model. This research uses a semi-empirical dune erosion model. As this model implements several assumptions and a simplified transport formulation, it raises some uncertainties and limitations, but it is highly useful for modelling long-term simulations in a fast way. As a result, it is possible to obtain probabilistic estimates due to the large number of simulations.

The recovery of a coastline during the calm periods in between storm events is complex to model as it depends on multiple processes, such as aeolian transport, nourishments, human activities and the presence of structures or vegetation. The relative importance of the specific transport processes varies with location and time. In this study, a constant rate for this coastline recovery was assumed, in accordance with findings in literature.

In order to model the long-term effects of SLR, two processes can be considered: an additional retreat of the coastline due to an elevated water level and an increase in storm intensity due to the same elevated water level. The first process can be modelled using the Bruun rule or with a simplified formula that translates the increased water level to a coastline retreat based on the beach slope. The second process is more difficult to predict, since large uncertainties are present in the current projections of SLR and their effect on coastal zones. To deal with these uncertainties, multiple defined scenarios of SLR can be implemented.

It is uncertain how coastal profiles will adapt to rising sea levels, although it is assumed that the cross-shore profile will change to be more resistant against SLR. Moreover, estimating the effect of SLR on storm erosion is highly dependent on the used erosion model. In this study, a dune erosion model was used which was calibrated for a specific coastline along the Dutch coast. As this erosion function is calibrated with historical measurements, the described adaptability of the profile to SLR is not included in this model. Therefore, it was decided to apply an adjusted method: the elevated water level due to SLR is not taken into account in the calculation of the storm-induced erosion volume, but only in the translation of the eroded volume to the final coastline retreat. Furthermore, it is important that no double counting occurs when estimating SLR effects, so the methods should be implemented with care and with sufficient knowledge of the underlying physical processes.

The total coastline evolution induced by the governing physical processes in cross-shore direction, i.e. storm erosion, recovery and long-term sea level rise (SLR) can be modelled by the PCR model. Due to the fact that most components are modelled separately, the model has a very low computational time. This makes the PCR model perfectly suitable for being used in a probabilistic framework. Moreover, the low computational time makes it possible to model multiple coastline transects, from which a full coastline can be simulated.

Regarding the gradients in LST, longshore sediment transport formulations can be used. Also in this case, these formulations can vary in complexity and thus in computational time. Again, according to the research objective, it was decided to implement a simplified transport formulation in this study. To achieve computational efficiency, this transport formula was implemented in the coastline model ShorelineS, which - instead of a coastal profile model - assumes a constant active profile height. The advantage of the ShorelineS model is that it is a free-form coastline model: it describes the coastline as a chain of grid points that can move, expand and shrink freely.

3. What is the added value of a framework that combines the relevant processes compared to existing methods?

The case study of the IJmuiden coastline showed that even for accreting coastlines, the cross-shore-induced coastline variability is still relevant. This variability can be in the order of tens of meters. For coastal zone management purposes it is important to predict the most landward position that a coastline might reach during a certain period, e.g. the maximum coastline retreat after a storm event. It was found in this study that for the RCP8.5 SLR scenario, this most landward coastline position can be more landward than the predicted longshore-induced position with values of 31.94 meters for a 50% probability, and even up to 170.34 meters for a 0.01% probability (i.e. 1 in 10,000 - often implemented in coastal management policies). This element is not taken into account when only considering longshore processes to predict the evolution of a coastline, an approach which is often found in literature.

The IJmuiden case study also showed that for coastline transects where no considerable longshore-induced coastline change occurs, the cross-shore-induced coastline variability is highly relevant. It was found in this study that for a particular coastline transect with a predicted accretion of 53.52 meters based on longshore processes only, the median of the predicted cross-shore-induced coastline retreat of 31.94 meters is very significant. For smaller exceedance probabilities, the cross-shore processes can even lead to a case in which this particular coastline transect shows no accretion anymore, but starts to erode. This is especially relevant for long-term assessments, as the effect of SLR and storm-induced erosion will increase over time. On the other hand, it is mentioned that in this study also a coastline transect was analysed which experienced 404.34 meters of accretion, for which the described median cross-shore-induced coastline change is less significant. However, also in this case it is relevant to consider the potential most landward coastline position in coastal zone management, especially for the smaller exceedance probabilities.

It can be concluded that the added value of the developed framework is that it detects and highlights the individual relevance of cross-shore and longshore processes for specific coastline transects. Moreover, it is able to predict the combined influence of both processes on the coastline evolution. For almost every coastal region in the world, it is highly important to study the relative contributions of both cross-shore and longshore processes to the total evolution of a coastline. This can be done with the developed framework. It is possible to predict the most landward coastline position during a certain studied period, while accounting for both cross-shore and longshore processes. In addition, the obtained stochastic estimates and the uncertainty range enable risk-based approaches, e.g. for the design of coastal structures or beach maintenance strategies.

8.1.2. Main research question

How can cross-shore and longshore nearshore processes be combined in long-term, probabilistic coastline modelling, in order to obtain stochastic projections of long-term coastline evolution?

In order to approach the main research question, four frameworks were developed based on the relevant physical processes as presented in the answers to the sub-questions:

1. Cross-shore and longshore processes are modelled separately;
2. Longshore processes respond to cross-shore storm erosion;
3. Cross-shore processes respond to changed coastline orientation induced by LST gradients;
4. Both processes are coupled and fully interact with each other.

In this research, it was studied whether Framework 1 is a suitable method to answer the main research question. The developed Framework 1 performs satisfactory in simulating cross-shore erosion volumes in line with field measurements and literature, as well as in hindcasting coastline changes induced by gradients in LST in accordance with previous studies. The framework also satisfied the aim of being computationally efficient, in order to obtain stochastic estimates of coastline development. As a result, Framework 1 can be seen as a useful method to combine cross-shore and longshore processes in long-term, probabilistic coastline modelling.

By accounting for time-varying coastline changes due to gradients in LST, the framework departs from modelling approaches that only cover cross-shore processes or only include constant values for the LST gradients in a cross-shore model. Furthermore, by integrating the range of uncertainties of wave climate and stochastic forcing, it departs from methods that only use a design storm or a benchmark event, i.e. the largest measured historical storm event. Finally, by providing probabilistic projections of long-term coastline evolution, it departs from modelling approaches in which only single, deterministic predictions are derived.

When implementing Framework 1, the coastline evolution of multiple selected coastline transects can be studied over time, e.g. for specific years within the simulation period. Also, the probabilities of exceedance for specific coastline recessions can be derived. This is highly useful for coastal zone management purposes. Moreover, multiple SLR scenarios can be implemented in the framework, in order to study the different long-term effects on the evolution of a coastline.

Framework 1 can be implemented for almost every coastal region in the world. Local wave data is needed for the statistical analysis to obtain the synthetic storm time series and for the calculation of longshore sediment transport volumes. In addition, local morphological data is necessary as input, to describe the (simplified) cross-shore coastal profile. However, the framework may be irrelevant for coastal areas where the coastline is fully dominated by storm erosion and no gradients in LST are present, or the other way around. Lastly, it is noted that the framework comes with several limitations due to the implemented assumptions. Hence, the methods should be implemented carefully and with sufficient understanding of the underlying physical processes.

8.2. Recommendations

Based on the relevance of this study, the obtained results and the discussed research limitations, several recommendations for further research are proposed.

Interaction cross-shore and longshore
In this research it was found that interaction between cross-shore and longshore processes is present in reality and that it influences the long-term evolution of coastlines. However, this effect was not implemented in the modelling framework. This forms a large limitation of the present study. It is therefore highly recommended to study the long-term coastline evolution induced by both cross-shore and longshore processes while including their interaction, in order to see how strongly it influences the long-term coastline variability.

The most important elements that have to be taken into account to incorporate this interaction is the orientation of the coastline and the variation in the coastal profile. As both models implemented in this research assume a constant cross-shore profile, the latter is not studied. Also, in this study, no change in coastline orientation after storm-induced erosion was modelled since the PCR model is not capable of simulating this. A solution can be to model multiple transects with the PCR model, with each having their own local wave conditions and morphological properties (dune height, etc.). Hence, the orientation of the coastline between these transects can be derived. If these transects show different coastline displacement after a storm event, the orientation has thus changed. Consequently, the (gradients in) LST might change as well, which would lead to a different coastline evolution. Another option is the use of a more advanced cross-shore model, which is capable of modelling cross-shore-induced variation in coastline orientation. However, it should be studied if this results in increased computational time due to increased complexity.

Framework 2 is highly suitable for this approach. Herein, the instantaneous storm-induced coastline change is implemented in the ShorelineS model during the simulation. Hence, if multiple transects are modelled with the PCR model and the corresponding coastline changes are implemented in ShorelineS at their specific location on the coastline, the ShorelineS model accounts for this storm-induced retreat within its own calculations. This would also enable accounting for sheltering effects behind coastal structures, as it could be assumed that no storm erosion (i.e. no coastline retreat) occurs in the corresponding shadow zone.

Probabilistic output for longshore component
In this study, only the cross-shore coastline displacement induced by cross-shore processes is presented in a probabilistic way. It is highly recommended to investigate the possibilities of obtaining probabilistic projections of coastline change induced by longshore processes. Low computational time is a requirement for this, which can be achieved by simplified analytical transport formulations or by less complex models. In the near future, it might even be possible to use ShorelineS for this purpose as further model developments are ongoing. Additionally, it is recommended to study stochastic projections of sea level rise and beach recovery in long-term coastline modelling.

Coastline recovery
The coastline recovery rate was assumed to be constant in the framework implementation. As a result, the time-varying process of dune build-up by aeolian transport is not considered. Also, the implementation of nourishments is not studied here, while they are known to have a large influence on the sediment availability in a coastal zone and therefore on the long-term coastline evolution. Moreover, human influences such as vegetation placement or removal, beach houses and beach maintenance activities are also not considered. In this study it is assumed to be acceptable to neglect the time-dependent processes as the focus is on the long-term evolution. However, for further research, it is recommended to thoroughly study the relevant processes contributing to coastline recovery and to include those processes separately in the developed framework of this research, to study their individual effects.

Other recommendations
A few other recommendations are discussed, which focus more on the specific implementation of the models:

- The used dune erosion function within the PCR model, i.e. the Dunerule model, is specifically calibrated for a transect along the Dutch coast by Li (2014). The universal applicability of this erosion function is thus not guaranteed. Moreover, the Dunerule model was found to be unrealistically sensitive to an increased water level induced by SLR. As a result, it is recommended to study different erosion functions within the PCR model, to see if these perform better for multiple coastal regions around the globe.
- An alternative option is to use the Dunerule model and to use historical data to fully calibrate it for a specific coastline transect to be studied. This depends on the purpose of the study, but it can be very useful if thorough analysis of that particular transect is required.
- Also, the implemented sediment transport formulation for the calculation of longshore transport is the simplified CERC1 formula. It is advised to study other transport formulations within the ShorelineS model. This could significantly improve the model calibration as well as the model predictions, since more complex transport formulations also include more input parameters such as the wave period and sediment grain size, but also wave breaking and refraction. However, the balance between the required accuracy and the computational time should be kept in mind here.
- In this study, a particular method is implemented to account for the (long-term) effects of climate change. Due to the numerous uncertainties in how climate change will evolve, it is recommended to further investigate how coastal profiles adapt to rising sea levels and to adjust dune erosion models to this. This might result in a more accurate prediction of a coastline's response to climate change impact.
- Lastly, it is recommended that further research is carried out to the proposed Frameworks 3 and 4. It should be further investigated if Framework 4 is feasible with respect to the research objective of small computational time. In addition, it can be studied if other models than the PCR model and the ShorelineS model could be a better fit for those frameworks.

References

Antolínez, J. A. A., Méndez, F. J., Anderson, D., Ruggiero, P., & Kaminsky, G. M. (2019). Predicting climate-driven coastlines with a simple and efficient multiscale model. *Journal of Geophysical Research: Earth Surface*, *124*, 1596–1624. https://doi.org/10.1029/2018JF004790

Bayram, A., Larson, M., Hanson, H., & Carr, C. (2007). A new formula for total longshore transport rate. *Proceedings of the Coastal Engineering Conference*, 3357–3369. https://doi.org/10.1142/9789812709554_0283

Bergillos, R. J., Masselink, G., & Ortega-Sánchez, M. (2017). Coupling cross-shore and longshore sediment transport to model storm response along a mixed sand-gravel coast under varying wave directions. *Coastal Engineering*, *129*, 93–104. https://doi.org/10.1016/J.COASTALENG.2017.09.009

Bitaki, A. (2019). *Estimating future coastline changes along Holland coast, under different sea level rise scenarios, using a probabilistic approach* (Master's thesis). Delft University of Technology. Delft, the Netherlands.

Bosboom, J., & Stive, M. J. F. (2021). *Coastal Dynamics*. TU Delft Open. https://doi.org/10.5074/T.2021.001

Bruun, P. M. (1962). Sea-Level Rise as a Cause of Shore Erosion. *Journal of the Waterways and Harbors Division*, *88*, 117–132.

Callaghan, D. P., Nielsen, P., Short, A., & Ranasinghe, R. (2008). Statistical simulation of wave climate and extreme beach erosion. *Coastal Engineering*, *55*, 375–390. https://doi.org/10.1016/j.coastaleng.2007.12.003

Church, J., Clark, P., Cazenave, A., Gregory, J., Jevrejeva, S., Levermann, A., Merrifield, M., Milne, G., Nerem, R., Nunn, P., Payne, A., Pfeffer, W., Stammer, D., & Unnikrishnan, A. (2013). Sea Level Change. *Climate Change 2013: The Physical Science Basis. Contribution of Working Group I to the Fifth Assessment Report of the Intergovernmental Panel on Climate Change* (pp. 1137–1216). Cambridge University Press.

Da Cruz, C. M. (2018). *Stochastic projections of coastline variations: Application to Hasaki Beach, Japan* (Master's thesis). UNESCO-IHE Institute for Water Education. Delft, the Netherlands.

Dastgheib, A., Jongejan, R., Wickramanayake, M., & Ranasinghe, R. (2018). Regional scale risk-informed land-use planning using Probabilistic Coastline Recession modelling and economical optimisation: East Coast of Sri Lanka. *Journal of Marine Science and Engineering*, *6*(4). https://doi.org/10.3390/jmse6040120

Dastgheib, A., Martinez, C., Udo, K., & Ranasinghe, R. (2022). Climate change driven shoreline change at Hasaki Beach Japan: A novel application of the Probabilistic Coastline Recession (PCR) model. *Coastal Engineering*, *172*. https://doi.org/10.1016/j.coastaleng.2021.104079

de Schipper, M. (2019). Lecture Notes CIE4309 Coastal Dynamics II. Delft University of Technology, Department of Hydraulic Engineering.

de Vries, S., Southgate, H. N., Kanning, W., & Ranasinghe, R. (2012). Dune behavior and aeolian transport on decadal timescales. *Coastal Engineering*, *67*, 41–53. https://doi.org/10.1016/J.COASTALENG.2012.04.002

DHI Group. (n.d.). LITPACK: Integrated littoral processes and coastline kinetics modelling. https://www.dhigroup.com/

Elghandour, A. M. (2018). *Efficient Modelling of coastal evolution: Development, verification and validation of ShorelineS model* (Master's thesis). UNESCO-IHE Institute for Water Education. Delft, the Netherlands.

Frey, A. E., Connell, K. J., Hanson, H., Larson, M., Thomas, R. C., Munger, S., & Zundel, A. (2012). *GenCade Version 1 Model Theory and User's Guide*. Version 1. U.S. Army Engineer Research and Development Center.

Gatto, V. M., van Prooijen, B. C., & Wang, Z. B. (2017). Net sediment transport in tidal basins: Quantifying the tidal barotropic mechanisms in a unified framework. https://doi.org/10.1007/s10236-017-1099-3

Hallermeier, R. J. (1978). Uses for a calculated limit depth to beach erosion. *Coastal Engineering Proceedings*, *1*(16), 88. https://doi.org/10.9753/icce.v16.88

Hallin, C. (2019). *Long-term beach and dune evolution: Development and application of the CS-model* (Doctoral dissertation). Delft University of Technology. https://doi.org/DOI:10.13140/RG.2.2.36390.37447

Hallin, C., Huisman, B., Larson, M., & Hanson, H. (2018). Long-term dune evolution under interacting cross-shore and longshore processes. *Coastal Engineering Proceedings*, *1*(36), sediment.73. https://doi.org/10.9753/icce.v36.sediment.73

Hallin, C., Huisman, B. J., Larson, M., Walstra, D. J. R., & Hanson, H. (2019). Impact of sediment supply on decadal-scale dune evolution — analysis and modelling of the kennemer dunes in the netherlands. *Geomorphology*, *337*, 94–110. https://doi.org/10.1016/j.geomorph.2019.04.003

Hanson, H., & Kraus, N. C. (1989). *GENESIS: Generalized Model for Simulating Shoreline Change. Report 1. Technical Reference*. U.S. Army Corps of Engineers.

Hanson, H., Larson, M., & Kraus, N. C. (2010). Calculation of beach change under interacting cross-shore and longshore processes. *Coastal Engineering*, *57*, 610–619. https://doi.org/10.1016/j.coastaleng.2010.02.002

Hanson, H., Larson, M., & Kraus, N. C. (2011). Modeling long-term beach change under interacting longshore and cross-shore processes. *Coastal Engineering Proceedings*, *1*(32), sediment.62. https://doi.org/10.9753/icce.v32.sediment.62

Hinkel, J., Lincke, D., Vafeidis, A. T., Perrette, M., Nicholls, R. J., Tol, R. S. J., Marzeion, B., Fettweis, X., Ionescu, C., & Levermann, A. (2014). Coastal flood damage and adaptation costs under 21st century sea-level rise. *Proceedings of the National Academy of Sciences of the United States of America*, *111*, 3292–3297. https://doi.org/10.1073/pnas.1222469111

Hinkel, J., Nicholls, R. J., Tol, R. S., Wang, Z. B., Hamilton, J. M., Boot, G., Vafeidis, A. T., McFadden, L., Ganopolski, A., & Klein, R. J. (2013). A global analysis of erosion of sandy beaches and sea-level rise: An application of DIVA. *Global and Planetary Change*, *111*, 150–158. https://doi.org/10.1016/J.GLOPLACHA.2013.09.002

Holthuijsen, L. H. (2007). *Waves in Oceanic and Coastal Waters*. Cambridge University Press.

Hughes, M. (2016). *Coastal waves, water levels, beach dynamics and climate change*. CoastAdapt, National Climate Change Adaptation Research Facility, Gold Coast.

Krijnen, I. (2021). *Modeling long-term beach and dune evolution with interacting longshore and cross-shore processes* (Master's thesis). Delft University of Technology. Delft, the Netherlands.

Kroon, A., de Schipper, M. A., van Gelder, P. H., & Aarninkhof, S. G. (2020). Ranking uncertainty: Wave climate variability versus model uncertainty in probabilistic assessment of coastline change. *Coastal Engineering*, *158*, 103673. https://doi.org/10.1016/J.COASTALENG.2020.103673

Larson, M., Erikson, L., & Hanson, H. (2004). An analytical model to predict dune erosion due to wave impact. *Coastal Engineering*, *51*, 675–696. https://doi.org/10.1016/j.coastaleng.2004.07.003

Larson, M., & Kraus, N. (1989). SBEACH: Numerical Model for Simulating Storm-Induced Beach Change. Report 1. Empirical Foundation and Model Development. *U.S. Army Corps of Engineers (USACE)*, 266.

Larson, M., Palalane, J., Fredriksson, C., & Hanson, H. (2016). Simulating cross-shore material exchange at decadal scale. Theory and model component validation. *Coastal Engineering*, *116*, 57–66. https://doi.org/10.1016/J.COASTALENG.2016.05.009

Lesser, G. R., Roelvink, J. A., van Kester, J. A., & Stelling, G. S. (2004). Development and validation of a three-dimensional morphological model. *Coastal Engineering*, *51*, 883–915. https://doi.org/10.1016/J.COASTALENG.2004.07.014

Li, F., van Gelder, P., Ranasinghe, R., Callaghan, D., & Jongejan, R. (2014). Probabilistic modelling of extreme storms along the Dutch coast. *Coastal Engineering*, *86*, 1–13. https://doi.org/10.1016/j.coastaleng.2013.12.009

Li, F., van Gelder, P., Vrijling, J., Callaghan, D., Jongejan, R., & Ranasinghe, R. (2014). Probabilistic estimation of coastal dune erosion and recession by statistical simulation of storm events. *Applied Ocean Research*, *47*, 53–62. https://doi.org/10.1016/j.apor.2014.01.002

Li, F. (2014). *Probabilistic estimation of dune erosion and coastal zone risk* (Doctoral dissertation). Delft University of Technology.

Luijendijk, A., Hagenaars, G., Ranasinghe, R., Baart, F., Donchyts, G., & Aarninkhof, S. (2018). The State of the World's Beaches. *Scientific Reports*, *8*. https://doi.org/10.1038/s41598-018-24630-6

McCall, R. T., de Vries, J. S. V. T., Plant, N. G., Dongeren, A. R. V., Roelvink, J. A., Thompson, D. M., & Reniers, A. J. (2010). Two-dimensional time dependent hurricane overwash and erosion modeling at Santa Rosa Island. *Coastal Engineering*, *57*, 668–683. https://doi.org/10.1016/J.COASTALENG.2010.02.006

McGranahan, G., Balk, D., & Anderson, B. (2007). The rising tide: Assessing the risks of climate change and human settlements in low elevation coastal zones. *IIED*, *19*, 17–37. https://doi.org/10.1177/0956247807076960

Mil-Homens, J. (2016). *Longshore Sediment Transport: Bulk Formulas and Process Based Models* (Doctoral dissertation). Delft University of Technology. http://repository.tudelft.nl/.

Neumann, B., Vafeidis, A. T., Zimmermann, J., & Nicholls, R. J. (2015). Future coastal population growth and exposure to sea-level rise and coastal flooding - A global assessment. *PLoS ONE*, *10*. https://doi.org/10.1371/journal.pone.0118571

Nicholls, R. J., Hanson, S. E., Lowe, J. A., Warrick, R. A., Lu, X., Long, A. J., & Carter, T. R. (2011). *Constructing Sea-Level Scenarios for Impact and Adaptation Assessment of Coastal Areas: A Guidance Document. Technical Guidelines of the Task Group on Data and Scenario Support for Impact and Climate Analysis (TGICA) of the Intergovernmental Panel on Climate Change (IPCC). 64 pp.*

Overgaauw, T. (2021). *Modelling shoreline evolution in the vicinity of shore normal structures* (Master's thesis). Delft University of Technology. Delft, the Netherlands.

Palalane, J., & Larson, M. (2019). A Long-Term Coastal Evolution Model with Longshore and Cross-Shore Transport. *Journal of Coastal Research*, *36*(2), 411–423. https://doi.org/10.2112/JCOASTRES-D-17-00020.1

Ranasinghe, R. (2016). Assessing climate change impacts on open sandy coasts: A review. *Earth-Science Reviews*, *160*, 320–332. https://doi.org/10.1016/j.earscirev.2016.07.011

Ranasinghe, R. (2020). On the need for a new generation of coastal change models for the 21st century. *Scientific Reports*, *10*, 1–6. https://doi.org/10.1038/s41598-020-58376-x

Ranasinghe, R., Callaghan, D., & Stive, M. J. F. (2012). Estimating coastal recession due to sea level rise: Beyond the Bruun rule. *Climatic Change*, *110*(3-4), 561–574. https://doi.org/10.1007/s10584-011-0107-8

Ranasinghe, R., & Stive, M. J. F. (2009). Rising seas and retreating coastlines. *Climatic Change*, *97*(3), 465–468. https://doi.org/10.1007/s10584-009-9593-3

Rijkswaterstaat. (2022). *JARKUS: the yearly coastal measurements (Dutch: de JAaRlijkse KUStmetingen)*.

Robinet, A., Idier, D., Castelle, B., & Marieu, V. (2018). A reduced-complexity shoreline change model combining longshore and cross-shore processes: The LX-Shore model. *Environmental Modelling and Software*, *109*, 1–16. https://doi.org/10.1016/j.envsoft.2018.08.010

Roelvink, D., Huisman, B., Elghandour, A., Ghonim, M., & Reyns, J. (2020). Efficient Modeling of Complex Sandy Coastal Evolution at Monthly to Century Time Scales. https://doi.org/10.3389/fmars.2020.00535

Roelvink, D., Reniers, A., van Dongeren, A., van Thiel de Vries, J., McCall, R., & Lescinski, J. (2009). Modelling storm impacts on beaches, dunes and barrier islands [- XBeach]. *Coastal Engineering*, *56*, 1133–1152. https://doi.org/10.1016/j.coastaleng.2009.08.006

Ruessink, B., Boers, M., van Geer, P., de Bakker, A., Pieterse, A., Grasso, F., & de Winter, R. (2012). Towards a process-based model to predict dune erosion along the Dutch Wadden coast. *Netherlands Journal of Geosciences - Geologie en Mijnbouw*, *91*(3), 357–372. https://doi.org/10.1017/S0016774600000494

Salman, A., Lombardo, S., & Doody, P. (2004). *Living with coastal erosion in Europe: Sediment and Space for Sustainability*. EUCC. http://resolver.tudelft.nl/uuid:483327a3-dcf7-4bd0-a986-21d9c8ec274e

Schepper, R., Almar, R., Bergsma, E., de Vries, S., Reniers, A., Davidson, M., & Splinter, K. (2021). Modelling cross-shore shoreline change on multiple timescales and their interactions. *Journal of Marine Science and Engineering*, *9*. https://doi.org/10.3390/jmse9060582

Shi, H., & Singh, A. (2003). Status and Interconnections of Selected Environmental Issues in the Global Coastal Zones. *AMBIO: A Journal of the Human Environment*, *32*, 145. https://doi.org/10.1639/0044-7447(2003)032[0145:saiose]2.0.co;2

Small, C., & Nicholls, R. J. (2003). A Global Analysis of Human Settlement in Coastal Zones. *Source: Journal of Coastal Research*, *19*, 584–599. https://about.jstor.org/terms

Stanica, A., & Ungureanu, G. V. (2010). Understanding coastal morphology and sedimentology. *Terre et environnement*, *88*, 105–111.

Steetzel, H. J., de Vroeg, H., van Rijn, L. C., & Stam, J.-M. (1998). Morphological Modelling using a Modified Multi-layer Approach. *Coastal Engineering*, 2368–2381. https://doi.org/10.1061/40549(276)229

Stolk, A. (1989). *Zandsysteem kust: een morfologische karakterisering*. Rijkswaterstaat, Ministerie van Verkeer en Waterstaat.

Svendsen, I. A. (1984). Mass flux and undertow in a surf zone. *Coastal Engineering*, *8*, 347–365. https://doi.org/10.1016/0378-3839(84)90030-9

Tonnon, P., Huisman, B., Stam, G., & van Rijn, L. (2018). Numerical modelling of erosion rates, life span and maintenance volumes of mega nourishments. *Coastal Engineering*, *131*, 51–69. https://doi.org/https://doi.org/10.1016/j.coastaleng.2017.10.001

TU Delft. (n.d.). Coastal Morphology [Accessed June 8, 2022]. https://www.tudelft.nl/citg/over-faculteit/afdelingen/hydraulic-engineering/sections/coastal-engineering/coastal-morphology

USACE. (1984). *Shore Protection Manual. Coastal Engineering Research Center* (Vol. 1). Washington, DC: US Army Corps of Engineers.

Vafeidis, A., Neumann, B., Zimmermann, J., & Nicholls, R. J. (2011). *MR9: Analysis of land area and population in the low-elevation coastal zone (LECZ)*. UK Government's Foresight Project, Migration and Global Environmental Change.

Van Rijn, L. C. (2013a). *Erosion of coastal dunes due to storms*. www.leovanrijn-sediment.com

Van Rijn, L. C. (2013b). *A simple general expression for longshore transport of sand, gravel and shingle*. www.leovanrijn-sediment.com

van Dongeren, A., Ciavola, P., Martinez, G., Viavattene, C., Bogaard, T., Ferreira, O., Higgins, R., & McCall, R. (2018). Introduction to RISC-KIT: Resilience-increasing strategies for coasts. *Coastal Engineering*, *134*, 2–9. https://doi.org/10.1016/J.COASTALENG.2017.10.007

van Prooijen, B., & van Maren, B. (2022). Lecture Notes CIE4308 Sediment Dynamics. Delft University of Technology, Department of Hydraulic Engineering.

Vitousek, S., Barnard, P. L., Limber, P., Erikson, L., & Cole, B. (2017). A model integrating longshore and cross-shore processes for predicting long-term shoreline response to climate change. *Journal of Geophysical Research: Earth Surface*, *122*, 782–806. https://doi.org/10.1002/2016JF004065

Vousdoukas, M. I., Mentaschi, L., Voukouvalas, E., Verlaan, M., Jevrejeva, S., Jackson, L. P., & Feyen, L. (2018). Global probabilistic projections of extreme sea levels show intensification of coastal flood hazard. *Nature Communications*, *9*. https://doi.org/10.1038/s41467-018-04692-w

Wainwright, D. J., Ranasinghe, R., Callaghan, D. P., Woodroffe, C. D., Cowell, P. J., & Rogers, K. (2014). An argument for probabilistic coastal hazard assessment: Retrospective examination of practice in New South Wales, Australia. *Ocean & Coastal Management*, *95*, 147–155. https://doi.org/10.1016/J.OCECOAMAN.2014.04.009

Waterman, R. E. (2010). *Integrated coastal policy via Building with Nature* (Doctoral dissertation). Delft University of Technology. Delft, the Netherlands. http://resolver.tudelft.nl/uuid:fa9a36f9-7cf8-4893-b0fd-5e5f15492640

Winter, C. (2011). *Observation- and Modelling of Morphodynamics in Sandy Coastal Environments*. Fachbereich Geowissenschaften der Universität Bremen. Bremen, Germany.

Wong, P. P., Losada, I. J., Gattuso, J. P., Hinkel, J., Khattabi, A., McInnes, K. L., Saito, Y., & Sallenger, A. (2014). Coastal Systems and Low-Lying Areas. *Climate Change 2014: Impacts, Adaptation, and Vulnerability. Part A: Global and Sectoral Aspects. Contribution of Working Group II to the Fifth Assessment Report of the Intergovernmental Panel on Climate Change* (pp. 361–409). Cambridge University Press.

A

JARKUS data

This chapter presents the used JARKUS data (Rijkswaterstaat, 2022) in this study. The JARKUS data set (an acronym for annual coastal measurements - de JAaRlijkse KUStmetingen) provides cross-shore bathymetric profile data of the Dutch coast since 1965, and it is composed of coastal transects perpendicular to coastline, spaced by alongshore intervals of 250 meter.

Figure A.1: Overview of JARKUS transects for coastal region south of IJmuiden.

Figure A.1 shows the JARKUS transects for the coastal region on the southern side of the IJmuiden port. In line with the used wave data from Transect 12 as depicted in Figure 5.10, it is decided to use data from JARKUS transect 5900, which represents the same location on the coastline (approximately). Consequently, the cross-shore coastal profile, the dune height, the dune toe elevation and the beach slope from this transect are depicted and implemented in the models for the present study.

It is noted that simplifications of the reality are inevitable if dune and beach characteristics from these observations is used, as the data represents only yearly measurements. It is known that sandy coasts are highly dynamic systems and change in size and shape continuously, but this short-term variability is not taken into account in this research.

A.1. Cross-shore profile

Figure A.2 shows the evolution over time of the cross-shore coastal profile of the studied JARKUS transect.

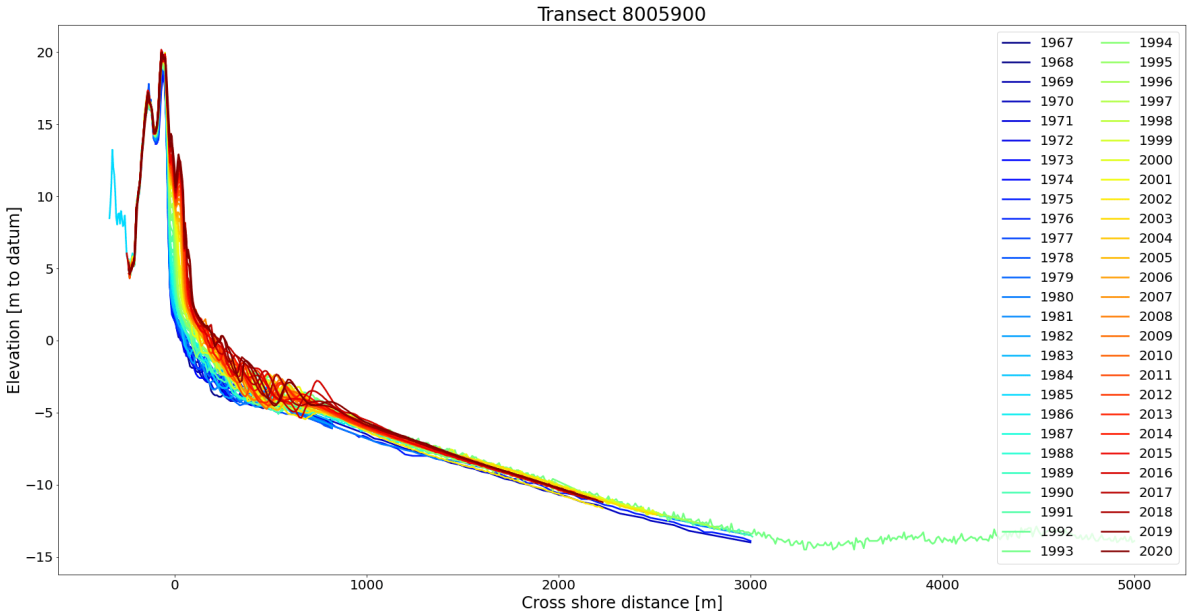

Figure A.2: Cross-shore profile evolution of JARKUS transect 5900.

A.2. Dune height

Based on the data as shown in Figure A.3, the dune height is taken as 19 m +MSL in this study. This is the safest value since a smaller dune height results in larger modelled dune erosion with the Dunerule model.

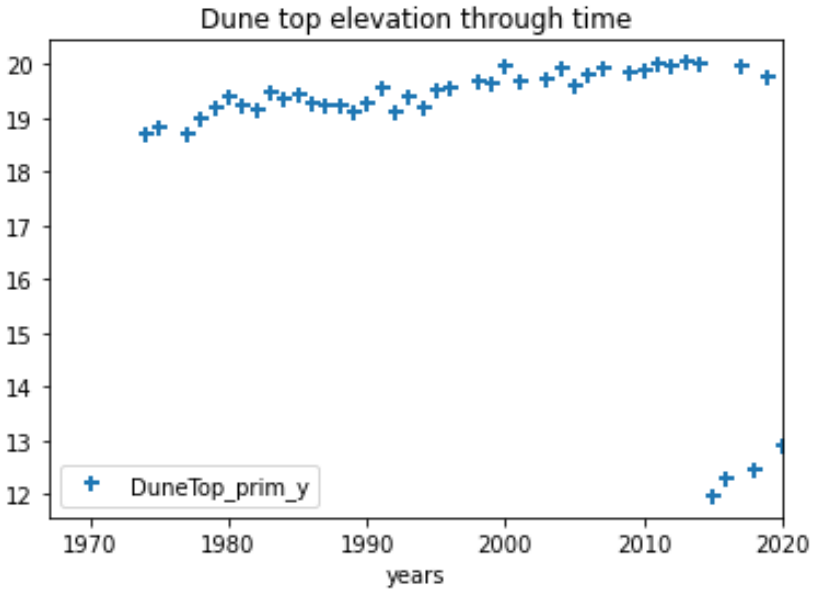

Figure A.3: Dune top evolution of JARKUS transect 5900.

A.3. Dune toe elevation

Figure A.4 shows the evolution of the dune toe elevation for the studied transect. In this study, a value of 3.0 m +MSL is taken.

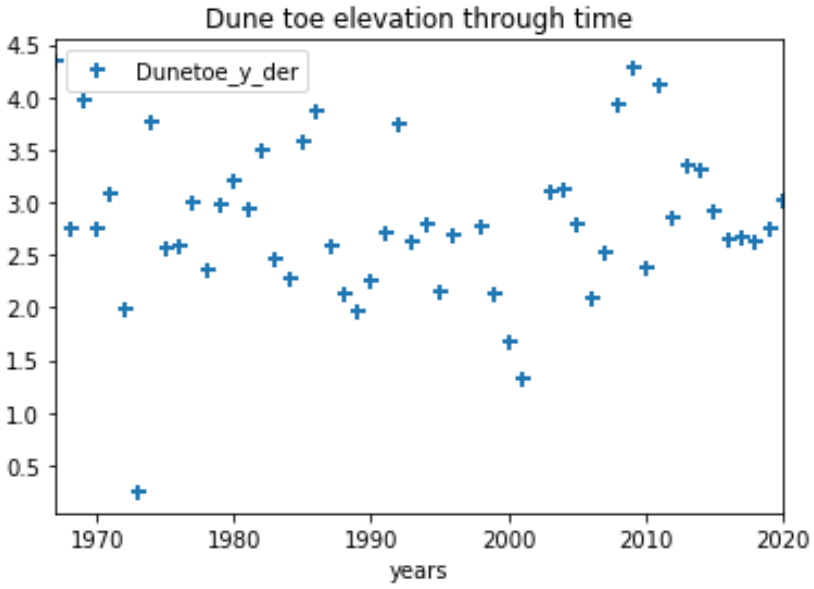

Figure A.4: Dune toe height evolution of JARKUS transect 5900.

A.4. Beach slope

Figure A.5 shows the variability of the beach slope at the particular coastline transect. A value of -0.025 (i.e. 1:40) is taken in this study, since a milder slope results in more severe effects of SLR, hence this is assumed to be a safe value.

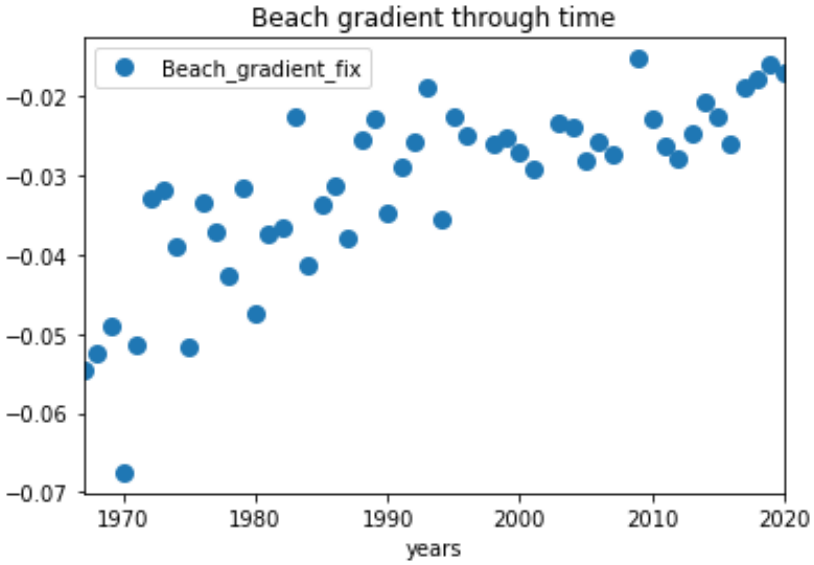

Figure A.5: Beach gradient evolution of JARKUS transect 5900.

A.5. Beach width

In Figure A.6 it is seen that the beach width at the studied transect varies significantly over the years. This variability is also visible along the full coastline, when more transects are analysed. In this research, an average value of 100 meter beach width is assumed, as this represents the most actual beach width measurements.

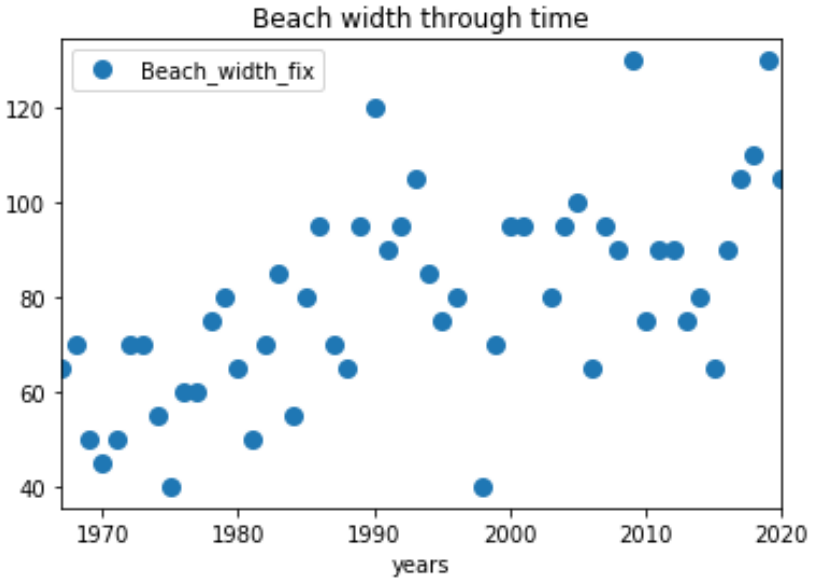

Figure A.6: Beach width evolution of JARKUS transect 5900.

A.6. Cross-shore location depth of closure

The cross-shore location of the DoC is mainly relevant for the calculation of SLR-induced coastline recession with the Bruun rule. As can be seen in Figure A.7, this cross-shore location varies significantly along the Dutch coast. For the Bruun rule application in the case study of this research, a (rather safe) value of 1500 meter is taken. It is noted that the calculated Bruun rule predictions are highly sensitive to this value, as discussed in Section 6.2.1.

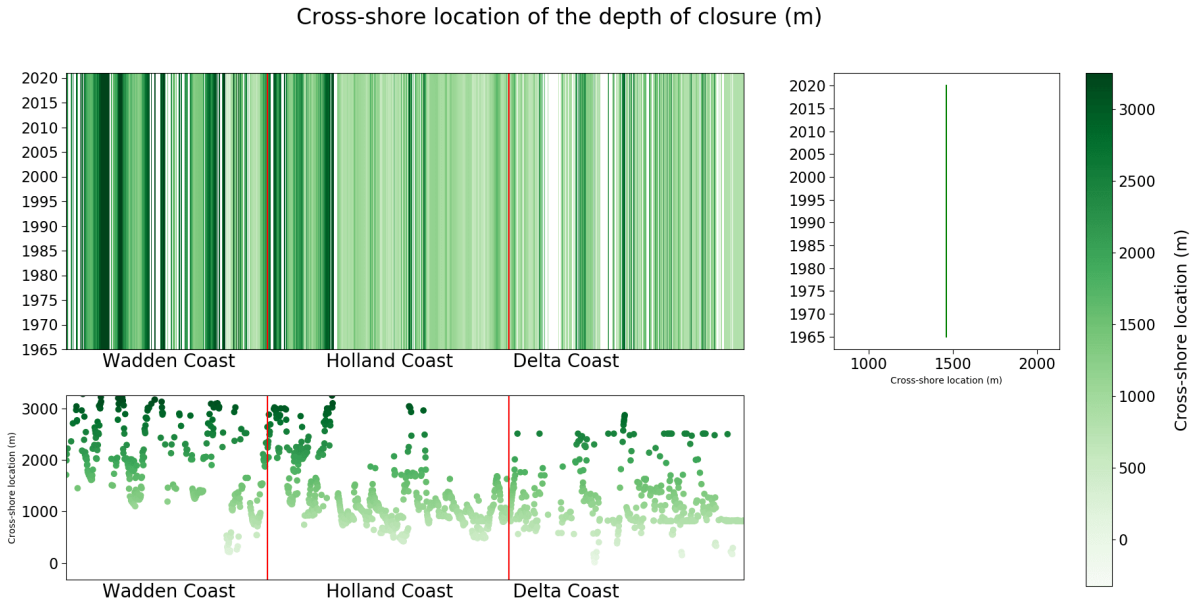

Figure A.7: Cross-shore locations of depth of closure along the Dutch coast.

B

Dunerule sensitivity

B.1. Results of SLR in Dunerule model

First, the impact of sea level rise (SLR) was studied by implementing the SLR in the water level parameter of the Dunerule erosion model, as follows:

$$R = 153 \cdot A_{dir} \cdot \left(\frac{h + SLR}{5}\right)^{\alpha_1} \cdot \left(\frac{H_{s,max}}{7.6}\right)^{\alpha_2} \cdot \left(\frac{D}{5}\right)^{\alpha_3} \cdot \left(\frac{T_p}{12}\right)^{\alpha_4} \tag{B.1}$$

$$\Delta y = \frac{R}{h_D - (h + SLR)} \tag{B.2}$$

However, the predictions of dune erosion volume turned out be highly unrealistic as a result of the large sensitivity of the Dunerule model to the water level parameter. This is most likely caused by the fact that the Dunerule model does not account for the potential adaptation of a coastal profile to increased sea levels. This sensitivity was already found by Van Rijn (2013a), who concluded that the water level and the sediment grain size are the most influential parameters in the Dunerule model. This phenomenon is further discussed in Section 5.1.5, in which it is also discussed which adjusted method is implemented in the present study to account for SLR effects.

In Figures B.1, B.2 and B.3, the results of the extremely large predicted coastline recession by the PCR model are shown. It is visible that for a scenario without SLR, the results are evidently equal to the results as presented in Section 6.2.1. However, when analysing the RCP8.5 SLR scenario, it is seen that an extremely large increase in coastline recession is visible, when compared to the presented results in Section 6.2.1.

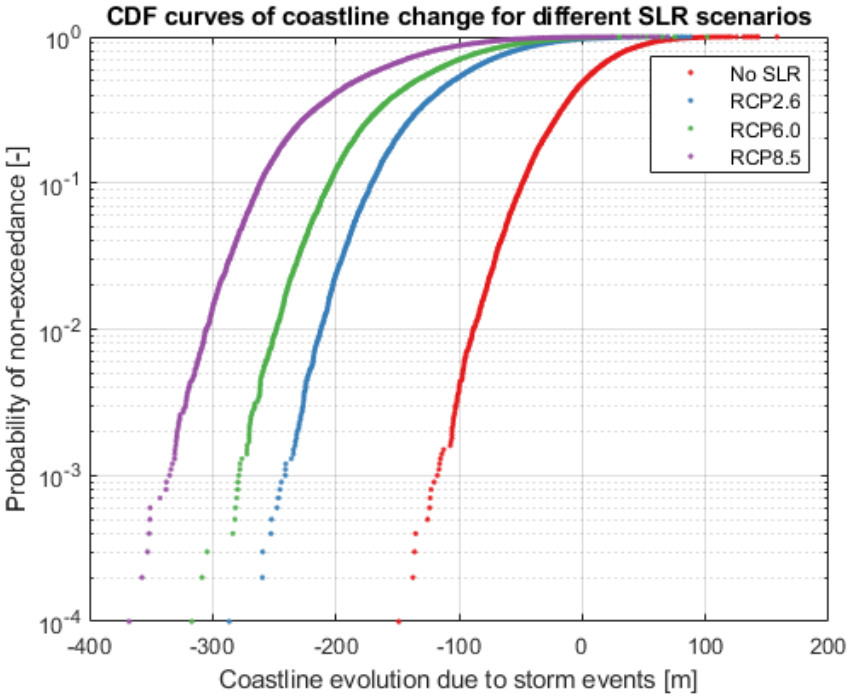

Figure B.1: PCR model: CDF curves of coastline evolution for different SLR scenarios.

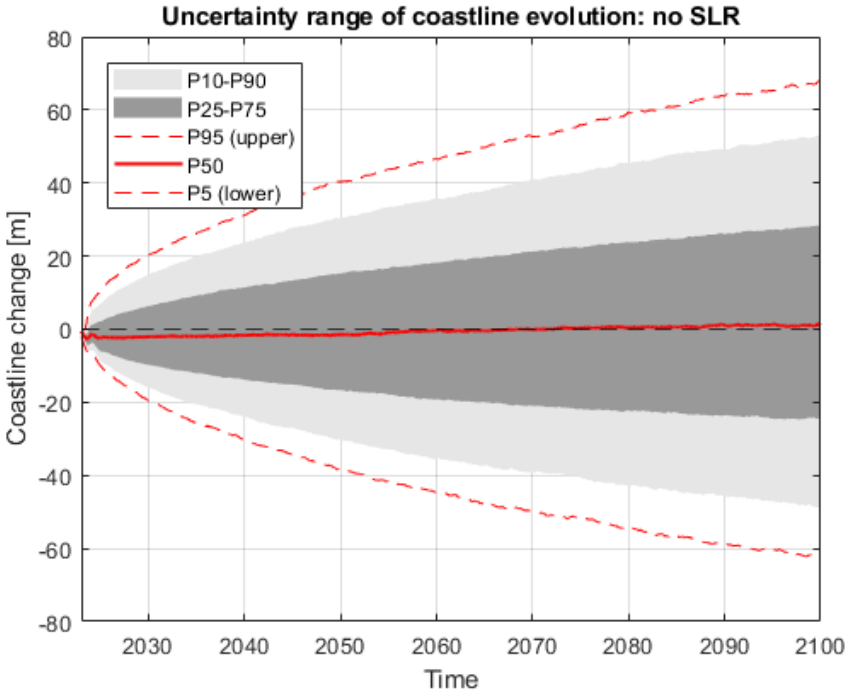

Figure B.2: PCR model: uncertainty range of coastline evolution for scenario without SLR.

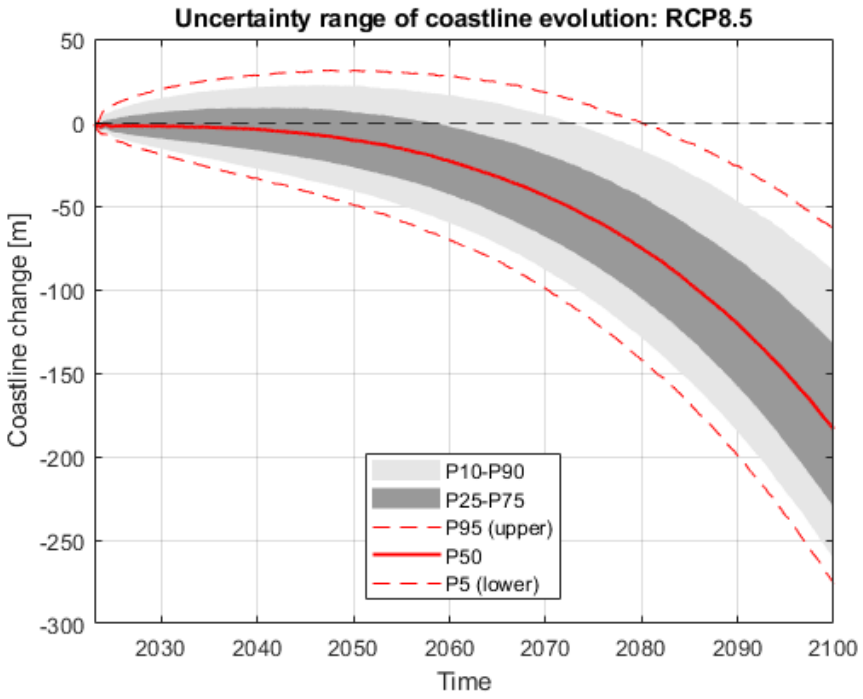

Figure B.3: PCR model: uncertainty range of coastline evolution for SLR scenario RCP8.5.

C

Other results

This chapter presents the obtained results that were not shown in Chapter 6 of the main report, i.e. the results for the SLR scenarios other than the presented SLR scenarios in Sections 6.2.1 and 6.2.3.

C.1. PCR model: uncertainty ranges of SLR scenarios

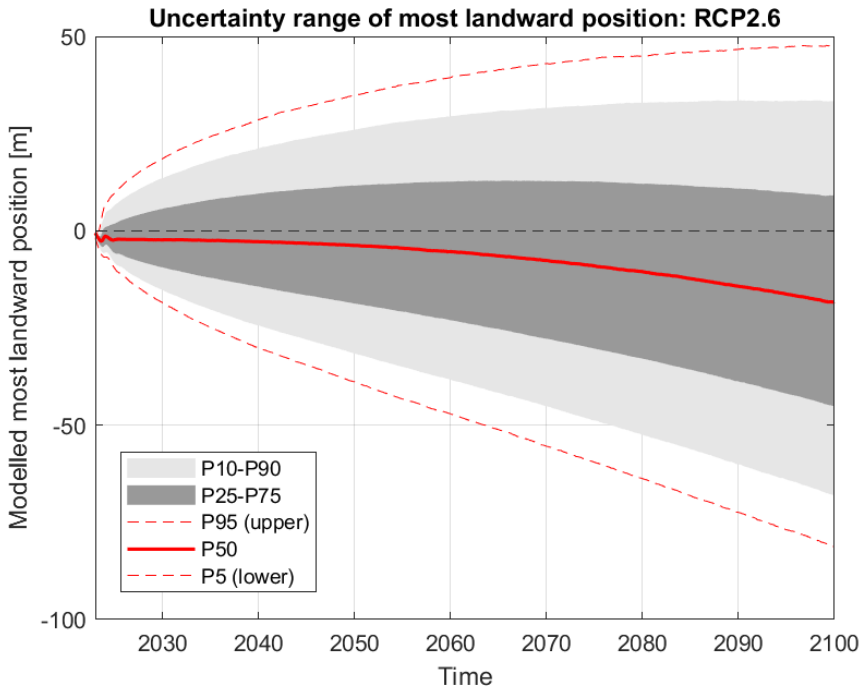

Figure C.1: PCR model: uncertainty range of coastline evolution for SLR scenario RCP2.6.

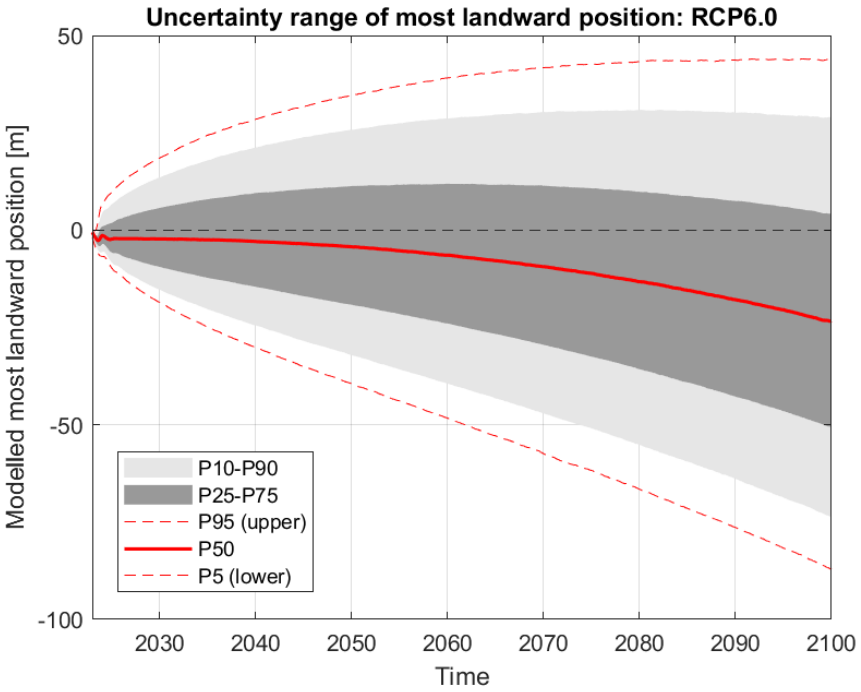

Figure C.2: PCR model: uncertainty range of coastline evolution for SLR scenario RCP6.0.

C.2. Framework 1: combined results for different SLR scenarios

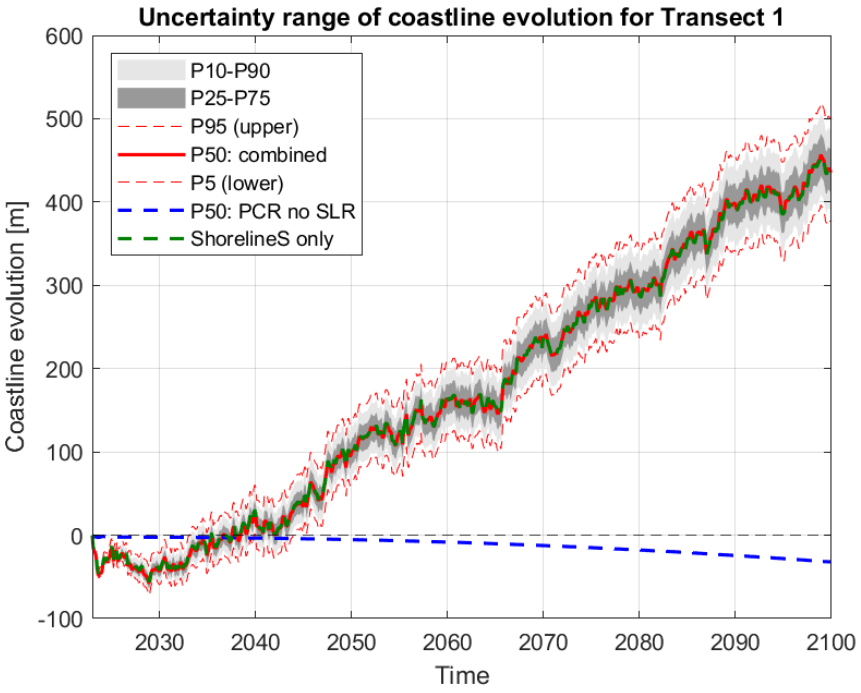

Figure C.3: Result Framework 1: projection for IJmuiden coastline Transect 1 for 2023-2100 (no SLR).

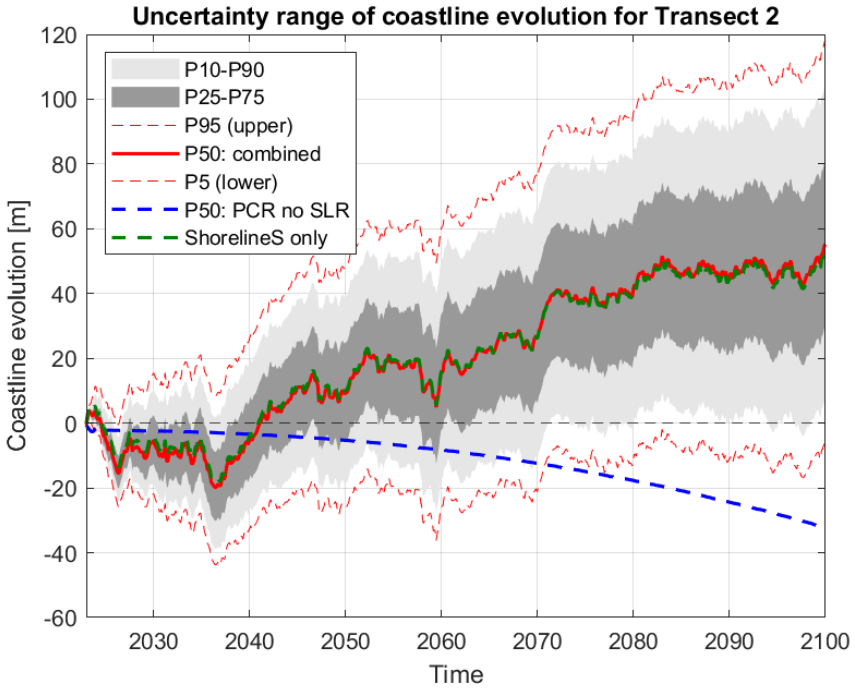

Figure C.4: Result Framework 1: projection for IJmuiden coastline Transect 2 for 2023-2100 (no SLR).

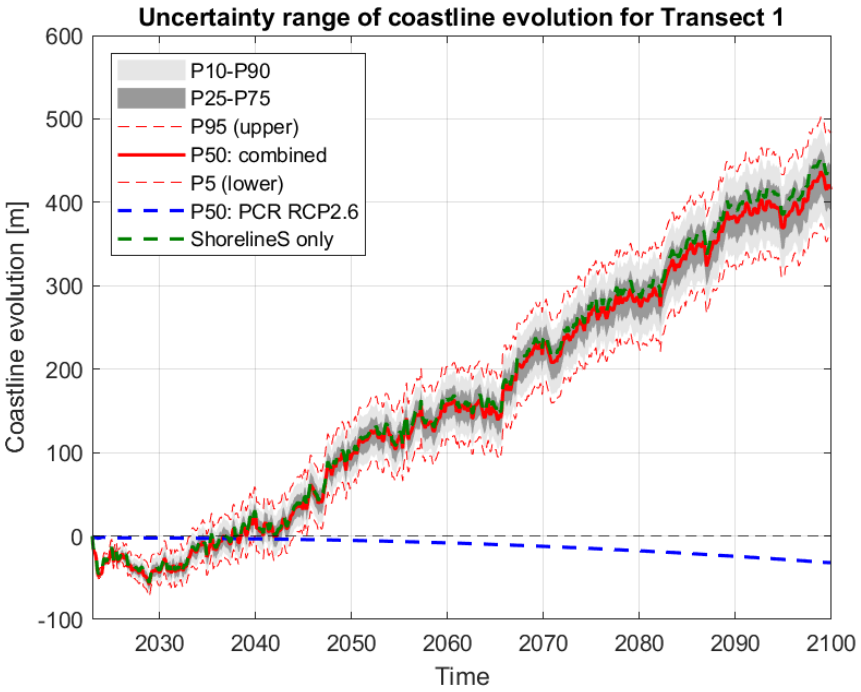

Figure C.5: Result Framework 1: projection for IJmuiden coastline Transect 1 for 2023-2100 (RCP2.6).

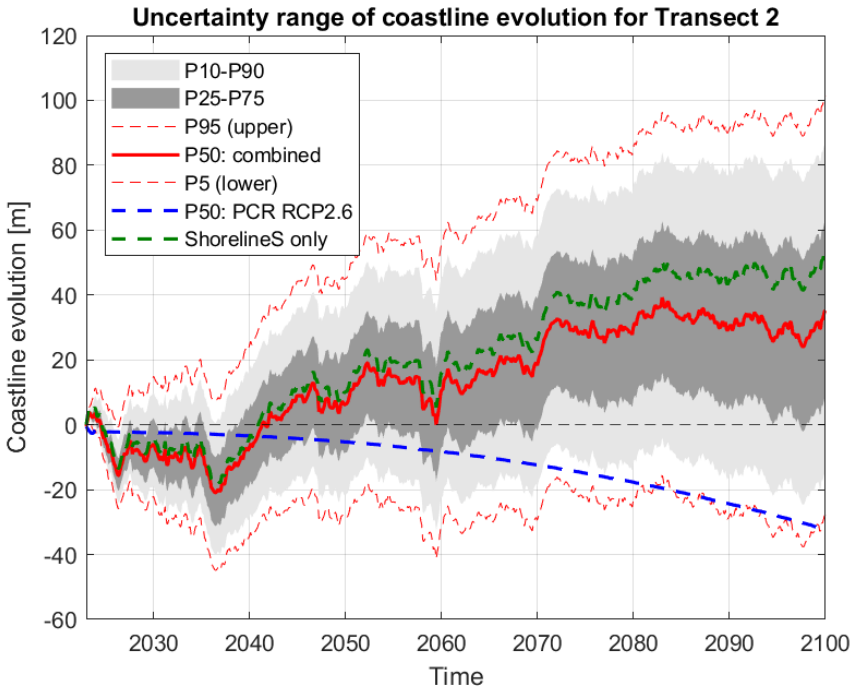

Figure C.6: Result Framework 1: projection for IJmuiden coastline Transect 2 for 2023-2100 (RCP2.6).

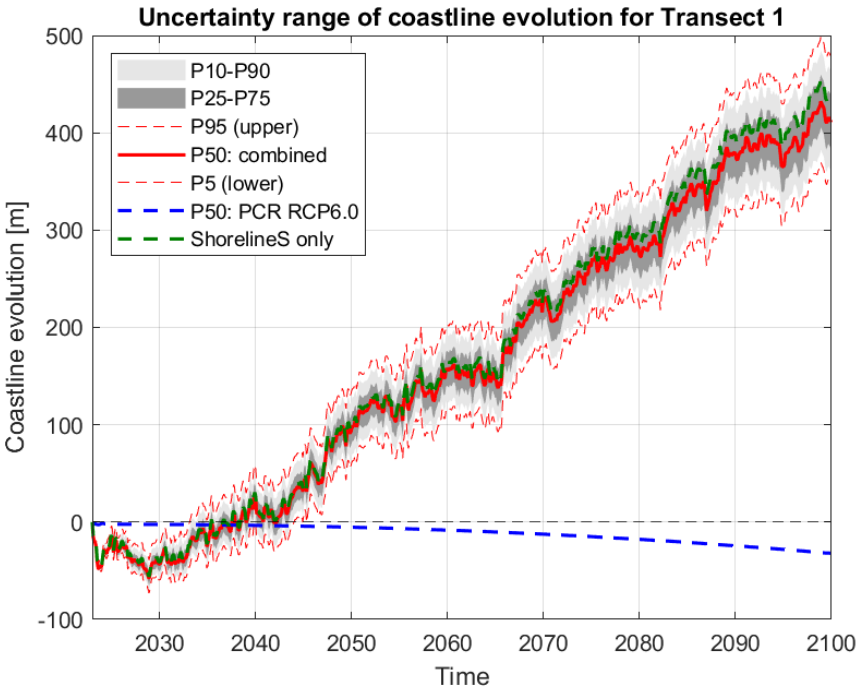

Figure C.7: Result Framework 1: projection for IJmuiden coastline Transect 1 for 2023-2100 (RCP6.0).

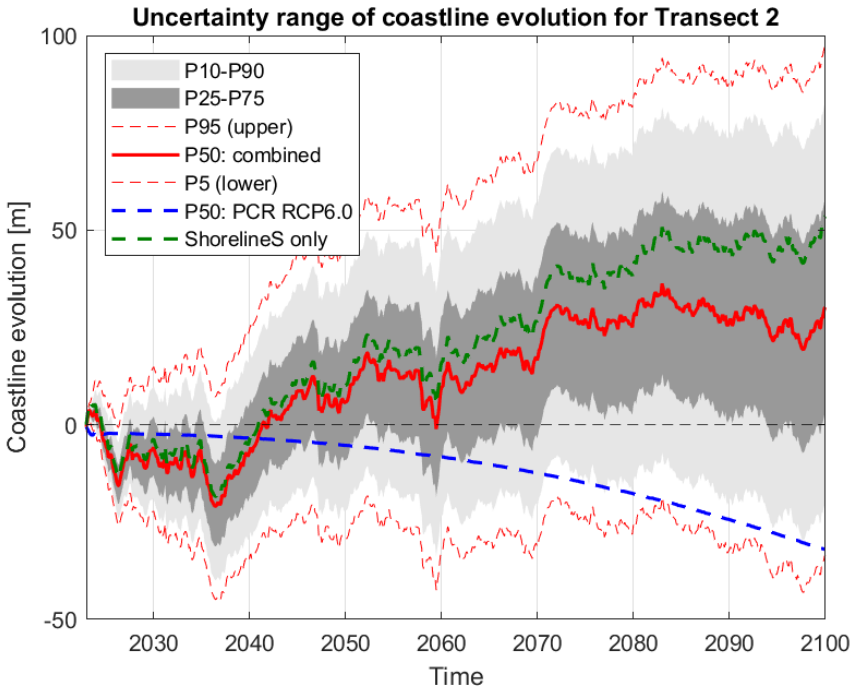

Figure C.8: Result Framework 1: projection for IJmuiden coastline Transect 2 for 2023-2100 (RCP6.0).

D

ShorelineS framework

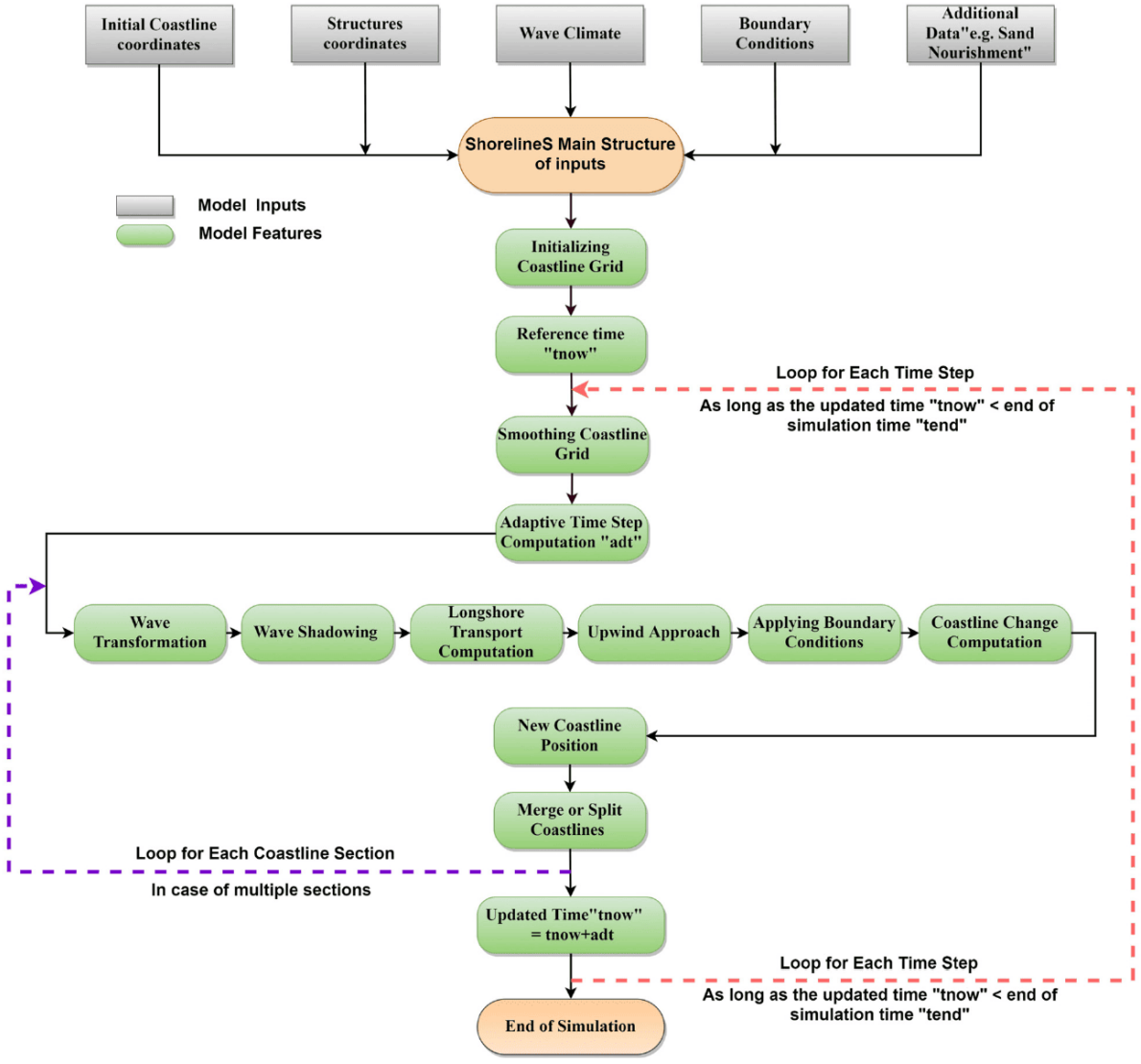

Figure D.1: Flow diagram of ShorelineS model implementation (Roelvink et al., 2020).